PHOTOPHYSICAL AND ELECTROCHEMICAL STUDIES ON PHENOTHIAZINE-BENZIMIDAZOLE HYBRIDS

A DISSERTATION

Submitted in partial fulfillment of the requirements for the award of the degree
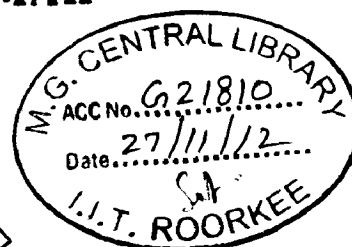
of

MASTER OF TECHNOLOGY

in

ADVANCED CHEMICAL ANALYSIS

By

SANDEEP KUMAR

DEPARTMENT OF CHEMISTRY
INDIAN INSTITUTE OF TECHNOLOGY ROORKEE
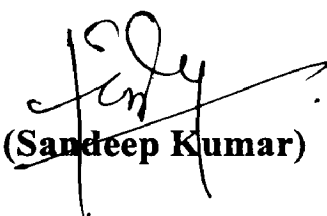ROORKEE - 247 667 (INDIA)
JUNE, 2012

CANDIDATE'S DECLARATION

I hereby declare that the work which is being presented in this dissertation entitled **"PHOTOPHYSICAL AND ELECTROCHEMICAL STUDIES ON PHENOTHIAZINE-BENZIMIDAZOLE HYBRIDS"** in partial fulfillment of the requirements for the award of the degree of **Master of Technology** in Chemistry with specialization in **"Advanced Chemical Analysis"**, and submitted in the **Department of Chemistry** at **Indian Institute of Technology Roorkee**, is an authentic record of the work carried out by me during the period August 2011 to April 2012, under the guidance of **Dr. K. R. Justin Thomas**, Assistant Professor, Department of Chemistry, Indian Institute of Technology Roorkee, Roorkee.

The matter presented in this dissertation work has not been submitted by me for the award of any degree of this or any other institute/ University. In keeping with the general practice of reporting scientific observation, due acknowledgement has been made wherever the work described is based on the findings of other investigators.

Date: June, 2012

Place. Roorkee   (Sandeep Kumar)

CERTIFICATE

This is to certify that the above statement made by the candidate is correct to the best of my knowledge.

(Dr. K. R. Justin Thomas)

Assistant Professor

Department of Chemistry

Indian Institute of Technology Roorkee

ROORKEE-247667 (INDIA)

i

Acknowledgement

During my research work I received a lot of cooperation, support and encouragement with my supervisor, colleagues and friends. It could be possible for me to finish my dissertation work with their dedication, prayers, wishes, blessings and support.

It is my great pleasure to thank God and the other people who helped me directly or indirectly in the course of my entire journey towards producing this thesis. First and foremost, I must thank my supervisor **Dr. K. R. Justin Thomas,** who helped me a lot in each and every step of my research work. Without his innovative guidance and encouragement, it would be impossible to bring my research work to completion. He always encouraged and enlightened me through his knowledge, intelligence and experience. He trained my scientific skills and aptitude to face every situation during my research and academic carrier that will be obliging for me in my future. He is, and always will be the inspiration to me throughout my life.

I would like to thank all the faculty members of the Chemistry Department for their invaluable help and suggestions during my research.

I express my sincere thanks to **Mr. O.P. Dhama** and Mr. Abdul Hauq, in-charge of instrumentation, Department of Chemistry for helping me a lot in carrying out UV-Visible spectroscopy, Fourier transform infrared spectroscopy (FT-IR), and fluorescence measurements. I am also thankful to Mr. Madan Pal, Department of Chemistry, for their technical help during my presentations in the department.

I express my sincere thanks to all my lab mates, particularly Govardhana Babu for assistance in synthesis and Sushil Kumar & Abhishek Baheti in spectral measurements. I am highly obliged for their co-operation, support and help in all the ways throughout my research work. They always motivated and encouraged me in my tough times, gave me moral support whenever I felt alone.

Finally, I am highly grateful to my family members specially my grandmother Smt. Satbiri Devi, my father, Shri Satya Veer Singh, my mother Mrs. Sharda Devi, my wife Mrs. Seema Singh, my son Yuvraj Singh and my daughter Devyani Singh for being the main inspiration and motivating source in this endeavor.

Finally, I must thank all those whom I have failed to state here but have helped in various ways during the course of my research.

(SANDEEP KUMAR)

ii

Table of Contents

Chapter 1

Phenothiazine- and benzimidazole-based

functional materials: A brief survey

1.1 Introduction

Recently, semiconducting organic materials have attracted considerable interest due to their potential application in electronics and optoelectronics. Among their many application fields, electroluminescence (EL) devices using small molar mass organic materials have become the most popular technology that have already been employed in practical applications such as flat-panel or flexible display devices.[1,2] A typical multilayer (often trilayer) electroluminescent device consists of a light emitting layer, an electron-transporting layer, as well as a hole transporting layer. Therefore, the EL performance significantly depends on the recombination efficiency of the holes and electrons injected from the anode and cathode, respectively. Large efforts are devoted to optimizing the charge flux balance for improving the device efficiency and limiting the energy consumption, because the hole-transporting material has a higher carrier drift than the electron-transporting material in most organic light emitting diode (OLED) materials. Bipolar materials with emission characteristics incorporating both hole- and electron-transporting segments can effectively stabilize exciton formation and balance the hole and electron charge in the emitting layer.[3-6] Moreover, the utilization of bipolar compounds will significantly simplify the device structure with double layers or even a single layer, which will largely limit the overall cost and accelerate its ongoing commercialization activities.

1

Similarly dye-sensitized solar cell (DSSC) systems based on highly porous nanocrystalline films of titanium dioxide are of considerable technological interest because of their demonstrated high-power conversion efficiency, potential low cost, and high semiconductor stability. The sensitizer is a critical component in DSSCs.[7,8] Both organometallic and organic sensitizers have been explored for application in DSSCs. Compared with organometallic complexes, organic dyes have the advantages of environmental friendliness, higher structural flexibility, lower cost, easier preparation and purification, larger spectral response in wider solar spectrum, etc. Most of the organic dyes featured an aromatic amine as a donor and cyanoacrylic acid unit as an acceptor. Such a donor-acceptor molecular configuration favored charge separation within the molecule and provided higher rates of electron collection at the terminal electrodes.

Since the dissertation is concerned about the synthesis of phenothiazine-benzimidazole hybrids for application in electronic devices, we present herein a brief survey of the utility of molecular materials constructed on phenothiazine or benzimidazole framework.

1.2 Phenothiazine containing organic materials

Phenothiazine is a well-known pharmaceutical compound bearing electron-rich sulfur and nitrogen heteroatoms. In one hand, it has low oxidation potentials, and stable radical cation can be easily generated.[9] In another hand, the phenothiazine ring is nonplanar with a butterfly conformation in the ground state, which is quite different from carbazole and fluorene. Such special conformation can impede the molecular aggregation and the formation of intermolecular excimer, which may lead to promising electronic and optical properties.[10] They have been used recently as spectroscopic probes in supramolecular assembly for photoinduced electron transfer studies[11,12] and as electron donor components in the materials science due to their low reversible oxidation potentials.[13,14] For example, donor–acceptor systems with phenothiazine as the electron

donor and phenylquinoline group as an electron acceptor provide an approach for the design of new materials exhibiting efficient eletrogenerated chemiluminescence.[9,15] And, phenothiazine-based conjugated polymers that were used as a light-emitting material have also been reported recently.[16,17]
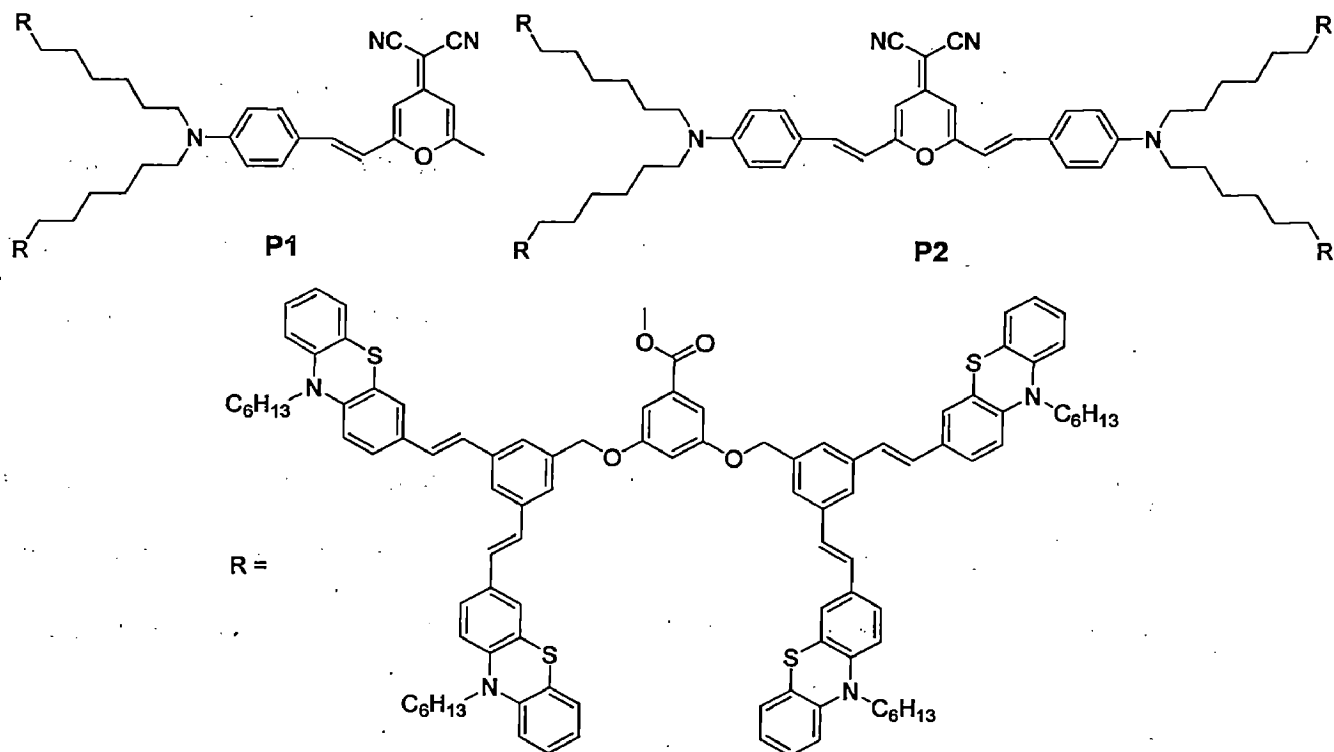

Figure 1. Structures of the red-emitting dendrimers containing light harvesting molecular dendritic wedge composed for electron-rich phenothiazine ring.

Kim et al reported[18] new red light emitting dendrimers, **P1** and **P2** (Figure 1) which were synthesized by reacting 2-[2-(2-{4-[bis(6-hydroxyhexyl)amino]-phenyl}vinyl)-6-methylpyran-4-ylidene]malononitrile or 2-[2,6-bis(2-{4-[bis(6-hydroxyhexyl)amino]-phenyl}vinyl)pyran-4-ylidene]malononitrile with 3,5-bis{3,5-bis[2-(10-hexyl-10*H*-phenothiazin-3-yl)vinyl]benzyloxy}benzoic acid by DCC catalyzed esterification. Two kinds of red emitting core dyes capable of electronic excitation via Förster energy transfer were encapsulated by

3

phenothiazine dendrons. Photoluminescence studies of the dendrimers demonstrated that, at the high density of a phenothiazine dendron, a significantly high-energy transfer to the core is achieved as a result of the large overlap between the absorption spectrum of a core emitting dye and the emission spectrum of the phenothiazine dendron. The electroluminescence spectra of multilayered devices showed red emissions, similar to those observed in the emission spectra of dendrimer thin films.

Barberis and Mikroyannidis reported[19] a novel cyan emitting compound, P3 (Figure 2) containing bis(phenothiazine core and four styryl units attached to it. It exhibited high thermal decomposition temperature (362 °C) and reasonable quantum yield (11%).
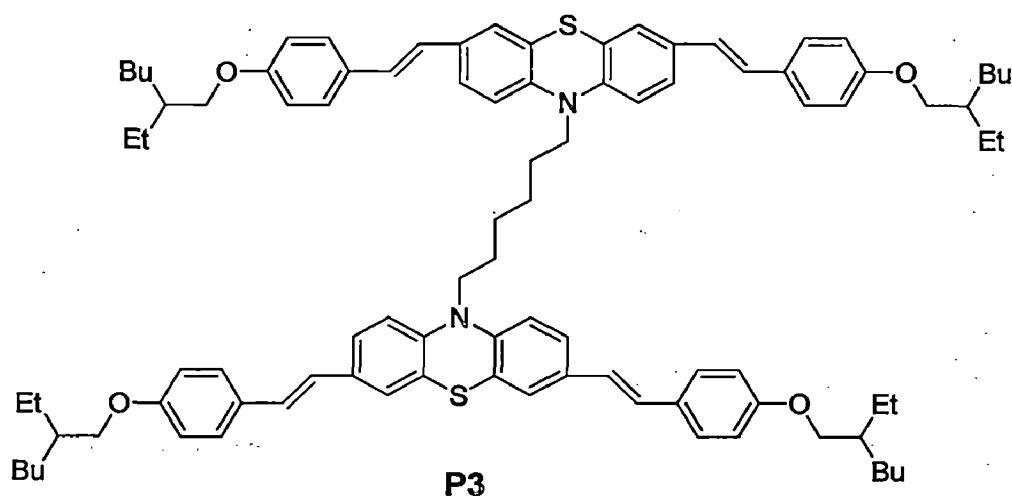
Figure 2. Structure of a bis(phenothiazine) derivative containing styryl units.

A novel class of conjugated dendrimers, **P4-P6** (Figure 3) bearing phenothiazines as peripheral groups and phenylenevinylene-group as a core has been synthesized through the Wittig–Horner reaction in moderate to good yield by Zhang and co-workers.[20] The absorption and fluorescence of all dendrimers show a good correlation to the conjugation length from the core to the periphery. The rather large Stokes shift shown by all these dendrimers could be

explained based on the more planar conformation of the phenothiazine ring in excited state compared with the ground state.
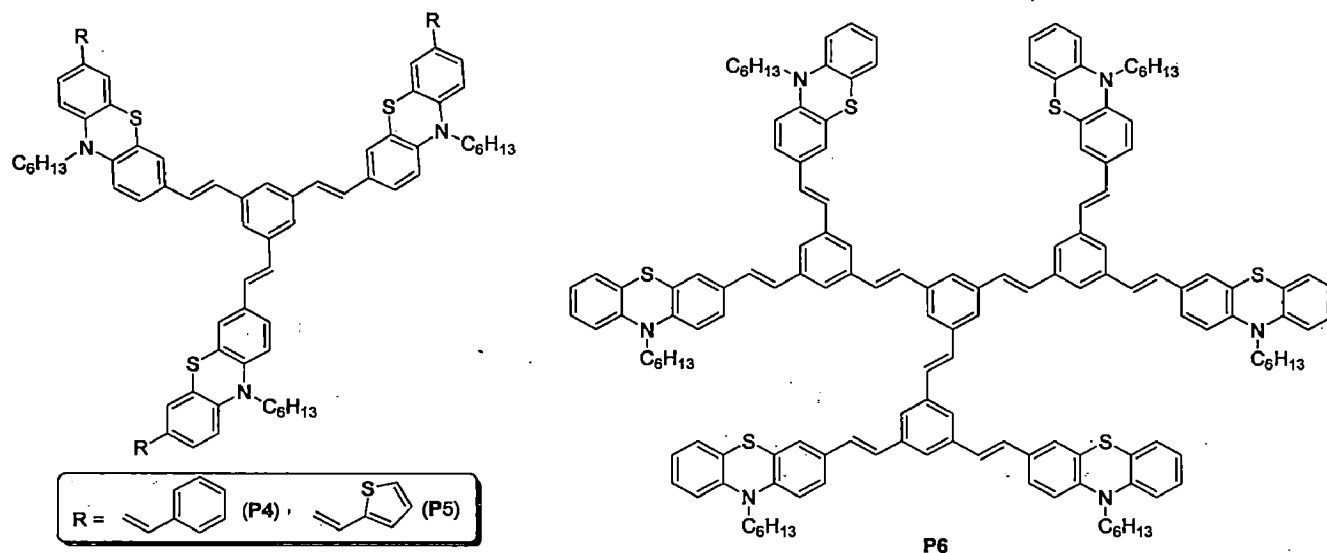

Figure 3. Structures of the dendrimers containing vinylphenothiazine chromophores

Photostability of phenothiazinyl-substituted ethylenes (P7-P10) (Figure 4) in both solution and in solid state (thin films) was investigated as a function of UV exposure time was studied by Kazlauskas et al.[21] Fluorescence intensity and spectral variation measurements in the presence and absence of ambient air were used to determine the effect of oxygen on the degradation of the compounds. The observed reduction in the fluorescence efficiency of air-saturated solutions and thin films subjected to UV was attributed to permanent photo-oxidative degradation. Photostability was higher in the cases of molecules that contained two bulky phenothiazinyl groups as compared to those containing only one phenothiazinyl group and a smaller phenyl substituent. Fully reversible fluorescence intensity decay in the degassed phenothiazine solutions was attributed to photoisomerization, whereas the partially reversible changes in fluorescence intensity that were observed for films in the absence of air were ascribed to both photoexcited

carrier capture by deep-traps acting as exciton quenching centres and degradation imparted by UV-induced bond scission.

P7

P8

P9

P10
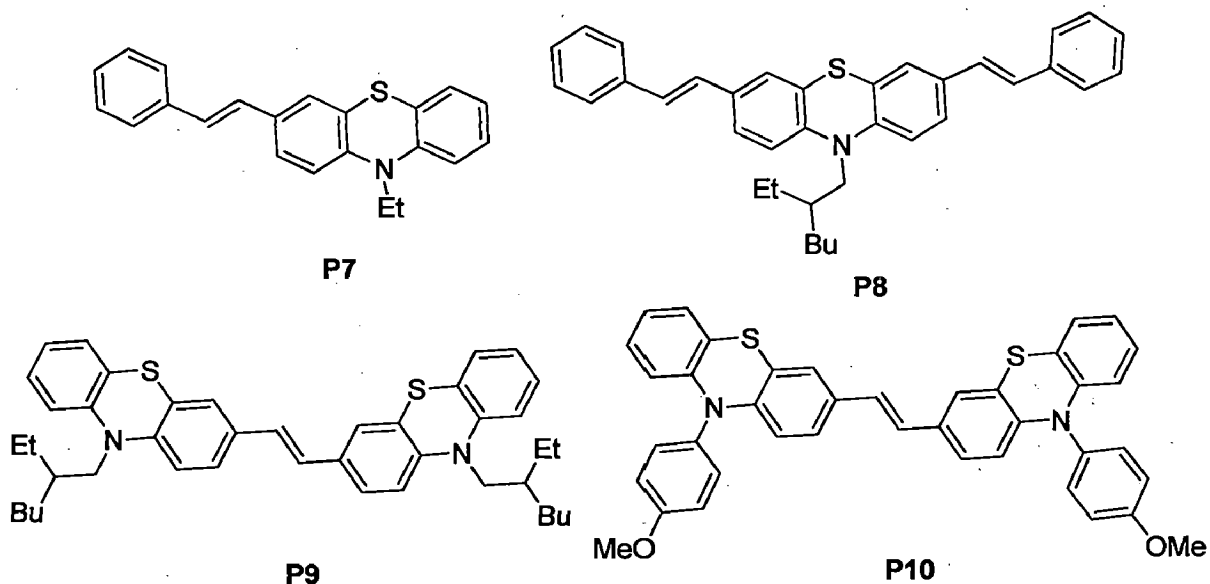
Figure 4. Structures of phenothiazinyl ethylenes.
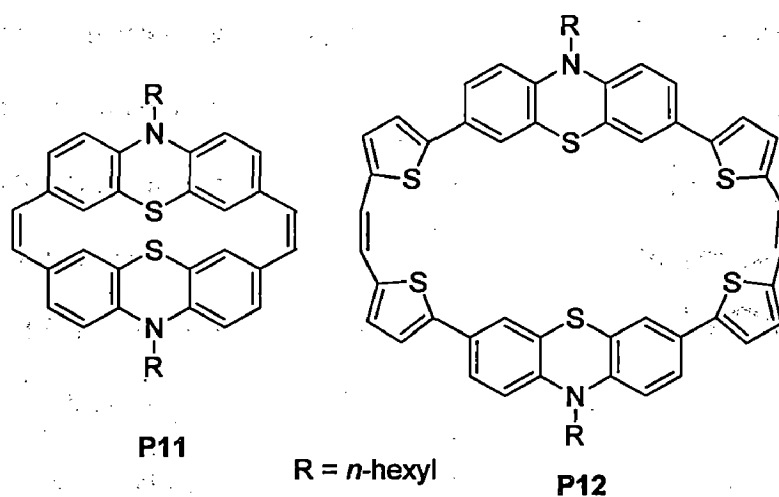

P11

R = n-hexyl

P12

Figure 5. Structures of cyclophanes containing phenothiaze bridges.

Müller and co-workers have developed a general synthesis to ethenylene and ethylene-bridged phenothiazinophanes, P11 and P12 (Figure 5) applying McMurry dimerization to phenothiazinyl aldehydes.[22] They exhibited intensive intramolecular electronic communication between the

6

phenothiazinyl subunits as observed from the cyclic voltammetry measurements. They displayed strong blue to green fluorescence with large Stokes shifts. DFT calculations support that the HOMOs of the cyclophanes possess a fully delocalized structure, and communication over the bridges rather likely occurs by σ-π interaction. In the solid state, the cyclophanes are arranged in unidimensional stacks, a favorable orientation for anisotropic hole-transport in OFET applications.

Qiu et al reported[23] the synthesis and characterization of a series of linear monodisperse vinylene-linked phenothiazine oligomers **P13-P18** (Figure 6). They have accomplished the synthesis by alternate Heck reaction and Wittig reaction in good yields. It was found that the absorption and fluorescence emission bands of the derivatives are red-shifted with increasing phenothiazine units due to the effective extension of conjugation.

n = 0 (P13), 2 (P14), 3 (P15), 4 (P16), 5 (P17), 6 (P18)
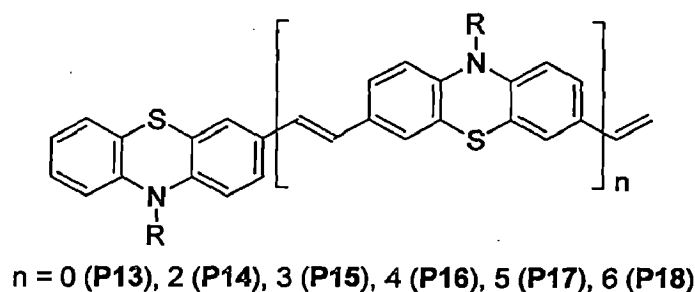
Figure 6. Structures of linear monodisperse vinylene-linked phenothiazine oligomers

Müller and co-workers[24] have synthesized phenothiazinyl dyads (**P19-P23**) and triad (**P24**) (Figure 7) with variable aromatic π-linkers in good yields by Suzuki coupling with suitable phenothiazinyl boronates. The dyads exhibited two reversible oxidation processes while the triads showed three reversible oxidation peaks. These oligofunctional heterocyclic oligomers are strongly electronically coupled and represent suitable functional units for novel redox active molecular wires. The phenylene- and biphenylene-bridged dyads display a very weak electronic

coupling when compared to the thienyl and phenothiazinyl bridged dyads. Strong red shift by altering the conjugating bridge from phenylene to thienylene was observed which arise due to the higher polarizability and reduced conformational biases of thiophene.

P19   n = 0 (R = CH$_3$; P20), 1 (R = n-hexyl; P21), 2 (R = n-hexyl; P22)

P23

P24
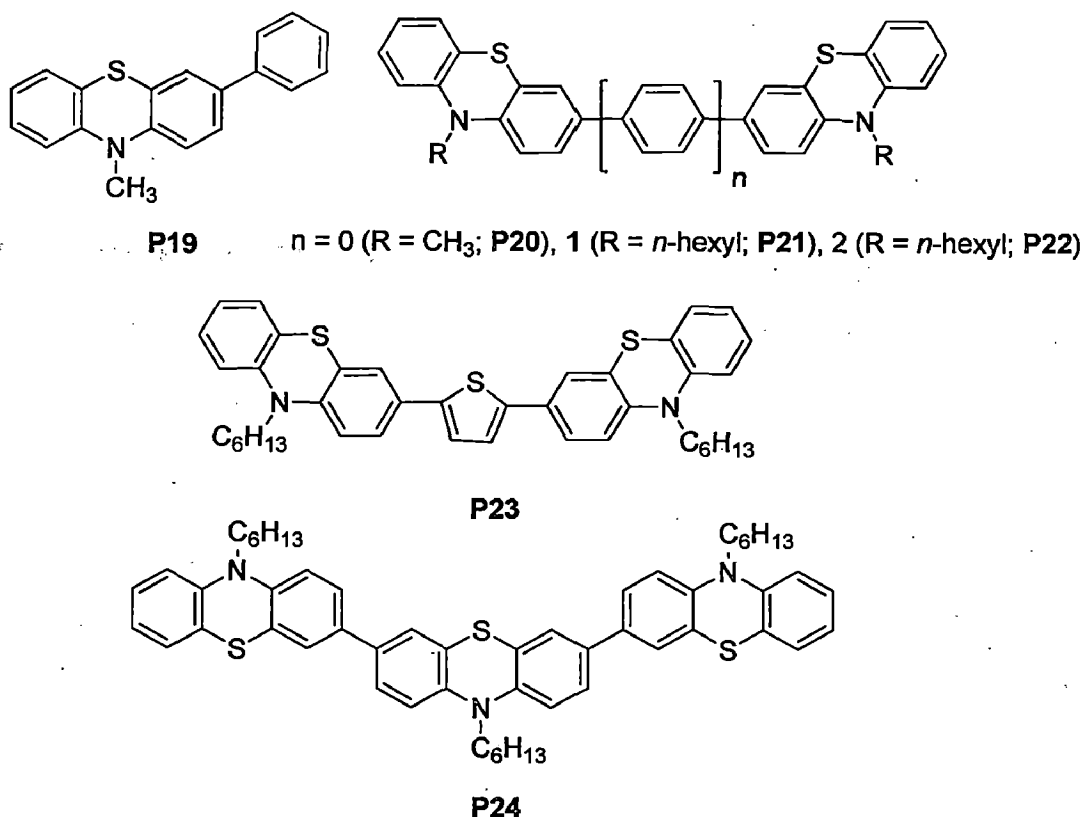
Figure 7. Structures of phenothiazine dyads (P19-23) and triad (P24).

Müller's group[25] reported the synthesis and the electronic properties of alkynylated phenothiazine dyads (P25 and P26) and phenothiazinyl triads (P27 and P28) (Figure 8). They have synthesized a series of alkynylated phenothiazines in moderate to excellent yields by sequences of aldehyde–alkyne transformations and/or Sonogashira cross coupling reactions from suitable phenothiazine aldehydes or bromides. The electronic properties (Table 1) of (hetero)aryl ethynyl-substituted N-methyl-phenothiazines strongly correlate with Hammett σ_p parameters

8

and indicate that remote substituents transmit their electronic information through π-electron delocalization and the σ-framework.

Table 1. Optical and electrochemical parameters for the alkynyl bridged phenothiazines recorded in dichloromethane

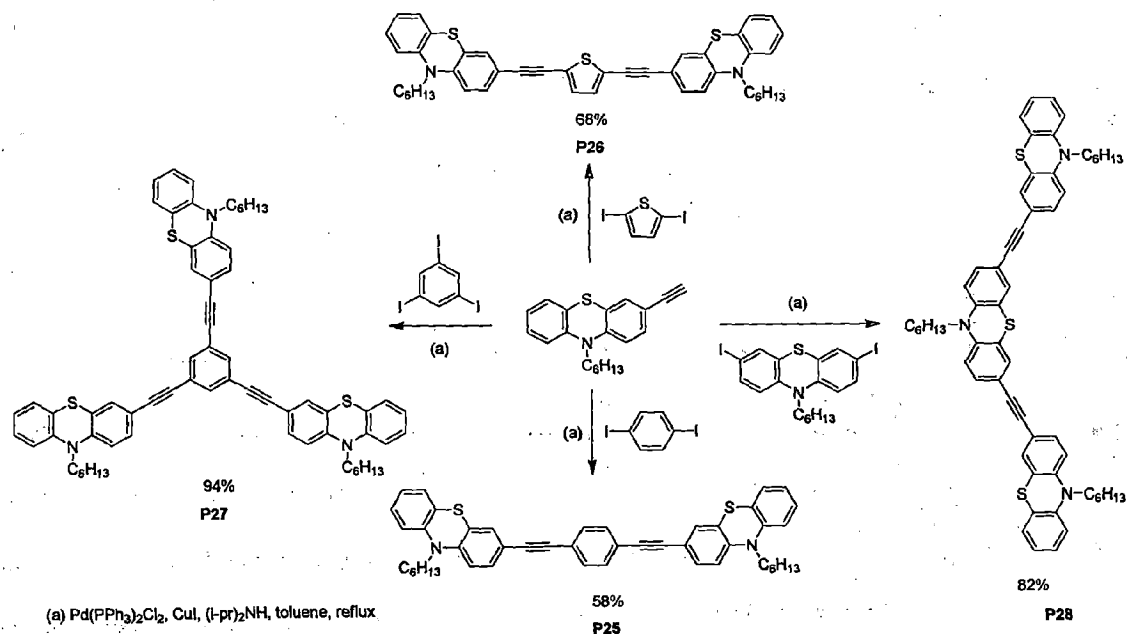| Compound	λ_{max}, nm (ε_{max}, $\times 10^{-3}$ M^{-1} cm^{-1})	λ_{em}, nm (Φ_F)	Stokes shift, cm^{-1}	E_{ox}, V
P25	272 (34.0), 286 (31.9), 304 (32.6), 318 (34.9), 384 (32.8)	499	6000	0.753
P26	270 (51.5), 333 (33.2), 394 (43.7)	496 (0.2)	5200	0.773
P27	278 (96.2), 295 (76.1), 356 (46.6)	470 (0.45)	6800	-
P28	238 (48.4), 276 (67.5), 296 (79.2), 388 (41.9)	481 (0.43)	5000	0.739, 0.886

Figure 8. Synthetic procedure for the dumbbell- and star-shaped alkynyl bridged di- and triphenothiazines

Bunz and co-workers[26] reported the synthesis and characterization of five novel phenothiazine-containing cruciforms (P29-P33) (Figure 9). Exposure of these cruciforms to

either trifluoroacetic acid or to metal salts such as magnesium triflate and zinc triflate led to strong chromic effects in absorption and in emission. In the case of magnesium triflate, a blue shift in emission was observed; in contrast, addition of zinc triflate resulted in either quenching or a red-shifted emission. Due to the electronic situation, these cruciforms displayed spatially separated frontier molecular orbitals, allowing the HOMO or the LUMO of the cruciforms to be addressed independently by addition of zinc or magnesium ions. These phenothiazine cruciforms may have potential application in array-type sensory applications for metal cations.
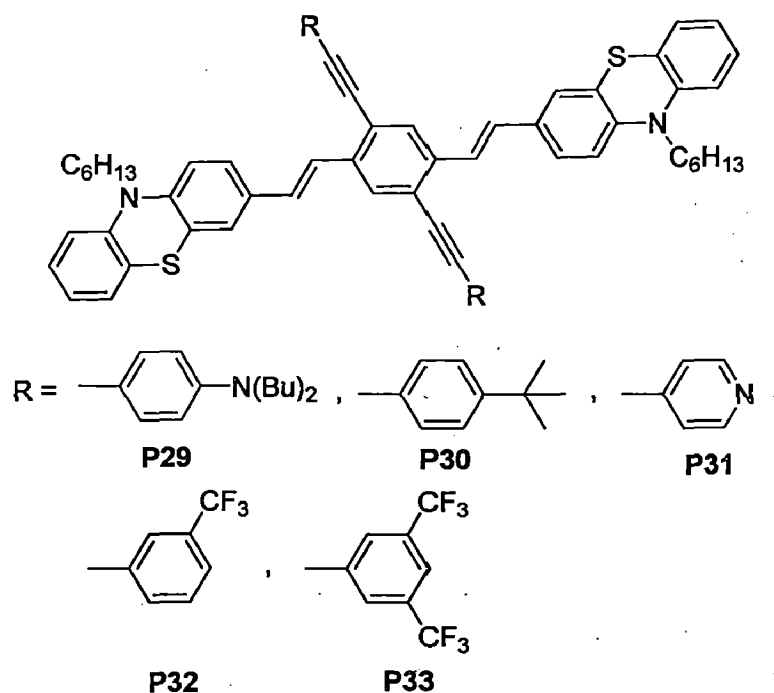
Figure 9. Structures of phenothiazine containing cruciforms

Müller and co-workers[27] reported the synthesis and photophysical and electrochemical characterization of new phenothiazinyl rhodanylidene acetic acid merocyanine dyes (P34-P36) (Figure 10). These dyes exhibited a distinct donor-π-acceptor behavior comprising phenothiazine derivatives as an electron donor and rhodanylidene acetic acid as an electron acceptor. Electron-rich or electron-deficient substituents in the phenothiazine moiety affected the physical and

chemical properties of the system (Table 2). An electron-rich substituent like a second phenothiazinyl group decreased the oxidation potential when compared to the unsubstituted phenothiazine and an efficient intramolecular charge transfer can take place. An electron withdrawing group, for example, a cyanide group reduced the electron density in the phenothiazine donor, which hinders oxidation of the dye. The substituent also influences the absorption region of the synthesized dyes. A pronounced conjugated π-system shifts the absorption to the red.
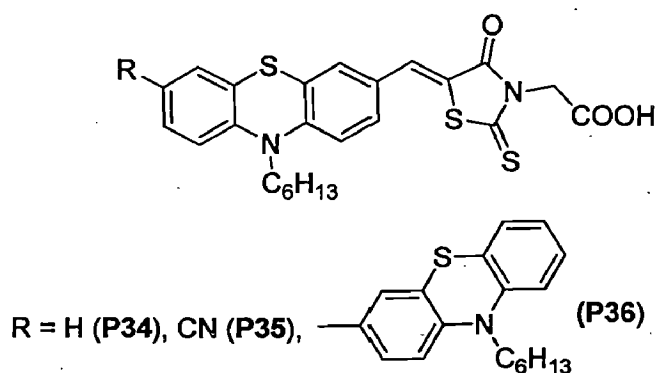

Figure 10. Structures of the phenothiazinyl rhodanylidene acetic acid merocyanines

Table 2. Optical and electrochemical properties of the phenothiazinyl rhodanylidene acetic acid merocyanines

Dye	λ_{max}, nm (ε_{max}, $\times 10^{-3} M^{-1} cm^{-1}$)	λ_{em}, nm (Φ_F)	Stokes shift, cm^{-1}	E_{ox}, V
P34	252 (18), 305 (14), 366 (14), 478 (20)	651 (0.01)	5600	0.898
P35	265 (18), 297 (21), 363 (16), 462 (22)	630 (0.21)	5800	1.116
P36	265 (36), 307 (16), 359 (24), 503 (18)	688 (<0.01)	5300	0.686

Sun and co-workers[28] designed and synthesized novel organic dyes (Figure 11) based on the phenothiazine chromophore for dye-sensitized solar cells. They exhibited solar energy-to-electricity conversion efficiency of up to 5.5% (Table 3) in comparison with the reference Ru-

complex (N3 dye) with an efficiency of 6.2% under similar experimental conditions. The phenothiazine dyes containing a cyanoacrylic anchor group possessed much better DSSC performance than those dyes containing a rhodanine-3-acetic acid group despite the later set of compounds showing promising absorption characteristics. This difference is attributed to the insulation present at the anchoring site.
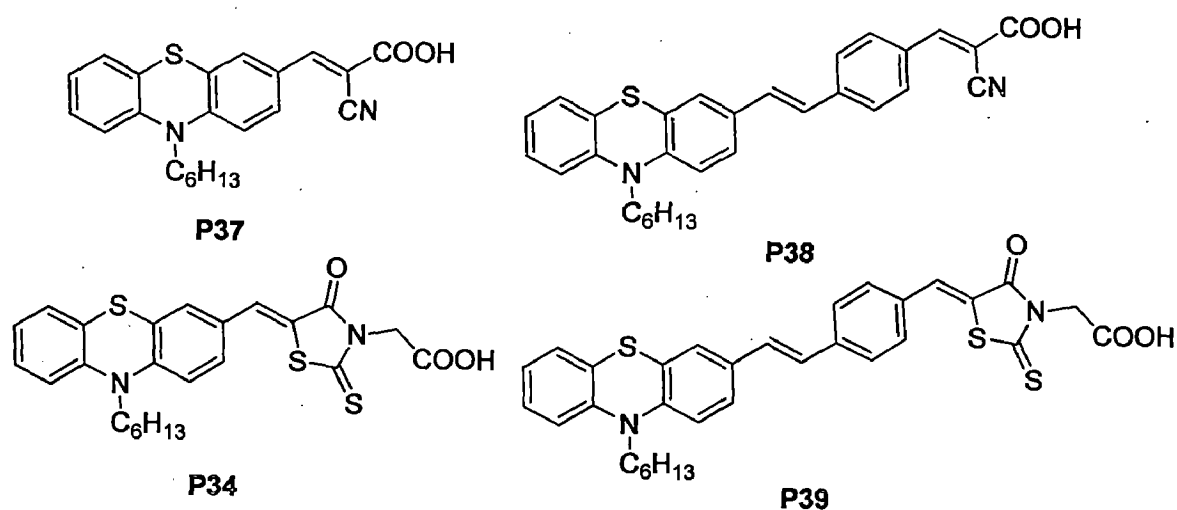
Figure 11. Structures of organic dyes featuring phenothiazine as donor

Table 3. Optical, electrochemical and DSSC properties of the organic dyes containing phenothiazine donor

Dye	λ_{max}, nm (ε_{max}, $\times 10^{-3}$ $M^{-1} cm^{-1}$)[a]	λ_{em}, nm[a]	E_{ox},V[a]	J_{SC}, mA cm^{-2}	V_{OC}, mV	FF	η, %
P34	481 (15.0)	689	1.03	4.8	532	0.74	1.9
P37	452 (19.4)	592	1.10	10.9	712	0.77	5.5
P38	457 (13.1)	653	0.92	10.7	673	0.67	4.8
P39	465 (27.8)	598	0.86	5.9	569	0.71	2.4
P40	469 (22.6)	-	-	15.0	675	0.68	6.8
P41	484 (34.7)	-	-	3.9	525	0.63	1.3

Kim and co-workers[29] designed and synthesized novel organic dyes (Figure 12) of double electron acceptor type based on phenothiazine framework (**P40** and **P41**), as photosensitizers for the dye-sensitized solar cell. They found that the organic dye (**P41**) with rhodanine-3-acetic acid group as acceptor gave much lower efficiencies, compared to that (**P40**) with cyanoacrylic acid unit, for both single and double electron acceptor type. It was attributed to the electronic decoupling between anchoring and TiO_2 conduction band accompanying the lack of π-conjugation of carboxylic group as anchoring on rhodanine-3-acetic acid group, despite that the dyes with rhodanine-3-acetic acid group had relatively broad and intense absorption spectra in the visible region. The DSSC based on the dye containing two cyanoacrylic acid acceptors showed the most efficient photon-to-electricity conversion efficiency compared to other dyes, which is the maximum η value of 6.8% under simulated AM 1.5 irradiation (100 mW/cm^2).
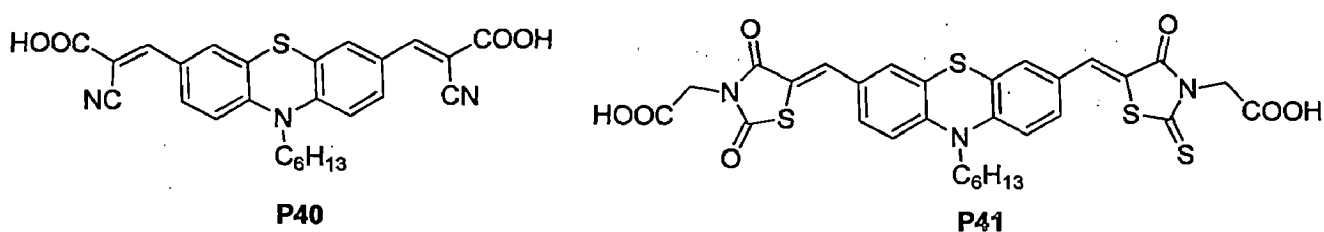

Figure 12. Organic dyes containing phenothiazine donor and two acceptors.

Double donor-acceptor branched dyes (**P42-P44**) with a phenothiazine unit as electron donor and a 2-cyanoacrylic acid unit as electron acceptor were synthesized by Cao et al[30] and used as sensitizers for solar cells. All of the dyes have an intense absorption band at 430-450 nm which is attributed to the π-π^* transition with Donor →Acceptor charge-transfer character. The molar extinction coefficients of the double donor double acceptor dyes are nearly twice as high as that of single donor single acceptor dyes because of the two donor-acceptor units. The conversion

13

efficiency of the DSSCs amounts up to 4.22% for **P43** (Table 4) (2.91% for **P37** under similar conditions) under AM 1.5 G irradiation. The results show that the performance of DSSCs can be effectively enhanced by the cooperation of two donor-acceptor containing branches in one molecule of the dyes.
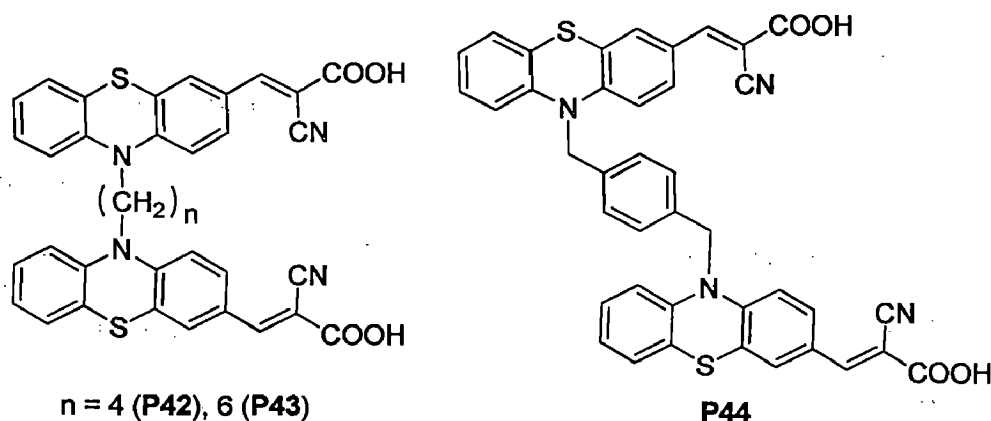

n = 4 (**P42**), 6 (**P43**)   **P44**

Figure 13. Organic dyes containing two phenothiazine donors and two acceptor groups.

Table 4. Optical, electrochemical and DSSC properties of the organic dyes containing phenothiazine donor

Dye	λ_{max}, nm (ε_{max}, $\times 10^{-3}$ M^{-1} cm^{-1})[a]	λ_{em}, nm[a]	J_{SC}, mA cm^{-2}	V_{OC}, mV	FF	η, %
P37	439 (1.6), 300 (2.9)	586	6.13	709	0.67	2.91
P42	433 (3.2), 310 (4.9)	589	7.86	740	0.71	4.13
P43	435 (3.1), 310 (4.9)	583	8.27	750	0.68	4.22
P44	439 (3.0), 314 (5.0)	577	6.98	740	0.69	3.56

[a] measured in THF solution; [b] vs NHE

Phenothiazine derivatives, **P45-P47** (Figure 14) with various conjugated linkers (furan, thiophene, and 3,4-ethylenedioxythiophene) were synthesized and used in dye-sensitized solar cells to study the effect of conjugated linkers on device performance.[31] The absorption spectra

show two major bands at ca. 300-400 nm and at ca. 400-600 nm. UV absorption was attributed to localized aromatic π-π* transitions. Visible absorption was ascribed to intramolecular charge transfer (ICT) transitions. The λ_{max} of the dye with thiophene linker was red-shifted (6 nm) when compared with the dye with furan linker (Table 5). This is due to better delocalization of electrons over the whole molecule when thiophene was used rather than furan. Among them, one with furan as a conjugated linker showed a solar energy-to-electricity conversion efficiency (η) of 6.58%, an improvement of over 24% compared with the reference cells' 5.29% under AM 1.5 G irradiation.
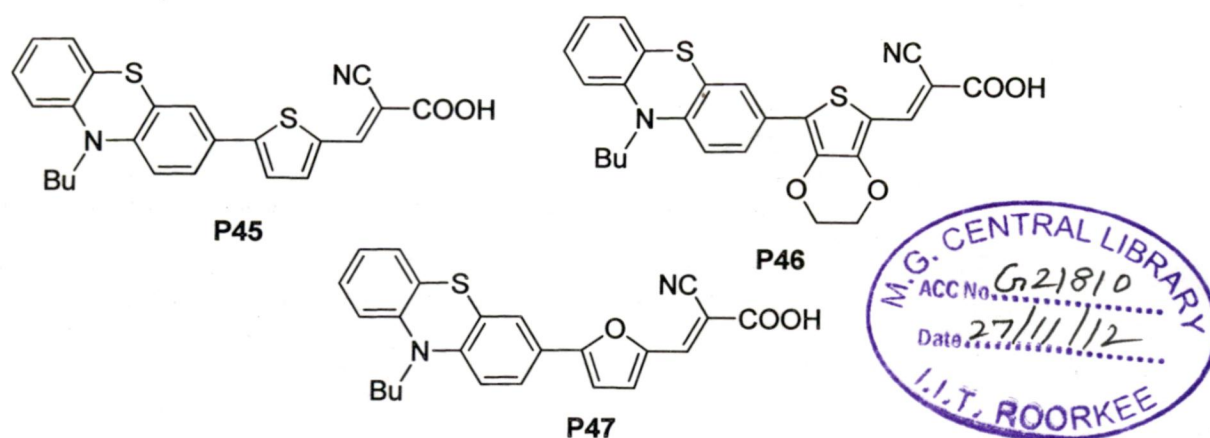

Figure 14. Organic dyes containing phenothiazine donors and various π-linkers.

Table 5. Optical, electrochemical and DSSC properties of the organic dyes containing phenothiazine donor and various π-linkers.

Dye	λ_{max}, nm (ε_{max}, $\times 10^{-3}$ M^{-1} cm^{-1}) [a]	λ_{em}, nm [a]	E_{ox}, V [a,b]	J_{SC}, mA cm^{-2}	V_{OC}, mV	FF	η, %
P45	448 (16.2)	634	0.89	12.05	725	0.72	6.32
P46	466 (26.0)	546	0.87	11.68	746	0.70	6.09
P47	442 (15.1)	641	0.78	12.18	772	0.70	6.58

[a] measured in dichloromethane solution; [b] vs NHE

15

Xie and co-workers[32] reported the synthesis and characterization of two novel organic dyes, **P48** and **P49** (Figure 15), containing electron rich phenothiazine as electron donor, oligothiophene vinylene as conjugation spacer and cyanoacrylic acid as acceptor. They found that an additional donor moiety in the organic sensitizers with three or more conjugation units deteriorates the PV performance of the DSSCs because of the occurrence of serious dye aggregation.
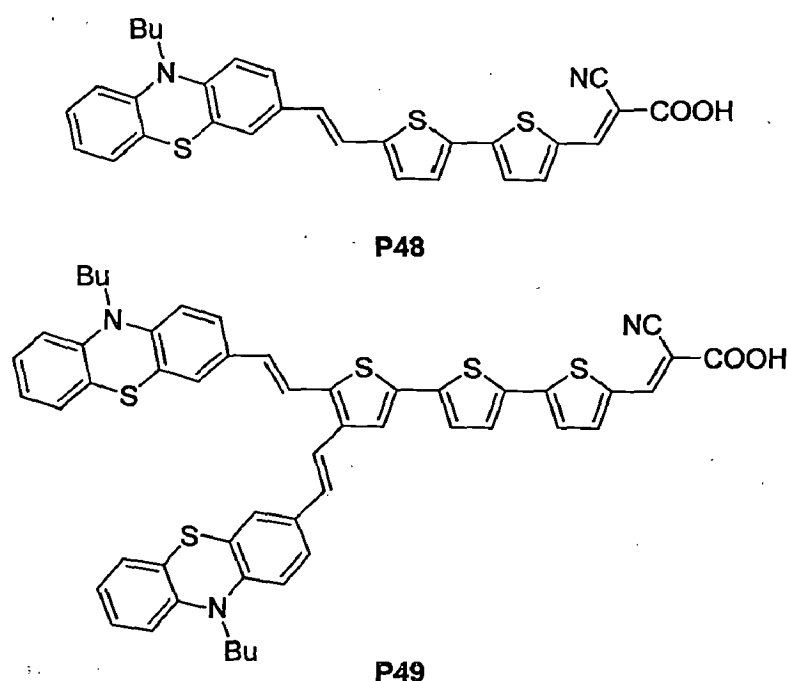

P48

P49

Figure 15. Structures of novel phenothiazine-based organic dyes with oligothiophene π-spacer.

Lin and co-workers[33] studied the effects of different acceptor groups in phenothiazine-triphenylamine dyes on the optical, electrochemical, and photovoltaic properties were studied. By replacing the cyanoacetic acid to rhodanine-3-acetic acid as electron acceptor, the absorption spectrum of **P51** (Figure 16) shows a significant red shift due to the rhodanine-3-acetic acid extends the π-conjugation system. The different acceptor groups in **P50** and **P51** show a great effect on the HOMO levels and a gentle effect on the LUMO levels. The overall conversion

16

efficiencies of 4.4% and 2.1% were obtained for DSSCs based on **P50** and **P51**, respectively. In comparison with **P51**, the photovoltaic performance of **P50** was significantly improved by replacing rhodanine-3-acetic acid to cyanoacetic acid. The conversion efficiency of solar cell based on the **P50** is increased about 110%. Theoretical calculations show that the delocalization of the excited state is broken between the 4-oxo-2-thioxothiazolidine ring and the acetic acid, which affects the electron injection from **P51** to the conduction band of TiO_2. The results indicate that cyanoacetic acid acceptor favors better properties of DSSCs than that of rhodanine-3-acetic acid acceptor in the phenothiazine-triphenylamine dyes.
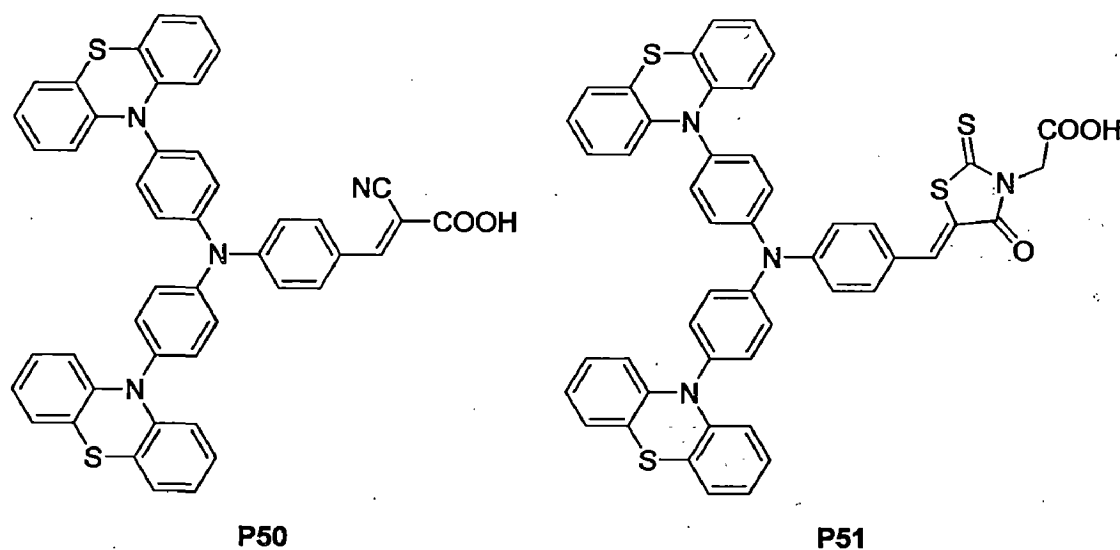

P50   P51

Figure 16. Structures' of triphenylamine-based dyes containing phenothiazine at peripheries.

Three new phenothiazine-based organic dyes (Figure 17) containing thiophene, 3-(5-(3-(4-(bis(4-methoxyphenyl)amino)phenyl)-10-octyl-10H-phenothiazin-7-yl)thiophen-2-yl)-2-cyanoacrylic acid (**P52**), 3-(5-(3-(4-(diphenylamino)phenyl)-10-octyl-10H-phenothiazin-7-yl)thiophen-2-yl)-2-cyanoacrylic acid (**P53**) and 2-cyano-3-(5-(10-octyl-3-(4-(2,2-diphenylvinyl)phenyl)-10H-phenothiazin-7-yl)thiophen-2-yl)acrylic acid (**P54**) were designed and synthesized as sensitizers for application in dye-sensitized solar cells by Tian and co-

workers.[34] For these dyes, the phenothiazine derivative moiety and the cyanoacetic acid take the roles of electron donor and electron acceptor, respectively. The absorption spectra, electrochemical and photovoltaic properties of P52–P54 and the cell long-term stability were extensively investigated. It was found that HOMO and LUMO energy level tuning can be conveniently accomplished by alternating the donor moiety. The DSSCs based on dye P53 showed the best photovoltaic performance: a maximum monochromatic incident photon-to-current conversion efficiency of 84.9%, a short-circuit photocurrent density of 10.84 mA·cm^{-2}, an open-circuit photovoltage of 592 mV, and a fill factor of 0.69, corresponding to an overall conversion efficiency of 4.41% under standard global AM1.5 solar light conditions. These results demonstrated that the DSSCs based on phenothiazine dyes could achieve both high performance and good stability.
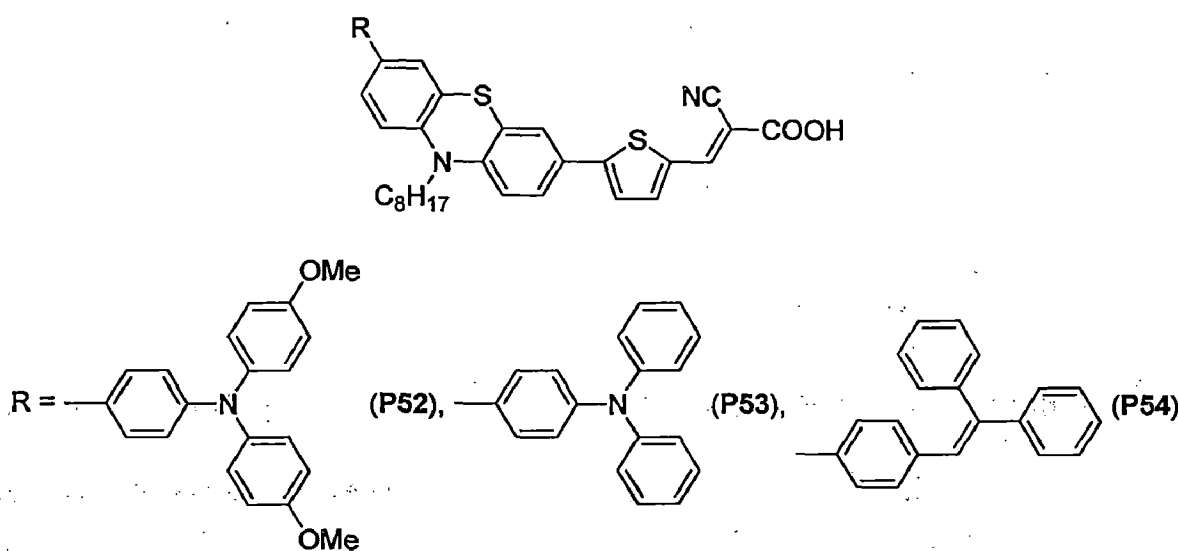

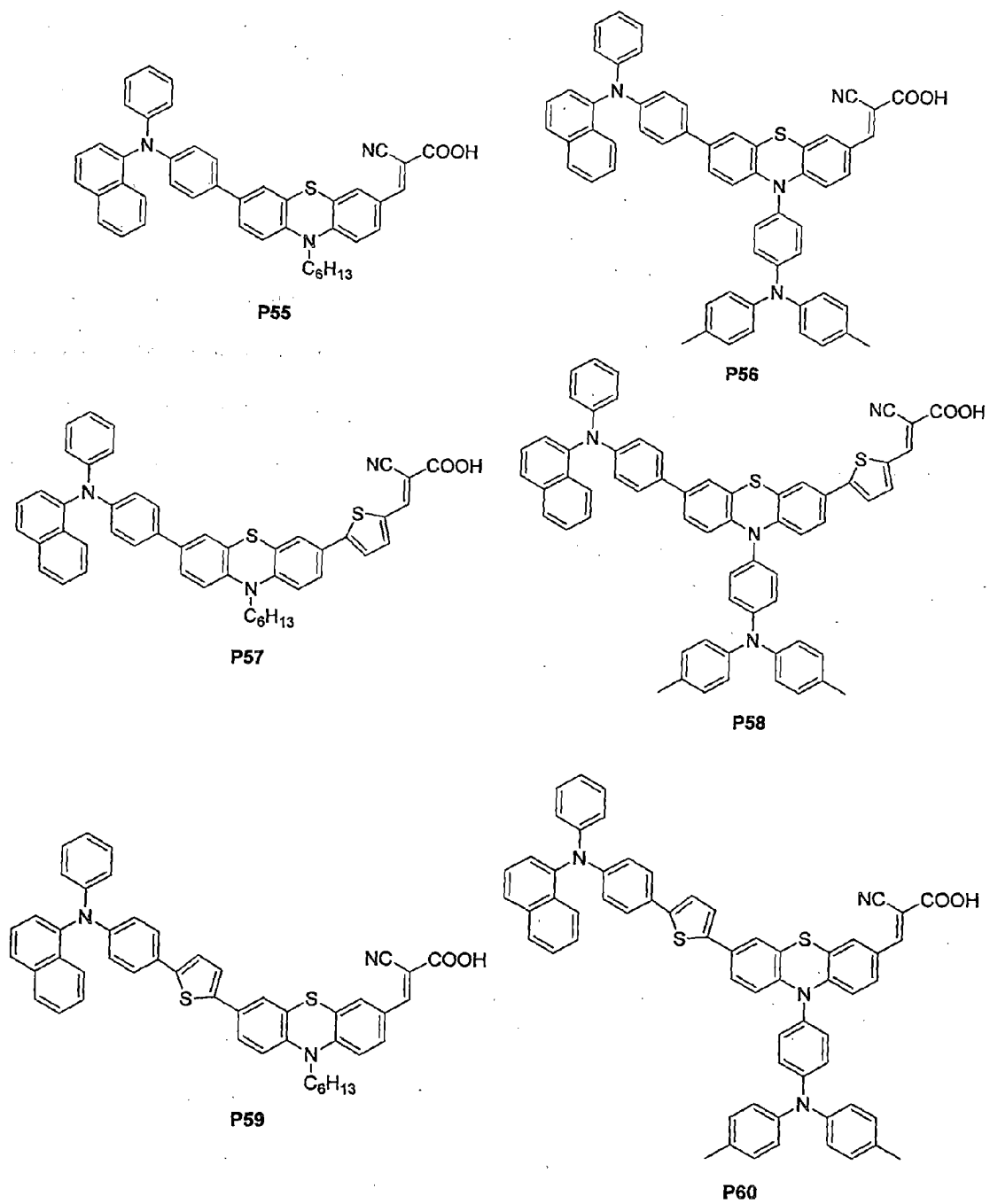Figure 17. Structures of organic dyes containing phenothiazine and different additional donor fragments.

P55

P56

P57

P58

P59

P60

Figure 18. Phenothiazine based dyes containing different peripheral amines and N-substitution

19

Chow and co-workers[35] synthesized a series of organic dyes, **P55-P60**, (Figure 18) containing a phenothiazine central unit and used in the fabrication of dye-sensitized solar cells. A cyanoacrylate moiety was added at the C(3) position of the phenothiazine as an electron acceptor, and a triarylamine moiety was attached at the C(7) position as an electron donor (Figure 18).

The DSSCs made with these dyes displayed remarkable quantum efficiency, ranging from 4.2–6.2% under an AM 1.5 solar conditions (100 mW cm^{-2}). A variety of substituents, i.e., methyl, hexyl and triphenylamino groups, were added at the N(10) of phenothiazine in order to optimize the incident photon-to-current conversion efficiency. Along the main chromophore a thiophenylene group was inserted at different positions to examine its influence on the properties of devices. The best performance was found in compound **P59**, in which a hexyl group was attached at the N(10) of phenothiazine and a thiophenylene at the C(7) position. It displayed a short-circuit current of 14.42 mA cm^{-2}, an open-circuit voltage of 0.69 V, and a fill factor of 0.63, corresponding to an overall conversion efficiency of 6.22%.

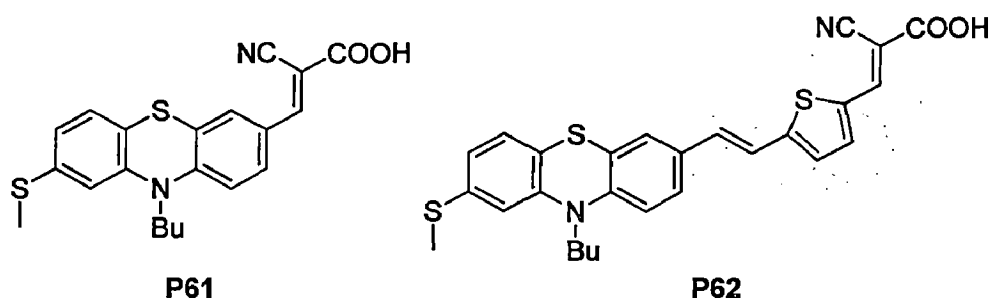**Figure 19.** Structures of phenothiazine-based organic dyes containing thioether functionality.

Two novel metal-free organic donor–π–acceptor dyes, **P61** and **P62** (Figure 19) were synthesized by Grätzel and co-workers[36] using electron-rich 10-butyl-(2-methylthio)-10*H*-phenothiazine as a donor and cyanoacrylic acid as an acceptor. The spectral response of the dye

was tuned by introducing a vinylene thiophene π-bridge. Extending the π-conjugated linker by introducing a vinyl thiophene group has helped to vastly enhance the optical properties of the resulting compound. The bathochromic shift of the absorption peak exhibited by P62 in the solution is only 27 nm, but the onset of the absorption has been pushed much further. Obtained optical and electrochemical properties of the dyes seemed to be promising in terms of employing them as light harvesters in dye-sensitized solar cells. The efficiencies of the devices under standard AM 1.5G (100 mW cm^{-2}) conditions reached 7.3% with volatile electrolyte.

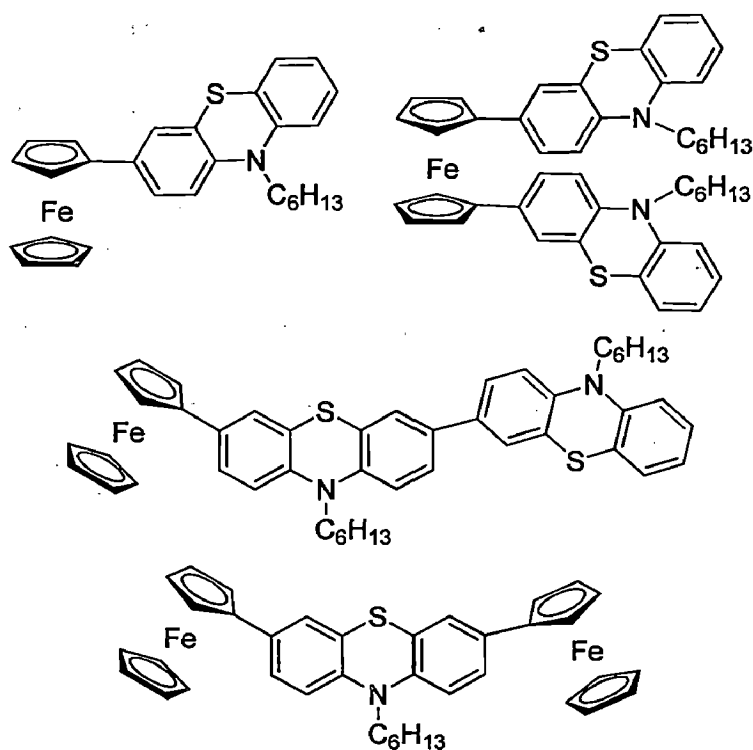Figure 20. Structures of phenothiazine-ferrocene hybrids.

Müller and co-workers[37] reported the synthesis and electrochemical investigations on oligomeric ferrocene–phenothiazine systems (Figure 20). They have synthesized these systems by Suzuki coupling of iodo ferrocenes with phenothiazinyl and diphenothiazinyl pinacolyl boronates. Structurally, these organometallic–organic hybrid electrophores with 1,10-

disubstitution on ferrocene adopt preferentially an eclipsed orientation as a consequence of partial intramolecular π-stacking. In cyclic voltammetry an effective electronic communication was observed if ferrocene adopts the central part of the oligomers and hence, the ferrocenyl moiety can be considered as an electronic communicator between the electronically active phenothiazine side chains.

1.3 Benzimidazole-based organic materials

Benzimidazole derivatives have been proven to be very effective to improve the injection and transport of electrons.[38,39] For instance, 1,3,5-tris(N-phenylbenzimidazol-2-yl)benzene (TPBI) is commonly used as both electron-transporter[40,41] and host material for fluorescent and phosphorescent dopants because of its good electron mobility ($\approx 10^{-5}$ cm^2 V^{-1} s^{-1}) and large HOMO-LUMO energy gap (≈ 3.5 eV) to confine charge carriers and excitons in the emissive layer. However, to enhance the hole transporting capability of the materials based on benzimidazoles and expand their utility in organic light emitting diodes, several structural variations have been attempted. We present below a brief survey of materials reported with benzimidazole fragment and additional functional moieties such as fluorene, carbazole, anthracene and triphenylamine.

Lin and co-workers[42] reported the synthesis and characterization of fluorene derivatives containing benzimidazole and arylamine units (Figure 21). The carrier mobilities for the amorphous compounds **B1** and **B2** were measured by the time-of-flight (TOF) transient photocurrent technique in vacuum at room temperature. Both compounds exhibit non-dispersive electron- and hole transport characteristics as indicated by the TOF transients. These blue-emitting compounds exhibit intriguing ambipolar carrier-transport properties and were used to

fabricate single-layer blue-emitting EL devices with very promising performances comparable to those of multilayer blue-emitting devices. High-performance single-layer devices with a phosphorescent dopant and these compounds as the hosts were also demonstrated.
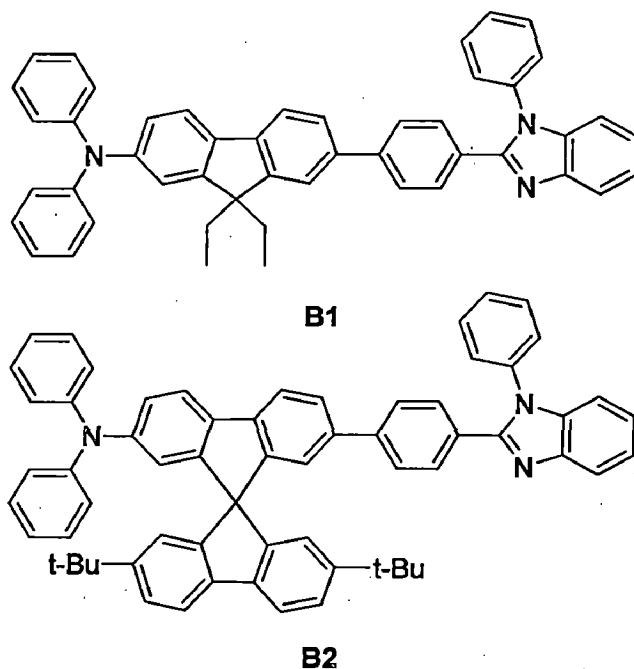

Figure 21. Structures of fluorene-benzimidazole hybrids containing additional amine unit.

Park and co-workers[43] developed two green host materials **B3** and **B4** by combining both of the hole-transporting carbazole moiety and electron-transporting benzimidazole moiety in one structure (Figure 22). These compounds have similar HOMO, LUMO levels and band-gap characteristics compared with CBP (4,4'-di(N-carbazolyl)biphenyl). The **B3** host exhibits very good device performances in the green phosphorescent organic light emitting diodes. The current and power efficiency is enhanced by 1.6 and 2.0 times at a given constant luminance of 1000 cd/m^2 compared with a CBP host device. The moderate efficiency of compound **B4** relative to that of **B3** is probably due to low triplet energy with the extension of conjugation at the N-naphthylcarbazole moiety and the localization of LUMO levels at the naphthyl group.
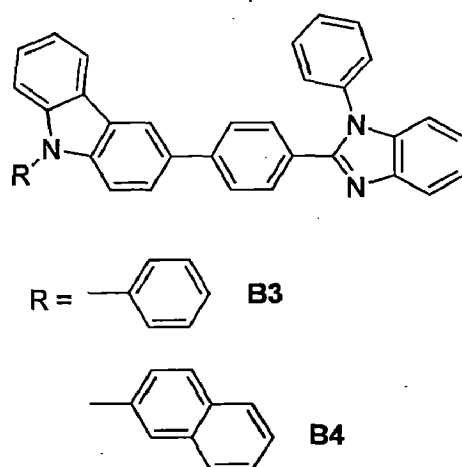
Figure 22. Structures of carbazole-benzimidazole hybrids.

Ge et al reported[44] the synthesis and characterization of two solution-processible bipolar molecules (Figure 23), tris(3'-(1-phenyl-1H-benzimidazol-2-yl)biphenyl-4-yl)amine (**B5**) and tris(2-methyl-3'-(1-phenyl-1H-benzimidazol-2-yl)biphenyl-4-yl)amine (**B6**), bearing both hole-transporting triphenylamine and electron-transporting benzimidazole moieties. They possess excellent thermal stability with high glass-transition temperature (T_g) of 148 and 144 °C, and the decomposition temperatures (T_d) of 552 and 515 °C in nitrogen, respectively. They exhibit good solubility in common solvents due to the meta-structured and star-shaped configuration allowing a solution processing. **B5** and **B6** were employed to fabricate phosphorescent organic light-emitting diodes (PHOLEDs) as the host materials doped with the guest of Ir(ppy)$_3$ by spin coating with a single-layer structure. The solution-processed **B6** device exhibited an improved performance relative to **B5** arising from the complete charge localization of HOMO and LUMO and an increase in the singlet–triplet (S_0-T_1) energy gap which originates from the decreased π-conjugation interrupted by the methyl group.

R = H (B5); Me (B6)
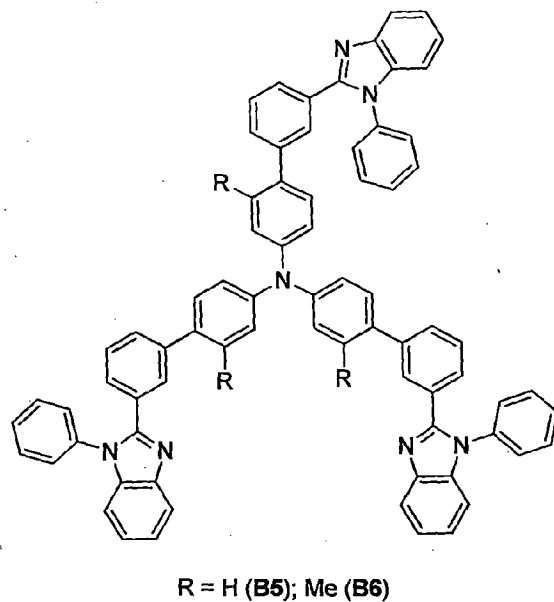
Figure 23. Structures of triphenylamine-benzimidazole conjugates used as triplet hosts.

B7
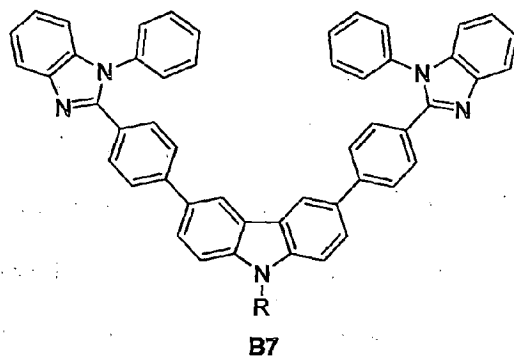
Figure 24. Structure of a carbazole-benzimidazole triad.

Hung and co-workers[45] reported a new benzimidazole/carbazole hybrid bipolar material (Figure 24, **B7**) for highly efficient deep-blue electrofluorescence, yellow–green electrophosphorescence, and two-color-based white OLEDs. The non-coplanar conformation of **B7** provides steric bulk, resulting in stable amorphous thin films and pronounced photoluminescence quantum efficiency. They applied **B7** to the fabrication of non-doped deep

blue-emitting devices with promising performance [η_{ext} = 3%; CIE = (0.16; 0.05)]. It also served as a host material when doped with 10 wt% of the yellow–green emitter (pbi)$_2$Ir(acac), to realize a green phosphorescent organic light emitting diode exhibiting high efficiency [η_{ext} = 19.2%; CIE = (0.42; 0.56)]. Combining the deep blue fluorescence of **B7** with the yellow–green phosphorescence of 0.1 wt% (pbi)$_2$Ir(acac) doped in **B7**, they obtained an efficient white light emitting electroluminescent device [η_{ext} = 7%; CIE = (0.31, 0.33)].

A series of bipolar anthracene derivatives (Figure 25) containing hole-transporting triphenylamine and electron transporting benzimidazole moieties were synthesized and characterized by Huang et al[46]. These compounds possess high thermal properties and quantum yield in toluene solution but their photoluminescence spectra are sensitive to the polarity of the solvent. Because the twist between the anthracene and phenyl rings can effectively reduce the charge transfer from the triphenylamine moiety to the benzimidazole moiety, these compounds emit light in the blue region. These derivatives indicate a high quantum yield in toluene because of the presence of the anthracene moiety. It is noteworthy that quantum yield increase with the increase of the phenyl rings, because less coplanarity and less π-electron conjugation of phenyl ring could reduce energy wastage in charge transfer and even nonradiative decay. They exhibited very high T_g values for **B8**, **B9** and **B10** at 144.1 °C, 152.7 °C, and 161.5 °C, respectively. Three types of devices were fabricated to investigate their electron-transporting and hole-transporting as well as light-emitting properties. The electroluminescence spectra for the three derivatives **B8**, **B10** and **B11** show that they emit blue light, while the **B9**-based devices produced white light at a low current density because of the electromer formation. Moreover, a single layer OLED device for **B11** exhibited a current efficiency of 3.33 cd A^{-1} with a pure blue color of CIE(x,y) of (0.16, 0.16) at 20 mA cm^{-2} and a maximum brightness of 8472 cd m^{-2} at 8.7 V.
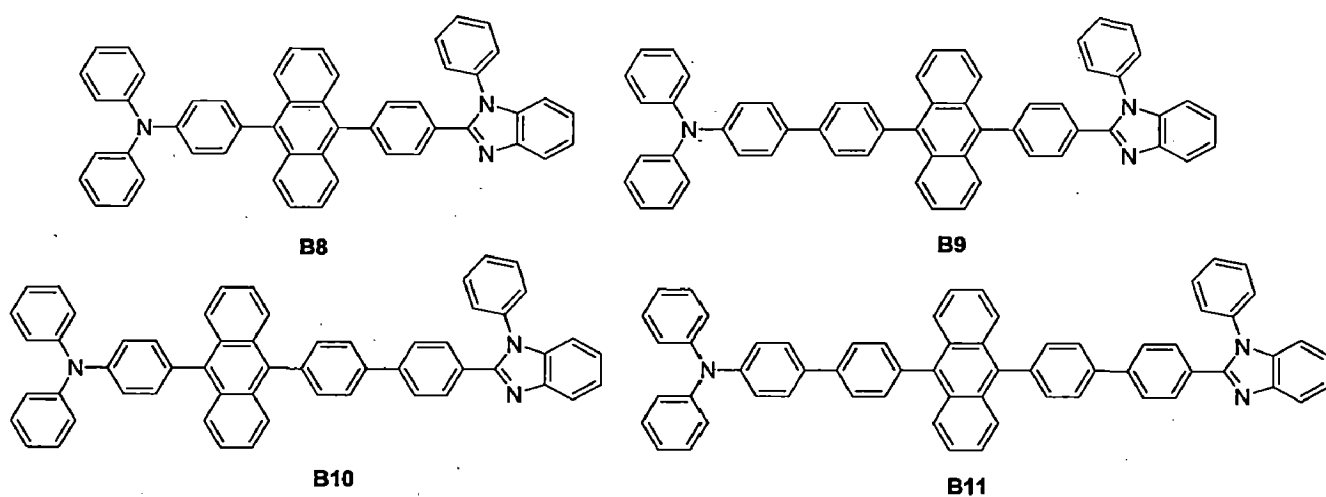
Figure 25. Structures of anthracene-benzimidazole hybrids.

Wong and co-workers[47] synthesized a series of bipolar hosts (Figure 26) containing hole-transporting carbazole and electron-transporting benzimidazole moieties and then examined the morphological, thermal, and photophysical properties and carrier mobilities of these bipolar host materials. Altering the linking topology (C- or N-connectivity of the benzimidazole) changed the effective conjugation length and led to different excited-state solvent relaxation behavior. The N-connected compounds (**B14, B15**) possessed higher triplet energies (E_T) than those of their C-connected analogues (**B12, B13**) by 0.23 eV. The higher values of E_T of **B14** and **B15** endowed them with the ability to confine triplet excitons on the blue-emitting guest. A blue phosphorescent OLED device incorporating **B14** achieved maximum external quantum efficiency, current efficiency, and power efficiency of 16.3%, 35.7 cd A^{-1}, and 23.3 lm W^{-1}, respectively, confirming the suitability of using N-connected bipolar hosts for the blue phosphor. The donor/acceptor interactions of the C-connected analogue resulted in a lower triplet energy, making it a suitable bipolar host for green phosphors. A green-phosphorescent device incorporating **B12** as the host doped with $(PBi)_2Ir(acac)$ achieved a maximum external quantum

27

efficiency, current efficiency, and power efficiency of 20.1%, 70.4 cd A^{-1}, and 63.2 lm W^{-1}, respectively.
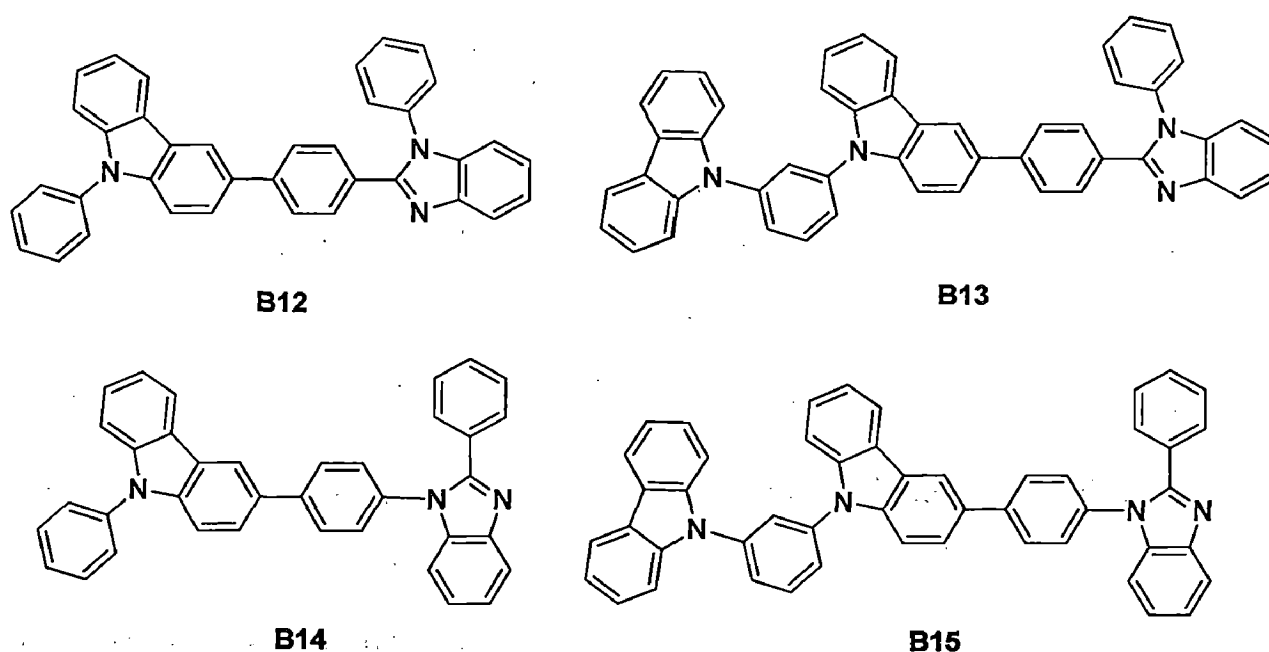

Figure 26. Structures of carbazole-benzimidazole hybrids displaying C-/N-connectivity variations.

Wong and co-workers[48] developed two novel donor–acceptor bipolar host materials (Figure 27), **B16** and **B17**, by incorporating electron-accepting benzimidazole and electron-donating indolo[3,2-*b*]carbazole into one molecule. The photophysical and electrochemical properties of the hybrids can be tuned through the different linkages (C- or N-connectivity) between the electronic donor and acceptor components. The promising physical properties of these two new compounds made them suitable for use as hosts doped with various Ir- or Os-based phosphors for realizing highly efficient phosphorescent organic light emitting diodes. Phosphorescent organic light emitting diodes using **B16** and **B17** as hosts incorporated with Ir-based emitters such as green (PPy)₂Ir(acac), yellow (Bt)₂Ir(acac), and two new red emitters (3,5dimethylPh-6-Fiq)₂Ir(acac) and (4-tBu-Ph-6-Fiq)₂Ir(acac) accomplished high external quantum efficiencies

ranging from 14 to 16.2%. Nevertheless, the red phosphorescent organic light emitting diode device incorporating **B17** doped with the red emitter osmium(II) bis[3-(trifluoromethyl)-5-(4-*tert*-butylpyridyl)-1,2,4-triazolate] dimethylphenylphosphine [Os(bpftz)$_2$(PPhMe$_2$)$_2$] achieved a maximum external quantum efficiency, current efficiency, and power efficiency of 22%, 28 cd A^{-1}, and 22.1 lm W^{-1}, respectively, with CIE coordinates of (0.65, 0.35). The external quantum efficiency remained high (20%) as the brightness reached to 1000 cd m^{-2}, suggesting balanced charge fluxes within the emitting layer, rendering devices with limited efficiency roll-off.

B16   B17
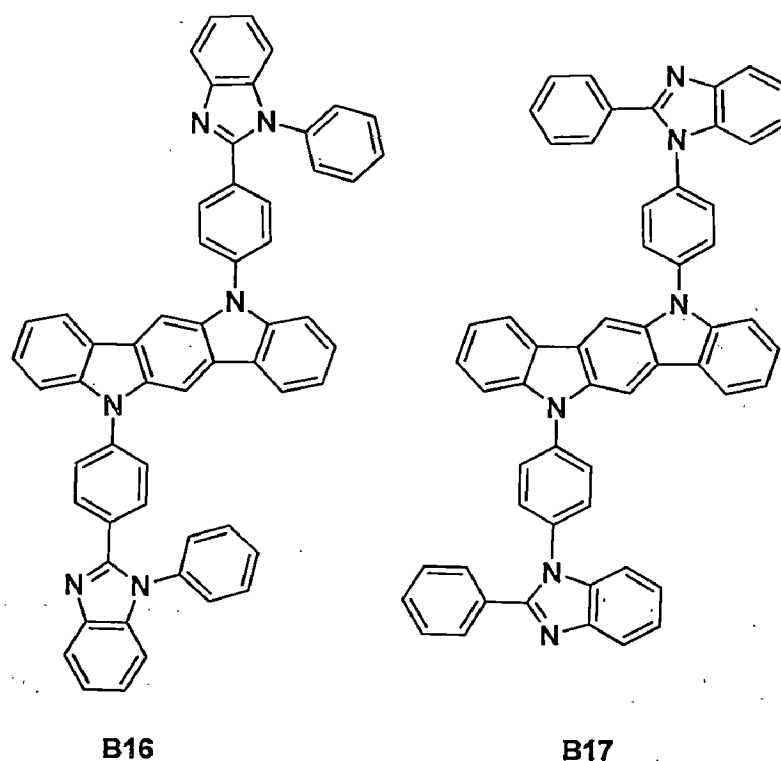
Figure 27. Structures of carbazole-benzimidazole triads with *C-/N*-connectivity variations.

A new series of benzimidazole/carbazole hybrids, **B18-B21** (Figure 28), with different linking spacers or linking topologies between the benzimidazole and carbazole moieties were facilely prepared, and their thermal, photophysical, and electrochemical properties were investigated by Ma and co-workers[49] With the incorporation of rigid benzimidazole moiety, these compounds

29

possess excellent thermal stability with high glass-transition temperatures of 137-186 °C and the thermal-decomposition temperatures of 479-544 °C. **B19** and **B20** with the *m*-terphenyl unit as the linking spacer between the carbazole and the benzimidazole moieties exhibit significant blue shifts as compared to **B18** and **B21** with the phenyl unit because the longer linking spacer alleviate intramolecular charge transfer.

B18

B19

B20

B21
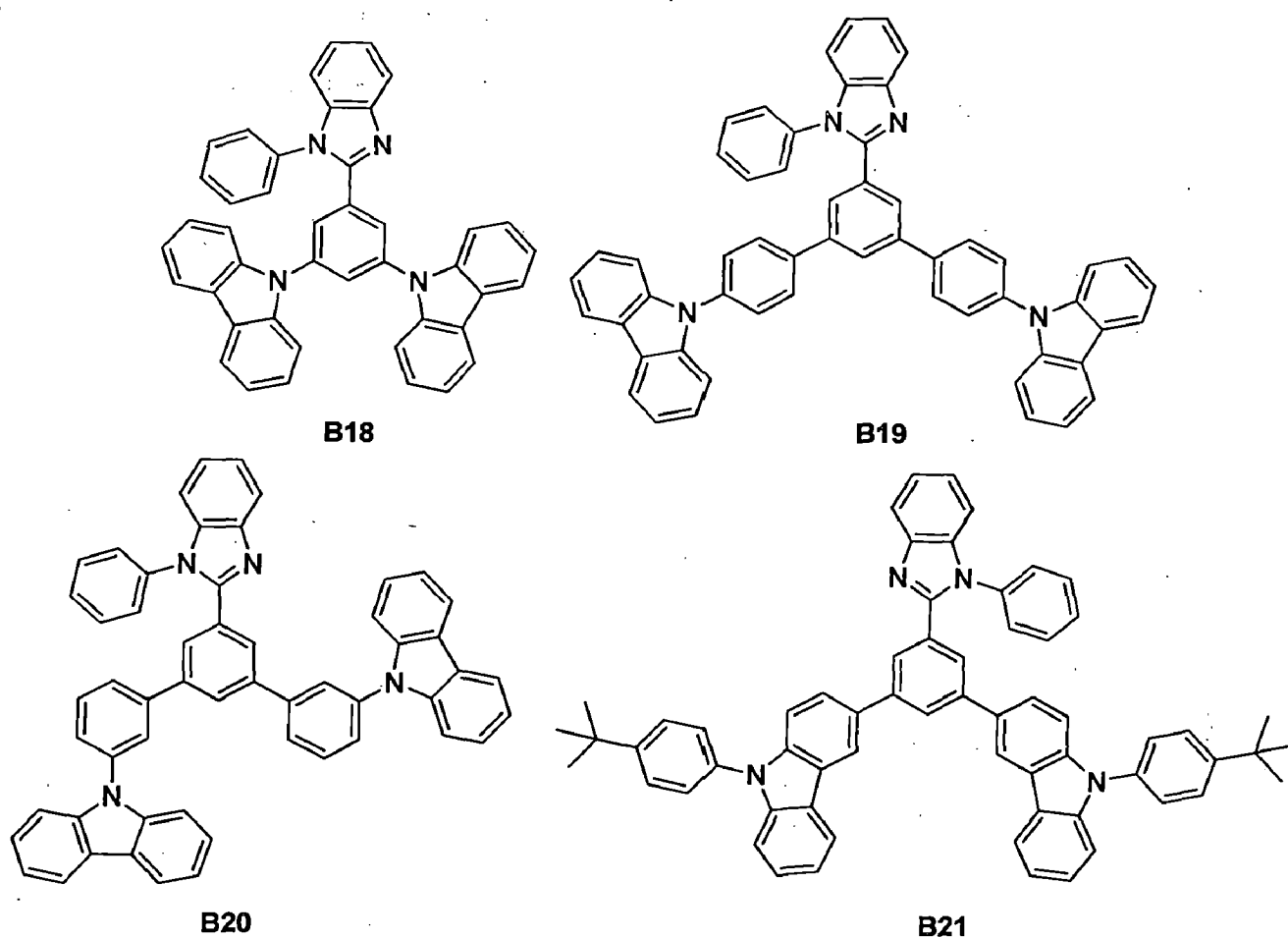
Figure 28. Structures of carbazole-benzimidazole triads having different linking topologies.

Their HOMO and LUMO energy levels vary in the range of 5.50-5.63 and 2.02-2.35 eV, respectively. Devices employing the new compounds as the host for the green emitter of $Ir(ppy)_3$ were fabricated with the configurations of ITO/MoO_3 (10 nm)/NPB (80 nm)/Host: 9 wt % $Ir(ppy)_3$ (20 nm)/TPBI (40 nm)/LiF (1 nm)/Al(100 nm). Their EL efficiencies follow the order of

B20 > B19 > B18 ≈ B21, which correlates with their triplet energy and the separation of HOMO and LUMO distributions at hole- and electron-transporting moieties. A maximum current efficiency of 70.2 cd A^{-1} and a maximum power efficiency of 73.4 lm/W were achieved when **B20** was used as the host. A facile strategy to manipulate the spatial distribution of energy levels and triplet energy of hosts by changing linking spacers or linking topologies is demonstrated.

Figure 29. Synthesis of a carbazole-benzimidazole triad
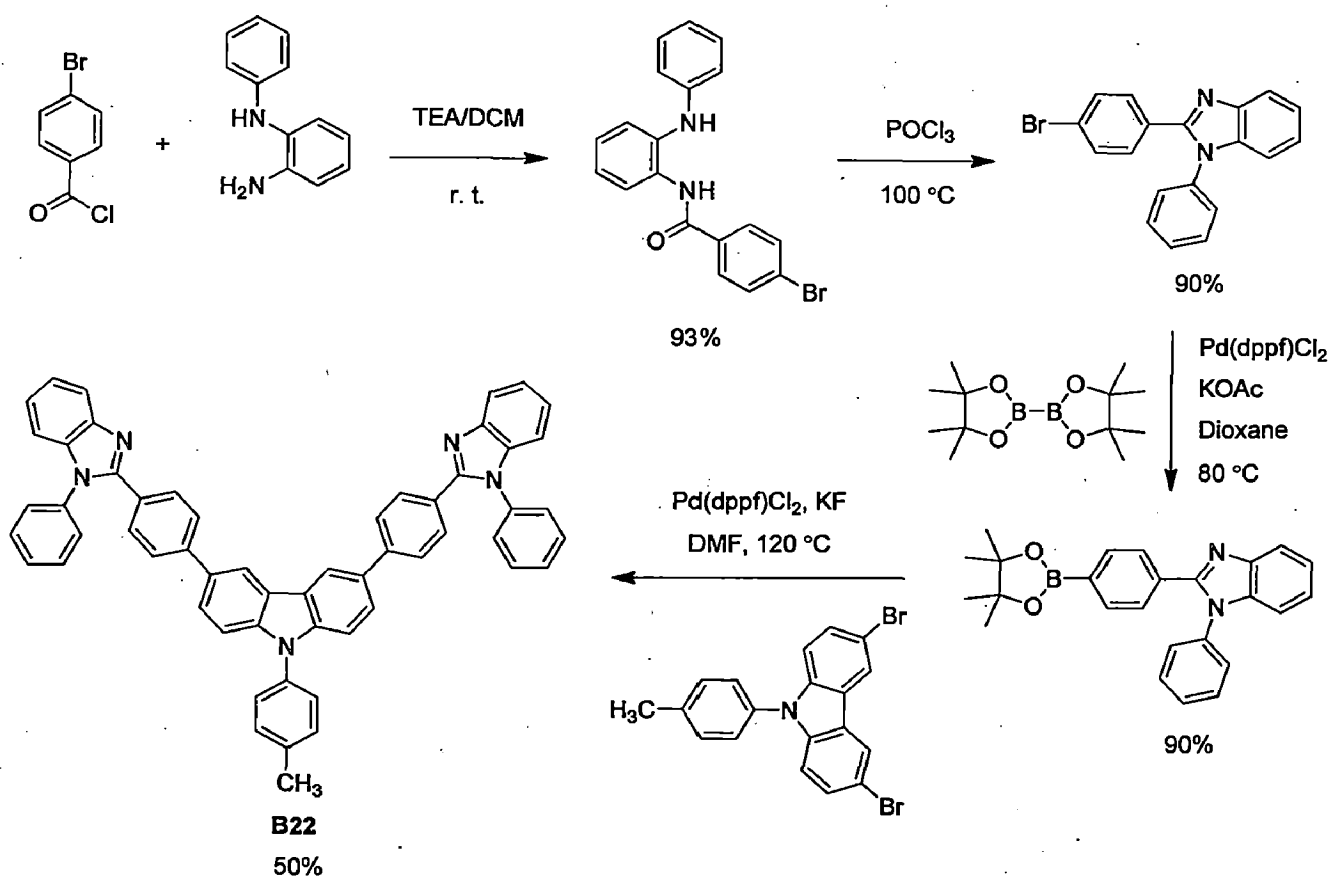
Jabbour and co-workers[50] reported the synthesis, photophysics, and electrochemical characterization of carbazole/benzimidazole-based compound, **B22** (Figure 29) and efficient fluorescent deep-blue light emitting devices based on **B22** with the peak external quantum efficiency of 4.1% and CIE coordinates of (0.16, 0.05). Efficient deep-blue emission as well as

high triplet state energy of **B22** enables fabrication of hybrid white organic light emitting diodes with a single emissive layer. Hybrid white emitting devices based on **B22** show the peak external quantum efficiency exceeding 10% and power efficiency of 14.8 lm/W at a luminance of 500 cd/m^2.

1.4 Aim and scope

From the survey presented above, it is clearly evident that phenothiazine and benzimidazole units are promising building blocks for the construction of molecular materials for application in electronic devices such as organic light emitting diodes and dye-sensitized solar cells. We felt that integration of phenothiazine donor with electron-deficient benzimidazole is a modular approach to obtain dipolar materials possessing balanced charge transport and good emission characteristics. Phenothiazines normally exhibit poor emission characteristics due to their inherent oxidation propensity. However, incorporation of electron-withdrawing groups such as cyano has been found to enhance the photophysical properties. It is our aim to synthesize phenothiazine-benzimidazole hybrids with elongated conjugated fragment attached to the phenothiazine nucleus.

Chapter 2

Synthesis and characterization of phenothiazine-

benzimidazole hybrids

2.1 Materials and methods

All commercially available materials were used as obtained from their sources. Dichloromethane (DCM) and toluene were distilled from phosphorus pentoxide. All chromatographic separations were carried out with hexane:DCM mixture on silica gel (60-120 mesh, Rankem).

^{1}H and ^{13}C NMR spectra were recorded on Bruker AV500 O FT-NMR spectrometer operating at 500 and 125 MHz respectively in CDCl$_3$ and (CD$_3$)$_2$SO (chemical shifts (δ) in ppm and coupling constants (J) in Hz). Me$_4$Si (0.00 ppm) served as internal standard, or residual signals for CHCl$_3$ (^{1}HNMR, δ = 7.26; ^{13}CNMR, δ = 77.36 ppm) or DMSO (^{1}HNMR, δ =2.5 ppm; ^{13}C NMR δ = 40.45 ppm). IR spectra were measured on NEXUS FT-IR (THERMONICOLET). The electronic absorption spectra were obtained with Evolution 600, Thermo Scientific UV-Vis spectrophotometer in dichloromethane and toluene solutions. Emission spectra were recorded in on selected solvents on a Schimadzu spectrofluorimeter. The samples were excited either at 340 nm (for coumarin 1 reference) or 420 nm (for coumarin 6 reference) during the quantum yield measurements. Qualitative emission spectra of the samples were obtained by exciting at the absorption maximum. Cyclic voltammetry experiments were performed with a CH Instruments electrochemical analyzer. All measurements were carried out at room temperature with a

conventional three-electrode configuration consisting of a glassy carbon working electrode, a platinum wire auxiliary, and a nonaqueous acetonitrile $Ag/AgNO_3$ reference electrode. The $E_{1/2}$ values were determined as $(E_p{}^a + E_p{}^c)/2$, where $E_p{}^a$ and $E_p{}^c$ are the anodic and cathodic peak potentials, respectively. The potential are quoted against ferrocene internal standard. The solvent in all experiments was dichloromethane and the supporting electrolyte was 0.1 M tetrabutylammonium hexafluorophosphate. Thermal studies such as TGA-DTA-DTG measurements were performed on Perkin-Elmer (Pyris Diamond) at heating rate of 10 °C/min under a nitrogen atmosphere.

2.2 Synthesis of the compounds

The compounds were synthesized as illustrated in Scheme 1. The starting materials required for the study, N^1-phenylbenzene-1,2-diamine,[51] 10-butyl-10H-phenothiazine,[53] 10-butyl-10H-phenothiazine-3-carbaldehyde,[53] 10-butyl-10H-phenothiazine-3,7-dicarbaldehyde[54] and 7-bromo-10-butyl-10H-phenothiazine-3-carbaldehyde[55]) were obtained by following the literature methods. All other chemicals and solvents were purchased from commercial source and used after prior purification by standard methods.

34
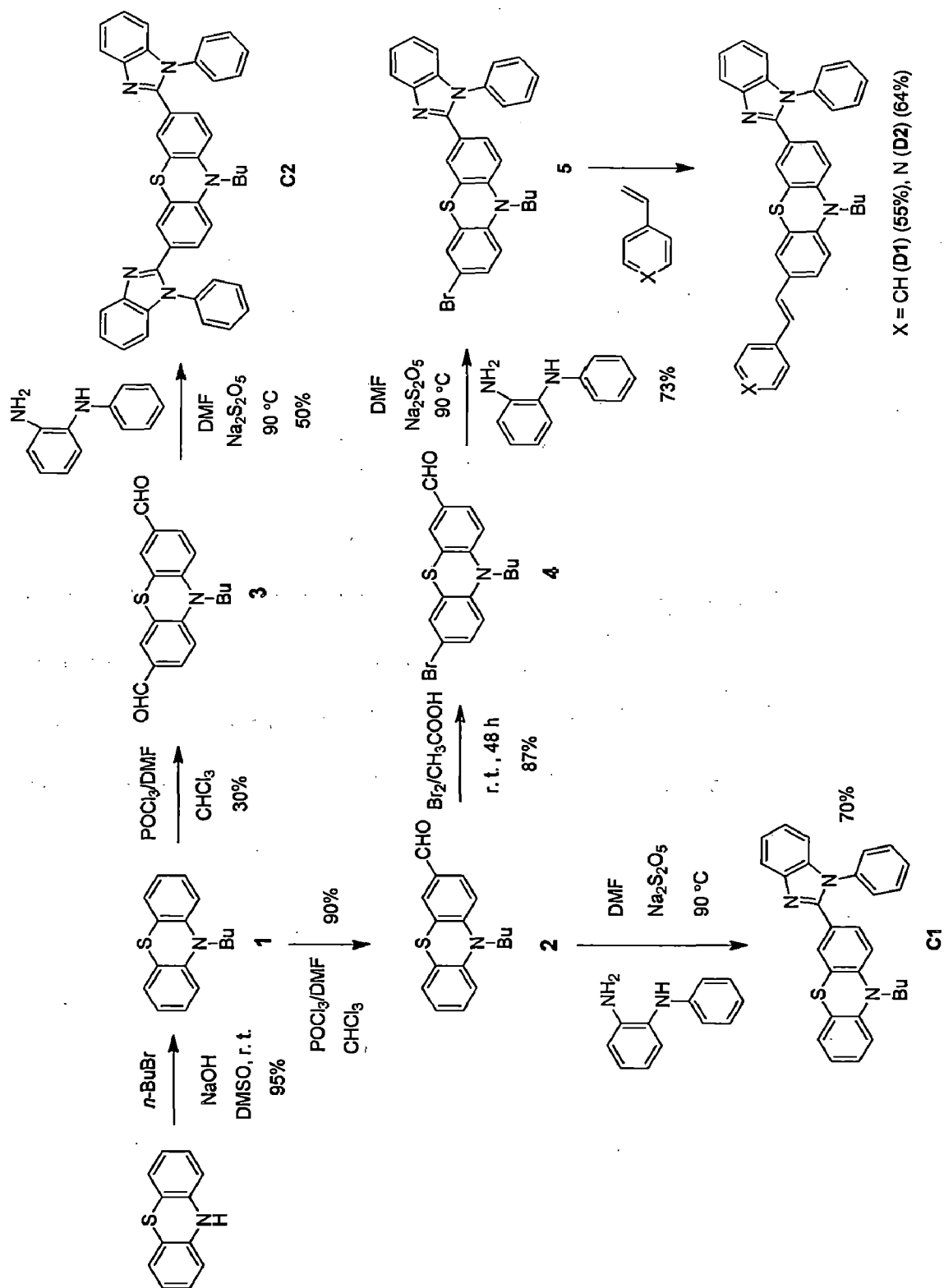
Scheme 1. Synthetic scheme for the compounds.

35

Synthesis of 10-butyl-3-(1-phenyl-1*H*-benzo[*d*]imidazol-2-yl)-10*H*-phenothiazine (C1)

A mixture of 10-butyl-10*H*-phenothiazine-3-carbaldehyde (2.83 g, 10 mmol), N^1-phenylbenzene-1,2-diamine (3.637 g, 13 mmol) and $Na_2S_2O_5$ (23.8 g, 20 mmol) in dimethyl formamide (10 mL) was taken in a round bottom flask and heated at 95 °C for 24 h. The progress of the reaction was monitored by TLC. After completion of reaction it was diluted with DCM, washed with water and brine solution respectively. Finally, the organic layer was separated, dried over anhydrous Na_2SO_4 and evaporated in a rotary evaporator to give a crude compound. It was finally purified by column chromatography on alumina by eluting with hexane/ethylacetate mixture. Yield: 70%. M.pt: 118-120 °C. ^{1}H NMR (CDCl$_3$, 500.13 MHz): δ 0.92 (t, $J = 7.5$ Hz, 3H), 1.39-1.47 (m, 2H), 1.71-1.79 (m, 2H), 3.80 (t, $J = 7.5$ Hz, 2H), 6.69 (d, $J = 8.5$ Hz, 1H), 6.3 (d, $J = 8.0$ Hz, 1H), 6.86-6.93 (m, 1H), 6.79 (dd, $J = 8.0$ Hz,1.5 Hz, 1H), 7.08-7.14 (m, 1H), 7.19-7.25 (m, 3H), 7.30-7.35 (m, 3H), 7.42-7.45 (m, 1H), 7.47-7.56 (m, 3H), 7.86 (d, $J = 8.0$ Hz, 1H); ^{13}C NMR (CDCl$_3$, 125.75 MHz): δ 13.8, 20.1, 28.8, 47.2, 110.2, 114.6, 115.4, 119.5, 122.7, 122.9, 123.0, 123.7, 124.2, 124.7, 127.2, 127.4, 127.5, 128.1, 128.3, 128.6, 129.9, 137.0, 137.3, 142.9, 144.4, 146.2, 151.6 ppm.

Synthesis of (*E*)-10-butyl-3-(1-phenyl-1*H*-benzo[*d*]imidazol-2-yl)-7-styryl-10*H*-phenothiazine (C2)

It was synthesized from N^1-phenylbenzene-1,2-diamine and 10-butyl-10*H*-phenothiazine-3,7-dicarbaldehyde by following the procedure described above for C1. M.pt: 266-269 °C. Yield: 73%. ^{1}H NMR (CDCl$_3$, 500.13 MHz): δ 0.94 (t, $J = 7.5$ Hz, 3H), 1.41-1.48 (m, 2H), 1.72-1.80 (m, 2H), 3.81 (t, $J = 7.5$ Hz, 2H), 6.69 (d, $J = 9$ Hz, 1H), 6.80 (d, $J = 9.0$ Hz, 1H), 6.86 (d, $J = 16.0$ Hz, 1H), 7.15 (d, $J = 16.0$ Hz, 1H), 7.19-7.24 (m, 4H), 7.31-7.37 (m, 6H), 7.43-7.47 (m, 1H), 7.48-7.57 (m, 4H), 7.86 (d, $J = 8.0$ Hz, 1H), 8.53-8.56 (m, 2H); ^{13}C NMR (CDCl$_3$, 125.75

MHz): δ 13.8, 20.1, 28.8, 47.3, 110.3, 114.5, 115.4, 119.6, 122.9, 123.1, 123.9, 124.2, 124.4, 124.9, 125.9, 126.3, 127.2, 127.3, 127.4, 127.5, 128.1, 128.4, 128.7, 129.9, 132.3, 137.1, 137.3, 143.0, 143.6, 145.8, 151.6 ppm.

Synthesis of 3-bromo-10-butyl-7-(1-phenyl-1H-benzo[d]imidazol-2-yl)-10H-phenothiazine (5)

It was synthesized from 7-bromo-10-butyl-10H-phenothiazine-3-carbaldehyde (4) and N^1-phenylbenzene-1,2-diamine by following the procedure described above for C1. Yield: 73%. ^{1}H NMR (CDCl$_3$, 500.13 MHz): δ 0.91 (t, J = 7.5 Hz, 3H), 1.37-1.45 (m, 2H), 1.68-1.75 (m, 2H), 3.75 (t, J = 7.5 Hz, 2H), 6.64-6.71 (m, 2H), 7.17-7.15 (m, 5H), 7.30-7.34 (m, 3H), 7.40-7.42 (m, 1H), 7.48-7.56 (m, 3H) 7.85 (d, J = 8 Hz, 1H).

Synthesis of (E)-10-butyl-3-(1-phenyl-1H-benzo[d]imidazol-2-yl)-7-styryl-10H-phenothiazine (D1)

A mixture of 3-bromo-10-butyl-7-(1-phenyl-1H-benzo[d]imidazol-2-yl)-10H-phenothiazine (4) (0.526 g, 1 mmol), styrene (0.2 mL, ~1.2 mmol) in DMF (8 mL) was taken in a pressure tube and nitrogen was passed through it. After the mixture was brought under nitrogen atmosphere, CH$_3$COONa (1.66 g, 20 mmol), (Bu)$_4$NBr (0.128 g, 0.4 mmol) and Pd(OAC)$_2$ (0.02 g, 0.04 mmol) were added and heated at 100 °C for 48 h. After completion of the reaction, it was poured into ice water and extracted with dichloromethane (3 x 20 mL). The combined organic layer was dried over anhydrous Na$_2$SO$_4$ and removal of volatile solvents from it afforded the crude product. It was purified by column chromatography on alumina using hexane/ethyl acetate mixture as eluant. Yield: 55%. M.pt: 135-137 °C. ^{1}H NMR (CDCl$_3$, 500.13 MHz): δ 0.94 (t, J = 7.5 Hz, 3H), 1.41-1.48 (m, 2H), 1.72-1.80 (m, 2H), 3.81 (t, J = 7.5 Hz, 2H), 6.69 (d, J = 9 Hz, 1H), 6.80 (d, J = 9.0 Hz, 1H), 6.86 (d, J = 16.0 Hz, 1H), 7.15 (d, J = 16.0 Hz, 1H), 7.19-7.24 (m,

4H), 7.31-7.37 (m, 6H), 7.43-7.47 (m, 1H), 7.48-7.57 (m, 4H), 7.86 (d, J = 8.0 Hz, 1H), 8.53-8.56 (m, 2H); ^{13}C NMR (CDCl$_3$, 125.75 MHz): δ 13.8, 20.1, 28.8, 47.3, 110.3, 114.5, 115.4, 119.6, 122.9, 123.1, 123.9, 124.2, 124.4, 124.9, 125.9, 126.3, 127.2, 127.3, 127.4, 127.5, 128.1, 128.4, 128.7, 129.9, 132.3, 137.1, 137.3, 143.0, 143.6, 145.8, 151.6 ppm.

Synthesis of (*E*)-10-butyl-3-(1-phenyl-1*H*-benzo[*d*]imidazol-2-yl)-7-(2-(pyridin-4-yl)vinyl)-10*H*-phenothiazine (D2)

It was obtained in 64% yield from 4-vinyl pyridine and 3-bromo-10-butyl-7-(1-phenyl-1*H*-benzo[*d*]imidazol-2-yl)-10*H*-phenothiazine (4) by following a procedure as described above for D1. M.pt: 125-128 °C. ^{1}H NMR (CDCl$_3$, 500.13 MHz): δ 0.94 (t, J = 7.5 Hz, 3H), 1.40-1.48 (m, 2H), 1.72-1.80 (m, 2H), 3.81 (t, J = 7.0 Hz, 2H), 6.69 (d, J = 8.5 Hz, 1H), 6.79 (d, J = 9.0 Hz, 1H), 6.96 (s, 1H), 7.18-7.25 (m, 5H), 7.30-7.36 (m, 6H), 7.39-7.56 (m, 6H), 7.86 (d, J = 8 Hz, 1H); ^{13}C NMR (CDCl$_3$, 125.75 MHz): δ 13.7, 20.0, 28.7, 47.4, 110.3, 114.6, 115.4, 120.0, 123.0, 123.2, 124.0, 124.1, 124.4, 124.6, 125.3, 126.6, 127.5, 128.1, 128.4, 128.7, 128.0, 130.9, 131.7, 137.3, 142.9, 144.7, 145.5, 150.1, 151.4 ppm.

Chapter 3

Photophysical and electrochemical characteristics

of phenothiazine-benzimidazole hybrids

3.1 Introduction

π-Conjugated donor-acceptor (D-A) molecules have been extensively studied due to their potential applications in electronics and optoeletronics, such as organic light-emitting devices (OLEDs),[56-58] nonlinear optics,[59,60] electrogenerated chemiluminescence (ECL),[61] photovoltaic cells,[62] and fluorescent sensors.[63] The unique structure of D-A molecules permits the alternation of optical and electrochemical properties by slight variation in structure by appropriate chemical modification to the donor and/or acceptor moieties. Donor-acceptor compounds were also synthesized to unravel the electronic interaction between them to establish the structure-property relationship of those molecules. In this report we present the syntheses of two series molecules whose structures are in donor-acceptor (D-A) configuration featuring phenothiazine as the donor and benzimidazole as acceptor. Additional groups such as styrene and ethenylpyridine units have been used to extend the π-conjugation of the phenothiazine nucleus. We describe herein the optical, electrochemical and thermal characteristics of the newly synthesized functional materials.

3.2 Synthesis and characterization

The most popular synthetic method for preparation of benzimidazoles is the condensation 1,2-diaminoarenes with a carbonyl equivalent such as aldehyde or carboxylic acid (Scheme 1). When the carbonyl equivalent is carboxylic acid the reaction requires strongly acidic conditions and sometimes very high temperatures. This condensation between the 1,2-diaminoarene and carboxylic acid in acidic conditions is often termed as Philips condensation.
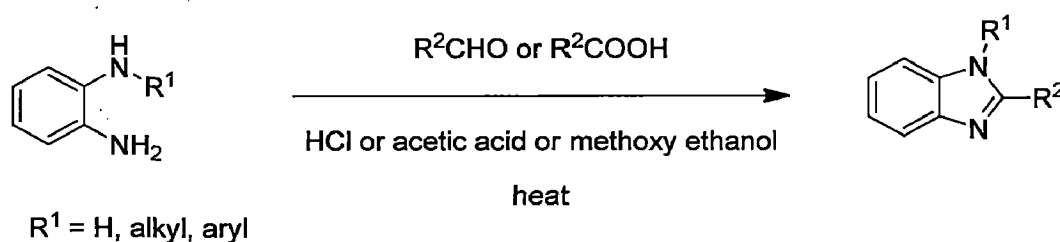

Scheme 1. Synthesis of benzimidazoles from 1,2-diamine and carbonyl compounds.

Use of aldehyde as carbonyl equivalent requires a stoichiometric oxidant for dehydration during the formation of benzimidazoles from the anil formed in the first step. The conditions which they were used are not fully compatible with a broad range of functional groups and substrates. Also the reactions by both precursors produce side products such as regioisomers and disubstituted products from the 1,2-diaminoarene. In 2008, Driver's group reported the $FeBr_2$-catalyzed synthesis of benzimidazole from 2-azidoaniline and achieved good yield (Scheme 2).

Scheme 2. Synthesis of benzimidazoles from o-nitroanilines and o-haloanlines.

Copper-catalyzed, three components coupling of 2-bromoaldehyde, primary amines, and sodium azide has recently been reported to construct $2H$-indazoles in high yields by this group. Recently, Yang et al. reported the synthesis of 2-substiuted benzimidazoles by a one step reaction with $Na_2S_2O_4$ used as a reducing agent. They were synthesized benzimidazoles from o-nitro anilines in the presence of hetero aldehydes and DMSO used as a solvent at 120 °C. This method eliminates the reduction of o-nitroanilines to 1,2-diamines. Using this method, 1,2-diamines or N-alkyl(aryl)-1,2-diamines can also be converted to the corresponding substituted benzimidazoles.

Scheme 3. Synthesis of benzimidazoles from o-nitroanilines.

We have synthesized the benzimidazole derivatives containing phenothiazine chromophores by reacting phenothiazine carboxaldehydes with N^1-phenylbenzene-1,2-diamine as illustrated in Scheme 4.

R = H (2), CHO (3), Br (4)

R = H (C1), Br (5)

R = (C1)
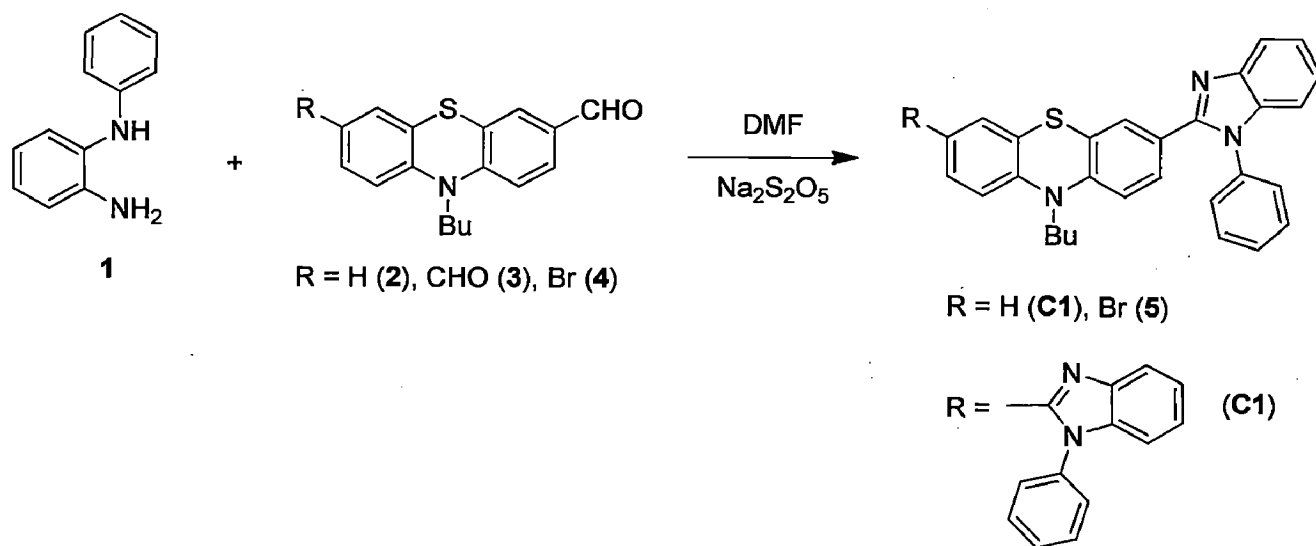
Scheme 4. Synthesis of phenothiazine-based benzimidazoles.

R = (D1)

R = (D2)
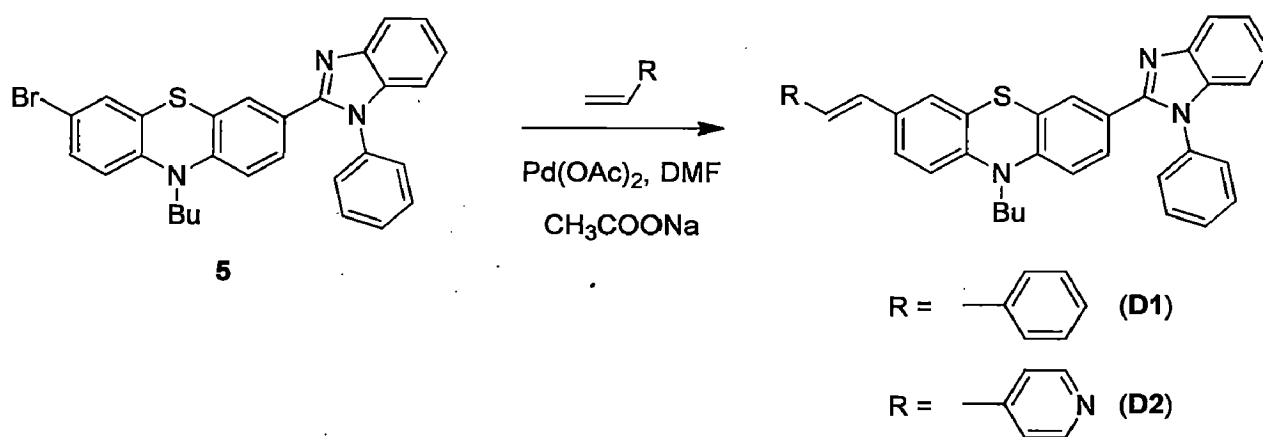
Scheme 5. Synthesis of styryl and vinylpyridine derivatives **D1** and **D2**.

The bromo derivative **5** served as a starting material for the functional compounds **D1** and **D2**. Aryl halides can be converted to polynuclear aromatic compounds by C-C coupling reactions, to arylamines by C-N coupling reactions, to substituted acetylene derivatives by Sonogashira

coupling reactions and to substituted alkenes by Heck coupling reactions. Using this literature knowledge we have first performed Heck coupling reactions on **5** with styrene and 4-vinylpyridine to obtain the derivatives **D1** and **D2**. The reactions went as expected and produced the compounds in reasonable yields (Scheme 5).

All the compounds are thoroughly soluble in common organic solvents such as toluene, dichloromethane, tetrahydrofuran, acetonitrile, etc. They showed intense yellow color in the solid state and as solutions. The structural compositions of the compounds were established by routine ^{1}H and ^{13}C NMR spectral measurements (see Chapter 2).
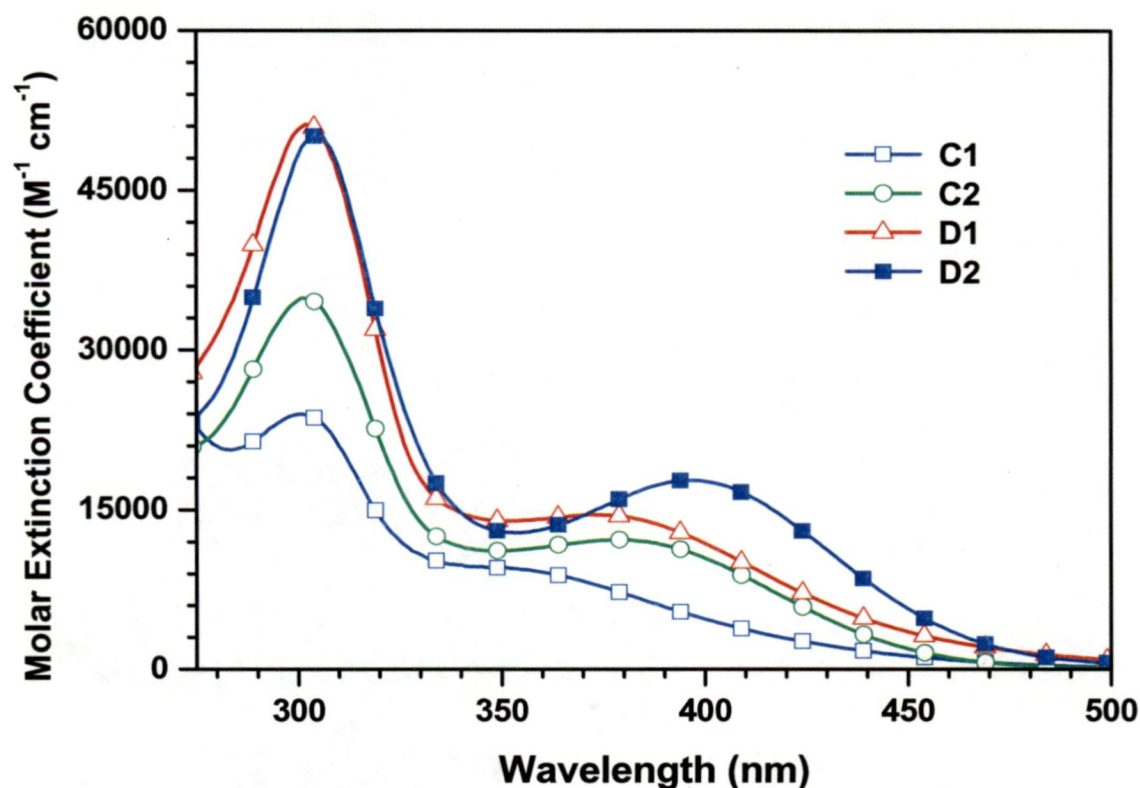

Figure 1. Absorption spectra of the compounds recorded in dichloromethane

3.3 Photophysical properties

The absorption spectra of the compounds **C1**, **C2**, **D1** and **D2** recorded in dichloromethane are displayed in Figure 1 and the pertinent data are compiled in Table 1. All the compounds

exhibited two absorption bands peaking at ~300 nm and >350 nm respectively. The shorter wavelength absorption corresponds to the electronic excitation originating from the phenothiazine localized π-π^* transition. The parent phenothiazine (*Eur. J. Org. Chem.* **2006**, 423-435) itself exhibited a strong absorption at 301 nm. Though the peak position of this band remained unaltered for all the compounds their intensity increased on introduction of additional chromophores on phenothiazine nucleus. The molar coefficient of this band followed the order: **C1 < C2 < D1 < D2**. This is in keeping with the extension of conjugation occurred in the molecules on inclusion of additional chromophores. The longer wavelength absorption is attributed to the delocalized π-π^* transition. Among the benzimidazoles **C1** and **C2**, **C2** exhibited red-shifted absorption and among **D1** and **D2**, **D2** displayed the longest wavelength absorption maxima (396 nm). The longest wavelength absorption for the dibenzimidazole derivative **C2** is 30 nm red-shifted when compared to the monobenzimidazole derivative **C1**.

Table 1. Photophysical properties of the compounds in dichloromethane

Dye	λ_{max}, nm (ε_{max}, $\times$ 10^4 M^{-1} cm^{-1})	λ_{em}, nm (Φ_F, %)	Stokes shift, cm^{-1}
C1	301 (23.93), 350 (9.53)	488	8080
C2	301 (34.85), 380 (12.15)	495	6114
D1	302 (51.13), 372 (14.50)	501	6922
D2	306 (50.09), 396 (17.71)	545	6904

The delocalized absorption of **D2** is red-shifted by 24 nm when compared to the corresponding peak observed for **D1**. At the same time this peak for **D1** is slightly blue shifted in comparison to **C2**. It appears that the styryl unit is inferior to benzimidazoles as it is a neutral chromophore. On the contrary the electron-withdrawing nature of benzimidazoles renders a

donor-acceptor nature to the molecule **C2**. Similarly, pyridine being a reasonable electron-accepting moiety introduces a strong donor-acceptor interaction and consequently red-shifts the absorption on comparison to **D1**.

Since the molecules displayed some donor-acceptor character, to identify the nature of interaction between the fragments absorption spectra of the compounds were also measured in solvents of different polarity. The absorption spectra of the compounds recorded in different solvents are displayed in Figures 2-5 and the relevant data are collected in Table 2. The absorption positions of the compounds remained unaltered on changing the solvent polarity. This indicates that the donor-acceptor interactions in the molecules are very minimal and the variations in absorption observed for the compounds are mainly due to the changes in the π-conjugation.
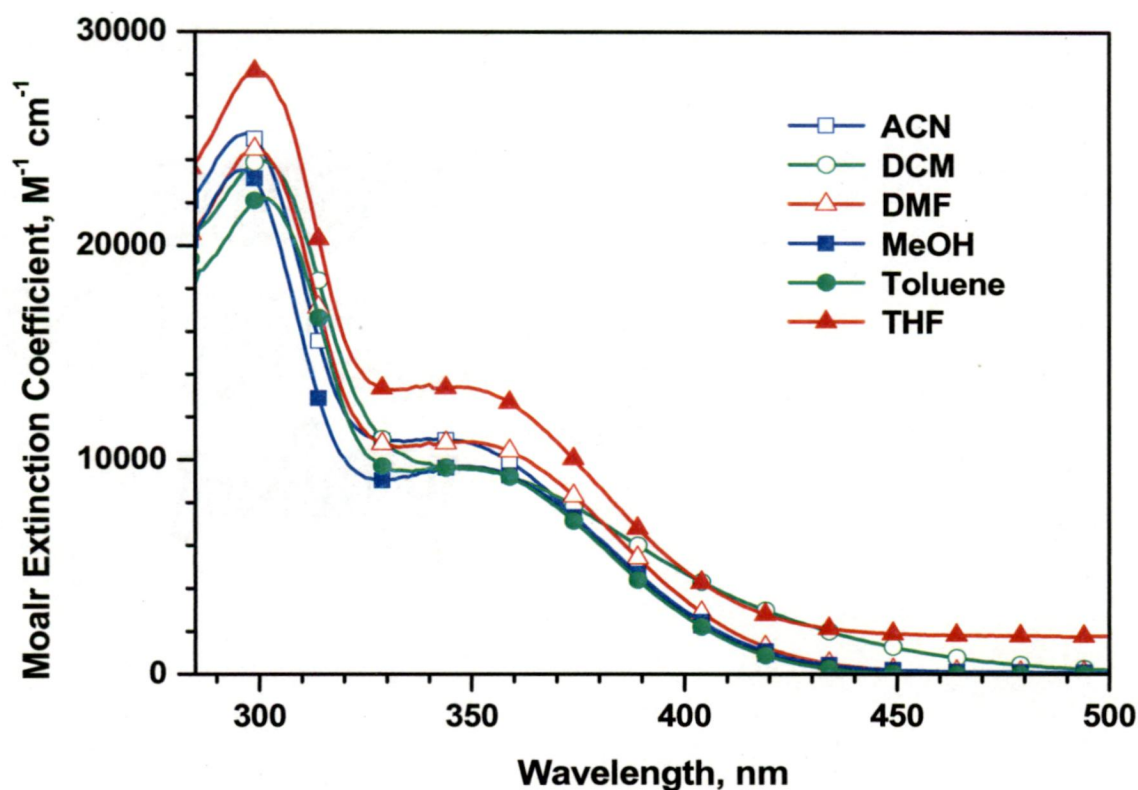

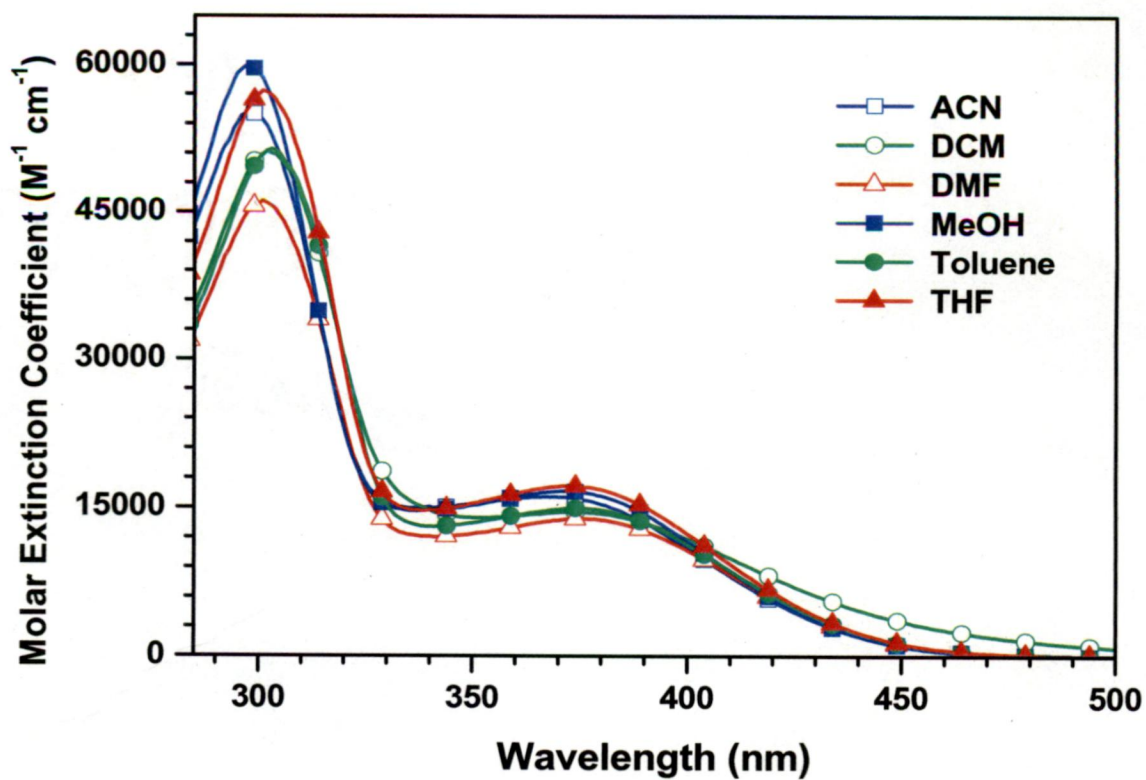**Figure 2**. Absorption spectra of **C1** recorded in different solvents.

Figure 3. Absorption spectra of **C2** recorded in different solvents.
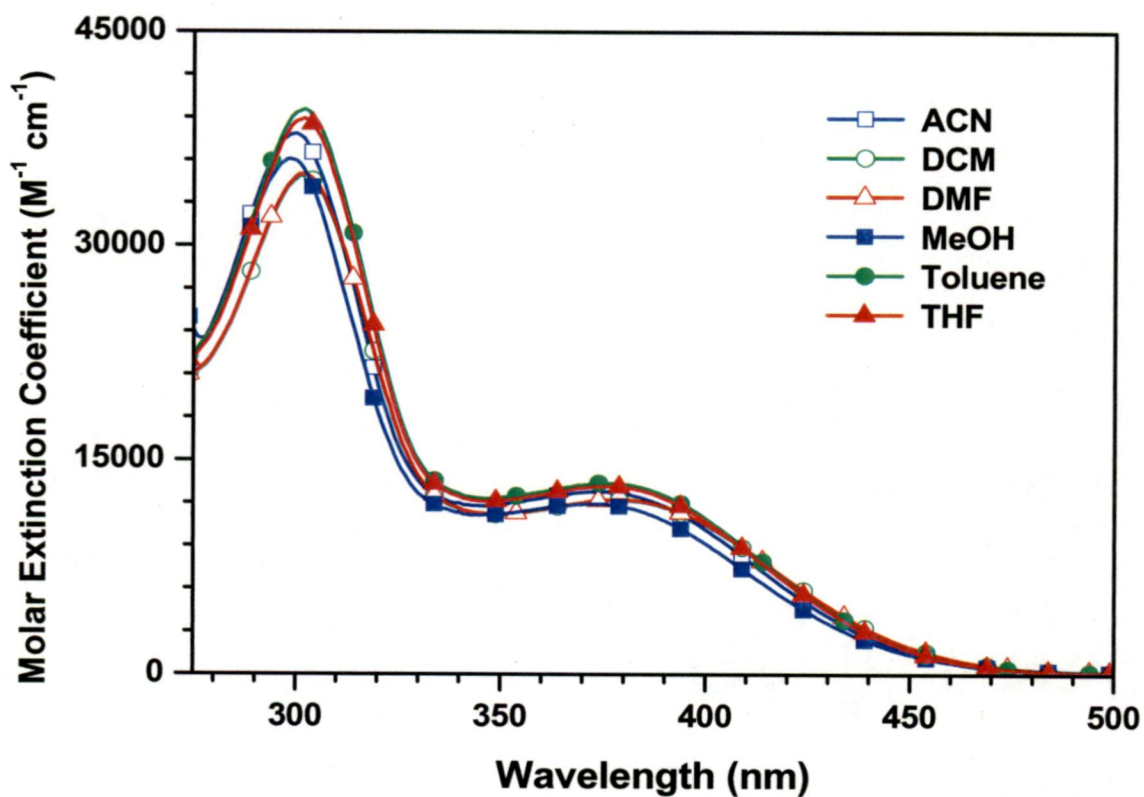

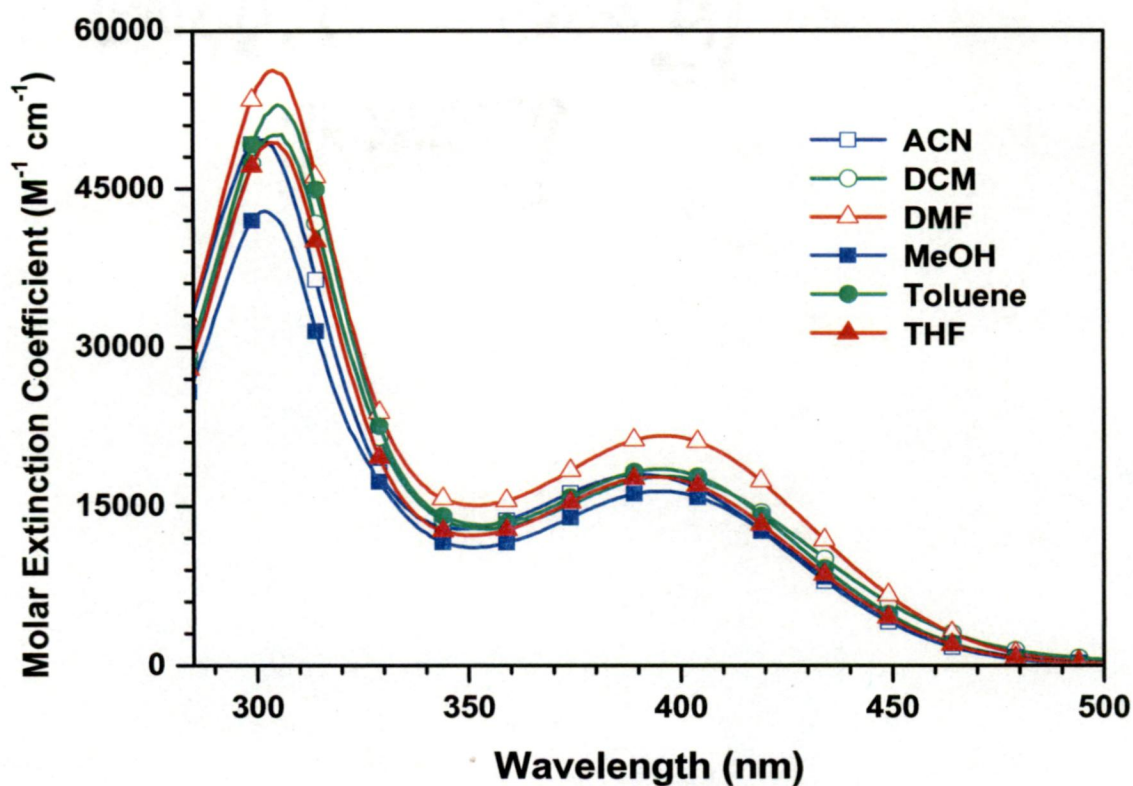**Figure 4**. Absorption spectra of **D1** recorded in different solvents.

Figure 5. Absorption spectra of **D2** recorded in different solvents.

The emission properties of the compounds were examined in dichloromethane by measuring fluorescence spectra (Figure 6). All the compounds showed a structureless emission profile. The emission maxima of the compounds exhibited the trend: **C1 < C2 < D1 < D2** similar to the absorption peak positions observed for them (Table 1). The compound **C1** showed large Stokes shift when compared to the other disubstituted phenothiazine derivatives (**C2**, **D1** and **D2**) indicating a significant structural change in the excited state for the former.

In contrast to the absorption spectra, the fluorescence spectra of all the compounds displayed a positive solvatochromism. The emission spectra recorded for the compounds in different solvents are displayed in Figures 7-10 and the important emission parameters are listed in Table 2. Pronounced solvatochromism was observed for the monobenzimidazole derivative, **C1** and the pyridine derivative, **D2**.

Table 2. Photophysical properties of the compounds in different solvents.

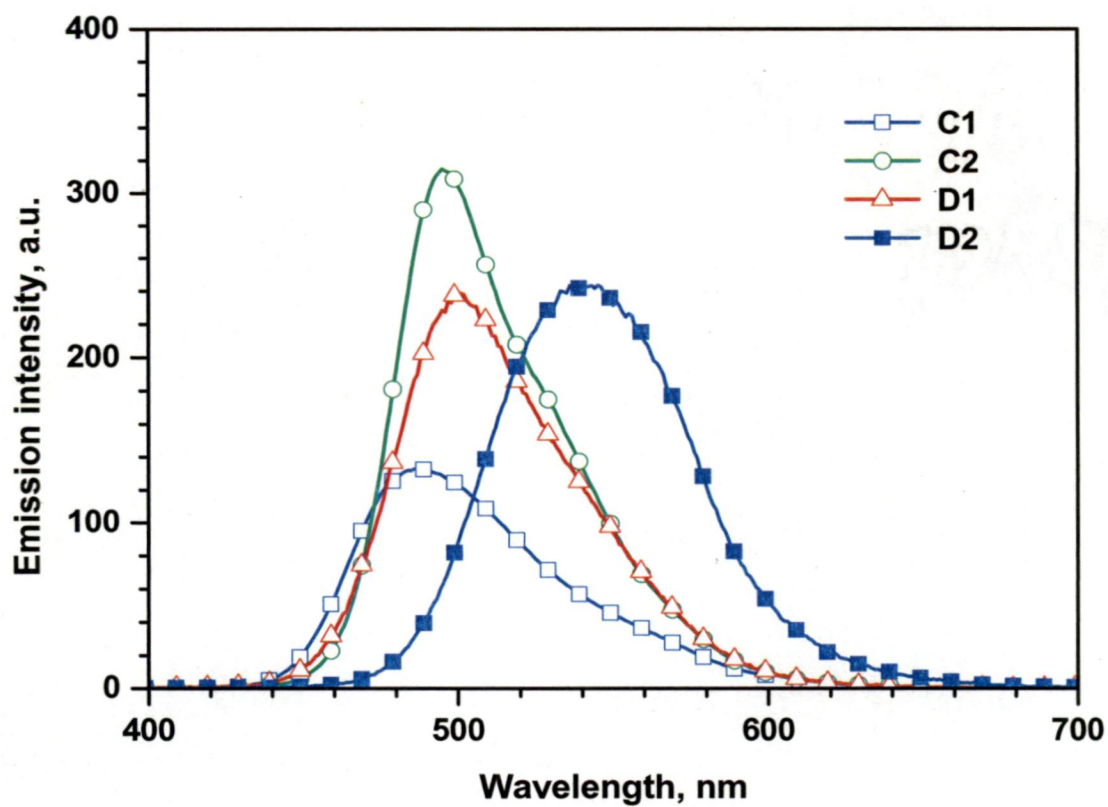| Dye	λ_{max}, nm (ε_{max}, × 10³ M⁻¹ cm⁻¹)					λ_{em}, nm (Φ_F, %)					Stokes shift, cm⁻¹				
	Toluene	THF	ACN	DMF	MeOH	Toluene	THF	ACN	DMF	MeOH	Toluene	THF	ACN	DMF	MeOH
C1	300 (22.20), 348 (9.62)	299 (28.11), 340 (13.48)	297 (25.21), 344 (10.90)	300 (24.49), 348 (10.81)	296, (23.48), 347 (9.66)	471	478	492	491	501	7504	8491	8745	8369	8858
C2	303 (51.38), 373 (14.87)	301 (57.26), 371 (17.12)	298 (55.09), 369 (16.05)	301 (46.10), 375 (13.81)	298 (59.90), 371 (16.60)	492	490	497	497	499	6485	6546	6980	6546	6914
D1	302 (39.45), 374 (13.33)	302 (38.85), 374 (13.12)	300 (37.80), 374 (12.74)	301 (34.95), 380 (12.18)	298 (36.01), 371 (11.88)	496	496	500	504	505	6577	6577	6738	6475	7152
D2	305 (52.90), 395 (18.42)	303 (49.33), 393 (17.68)	301 (49.61), 391 (17.90)	304 (56.19), 397 (21.54)	302 (42.85), 395 (16.33)	514	525	547	546	550	5861	6398	7294	6874	7135

Figure 6. Emission spectra of the compounds recorded in dichloromethane.
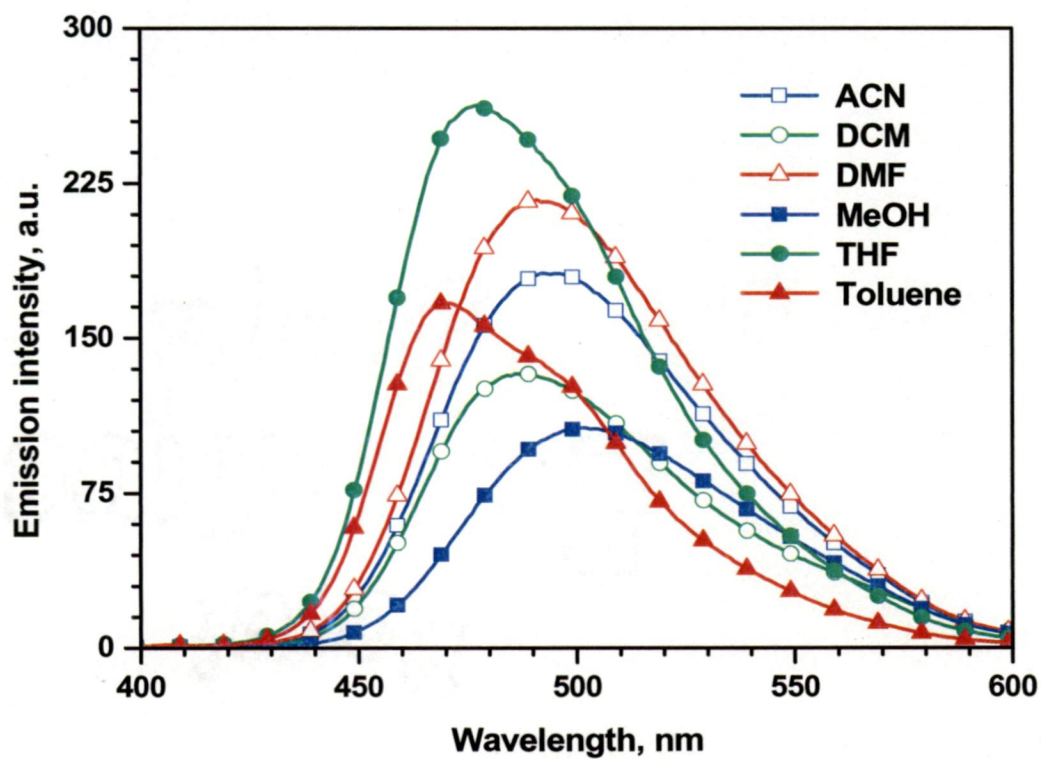

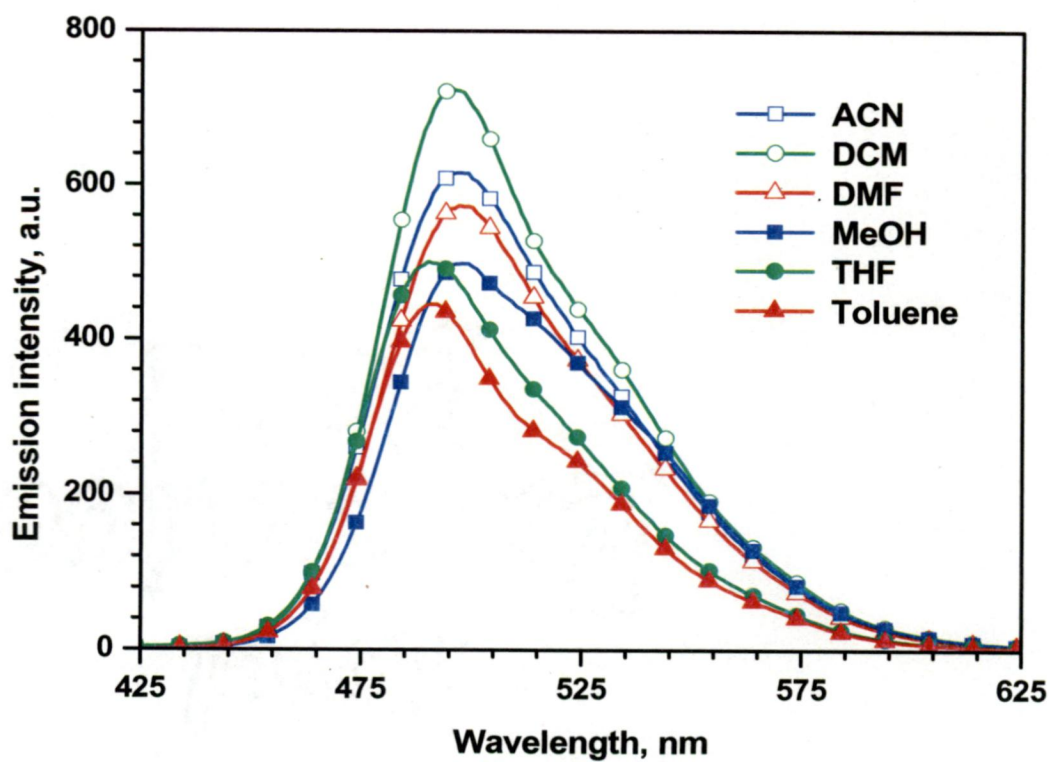**Figure 7.** Emission spectra of **C1** recorded in different solvents.

49

Figure 8. Emission spectra of **C2** recorded in different solvents.
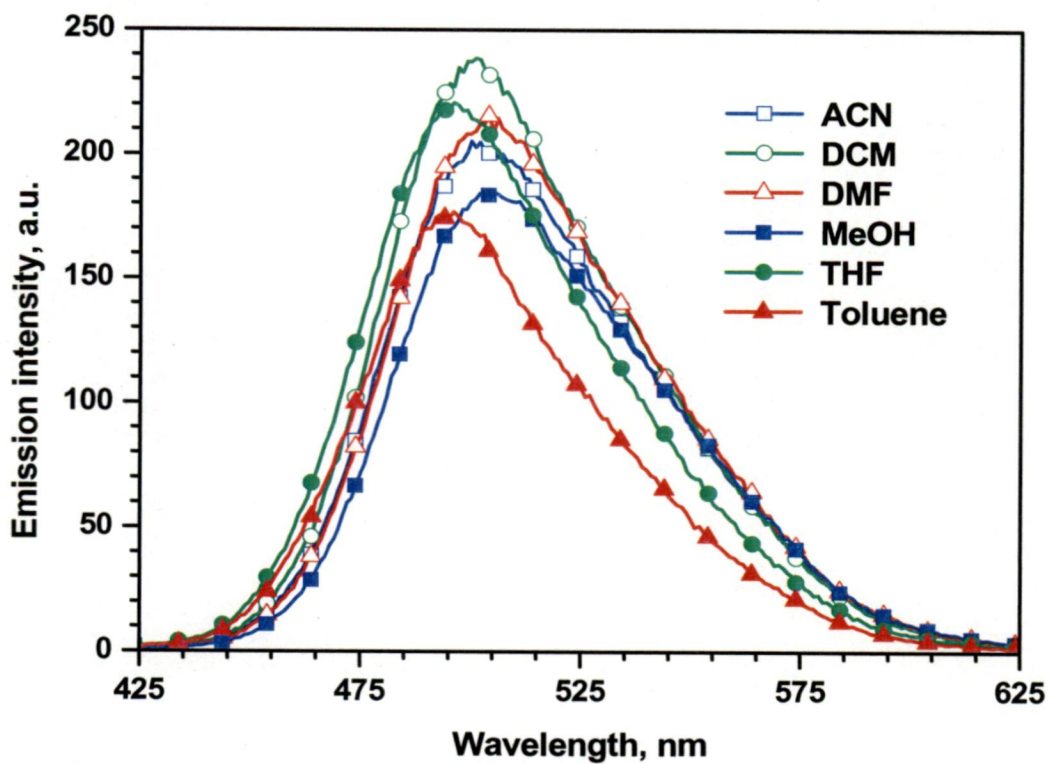

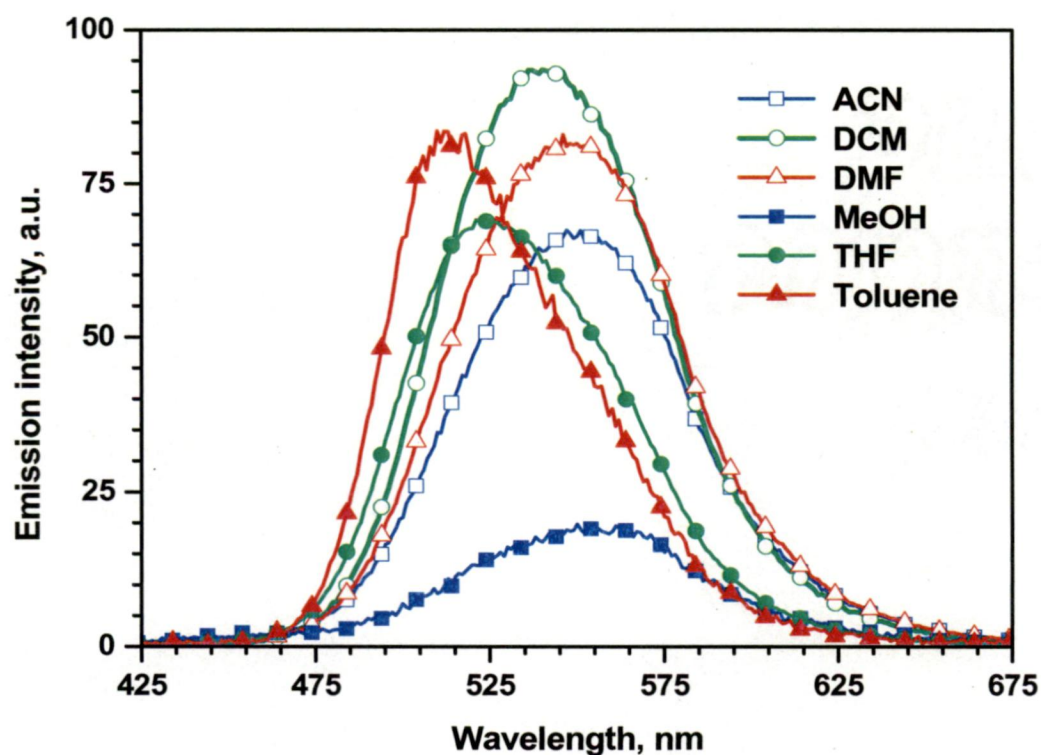**Figure 9**. Emission spectra of **D1** recorded in different solvents.

Figure 10. Emission spectra of **D2** recorded in different solvents.

Most red-shifted emission was observed for methanol solutions. A maximum red shift of 30 nm and 36 nm were observed for **C1** and **D2** respectively in methanol when compared to the spectra recorded in toluene. It appears that the dyes are more stabilized in highly polar solvent such as methanol, acetonitrile and dimethylformamide. It might arise due to the preferential solvation of the dyes in polar solvents. If the donor-acceptor interactions alone are important to stabilize the molecules in polar solvents, the dibenzimidazole derivative, **C2** should also show large solvatochromic shifts as it contains two electron-accepting benzimidazole moieties. Absence of such behavior by **C2** indicates that the hydrophobic structure of **C2** and **D1** retard the effective association of the dye molecules by polar solvents. Interestingly, the bathochromic shifts observed in **C1** and **D2** were accompanied by significant broadening of the emission band, which is the characteristic of charge transfer transition. We attribute this large solvatochromic effect to the large induced dipole moment at the excited state generated by the charge transfer

51

from the electron donating phenothiazine core to the electron withdrawing benzimidazole subunit in **C1** and to pyridine also in **D2**. It is interesting that the introduction of addition chromophore (benzimidazole/styryl/vinylpyridine) at the phenothiazine chromophore produced a red-shift in the emission 7-57 nm (Table 1). It suggests a simpler pathway to tune the excited state properties of phenothiazine chromophore.

The solvatochromic data for the dyes were examined for correlations between absorption and emission properties with the solvent parameters such as orientation polarizability and $E_T(30)$ parameter. It has been noticed that the highly solvatochromic compounds **C1** and **D2** exhibited quite good correlation with these parameters (Figure 11 and 12). This suggest that general solvation effect and dipole interactions of predominant in the dye-solvent interactions.
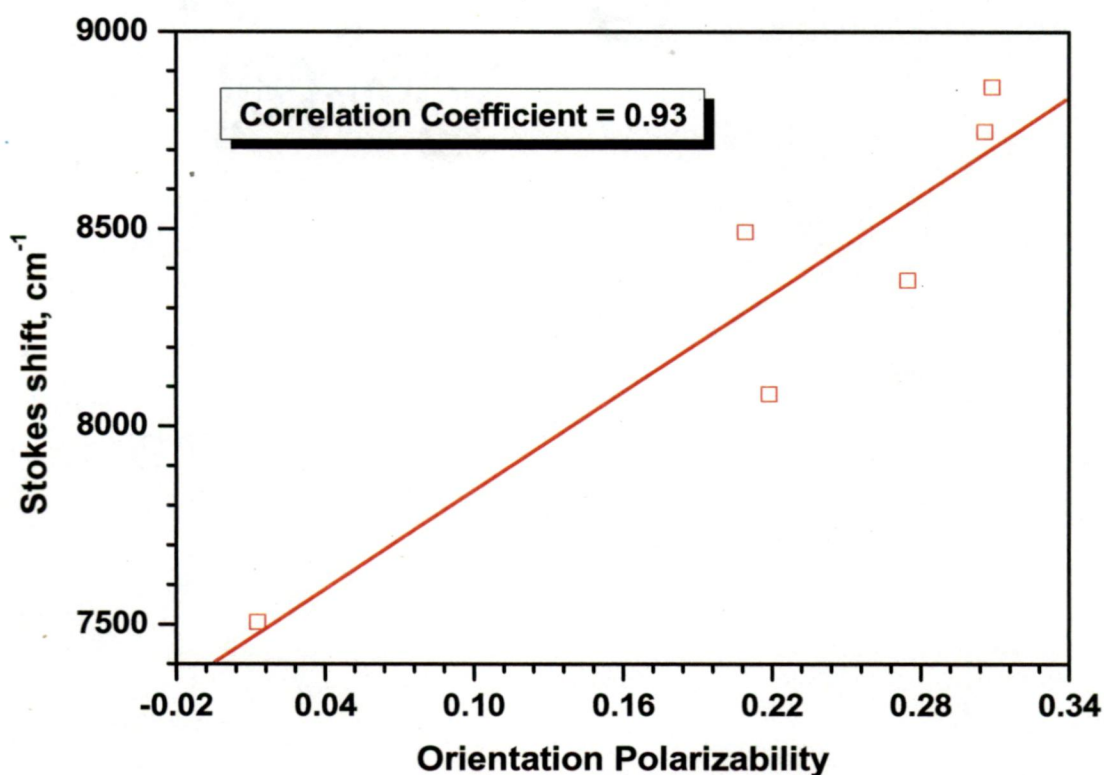

Figure 11. Lippert-Mataga plot for **C1**.

52

Supporting Information

Table of Contents

Figure S1. ^{1}H NMR spectrum of **2** recorded in CDCl$_3$.

0.951
0.981
1.446
1.460
1.475
1.490
1.505
1.520
1.784
1.799
1.814
1.828
1.843

3.926
3.940
3.955

7.580
7.584
7.654
7.657
7.670
7.674

9.839

3.00
2.19
2.12
2.03
2.05
2.01
2.17
1.96

ppm
1 2 3 4 5 6 7 8 9 10 11
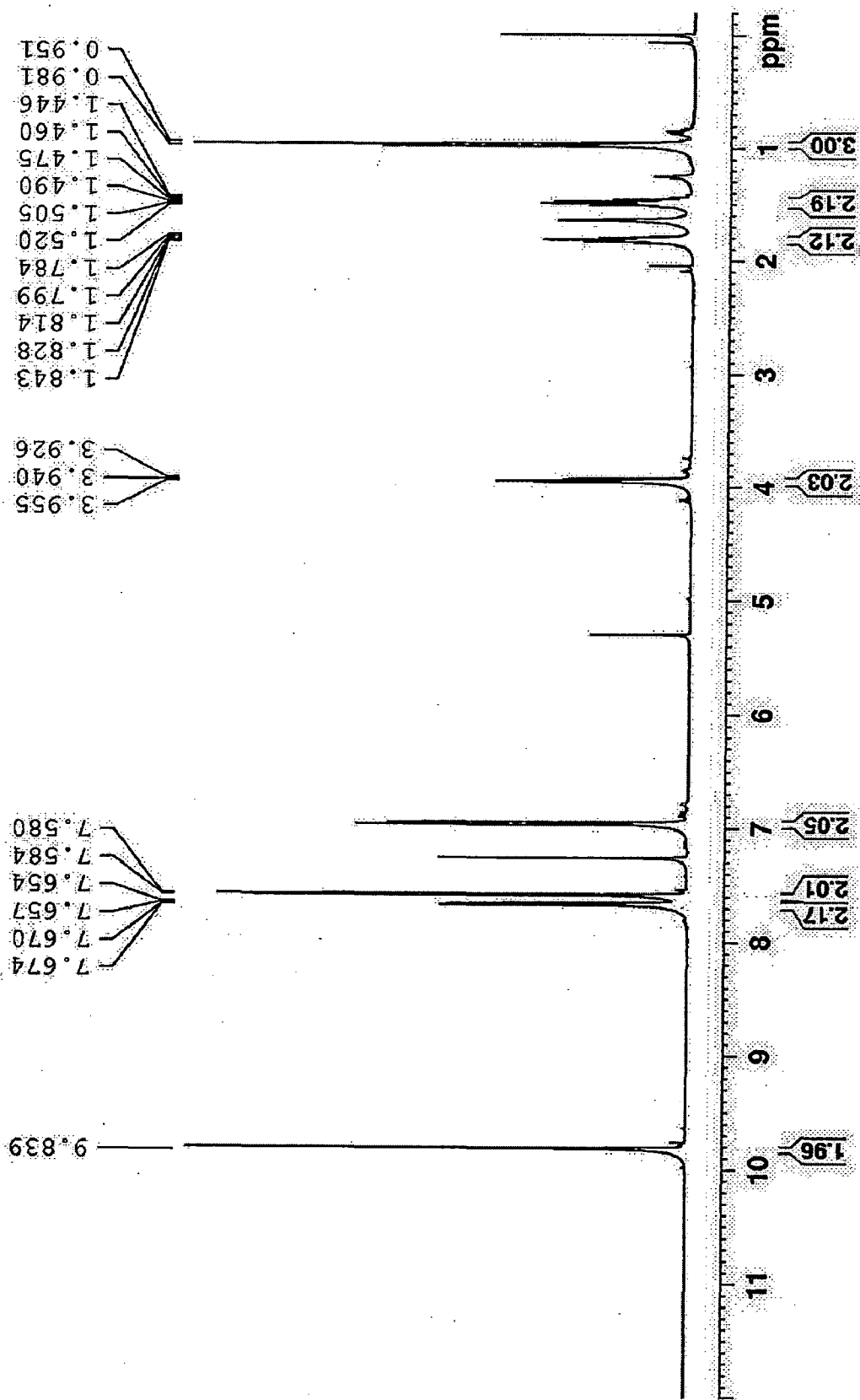
Figure S2. ^{1}H NMR spectrum of **3** recorded in CDCl$_3$.
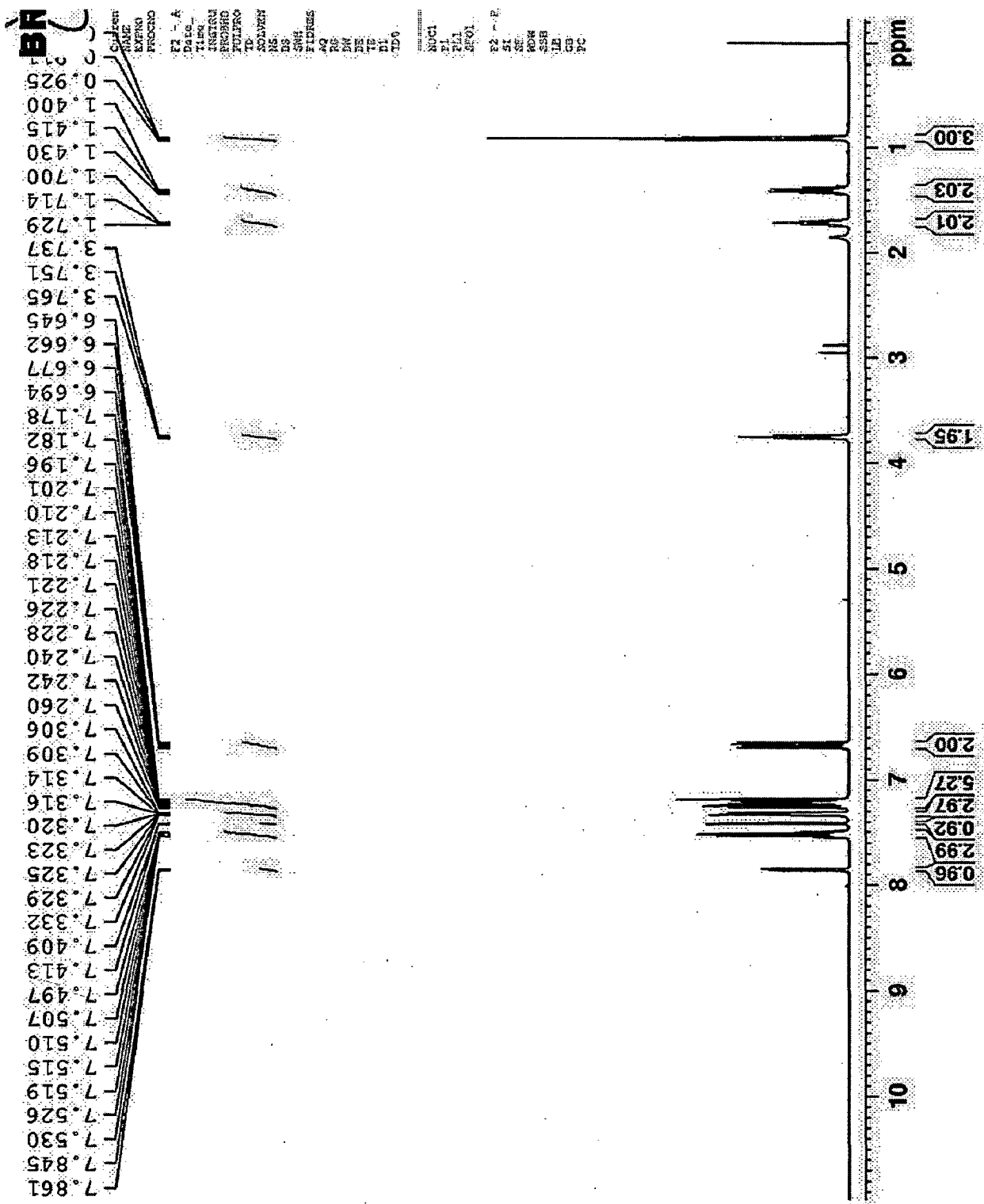
Figure S3. ^{1}H NMR spectrum of **5** recorded in CDCl$_3$.

0.909
0.924
0.939
1.421
1.436
1.451
1.736
1.750
1.765
3.784
3.799
3.813
6.685
6.702
6.818
6.834
6.901
6.903
6.916
7.069
7.072
7.085
7.088
7.128
7.209
7.211
7.222
7.235
7.238
7.321
7.323
7.329
7.334
7.337
7.434
7.439
7.490
7.501
7.504
7.506
7.511
7.523
7.527
7.540
7.851
7.867

3.14
2.17
2.09
2.00
0.89
0.96
1.07
0.98
1.12
3.21
2.98
0.74
3.06
0.90

ppm
0.5 1.0 1.5 2.0 2.5 3.0 3.5 4.0 4.5 5.0 5.5 6.0 6.5 7.0 7.5 8.0 8.5
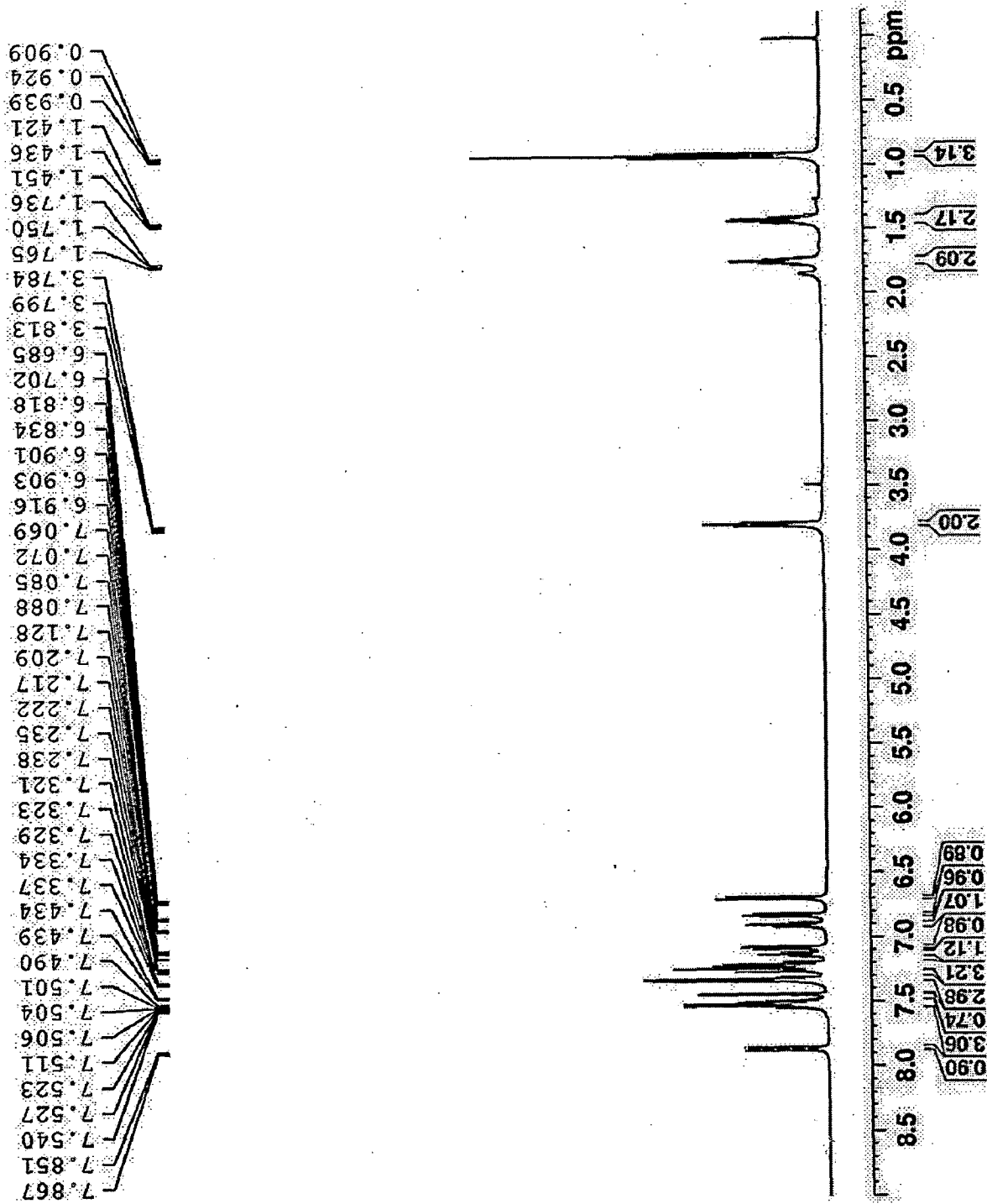
Figure S4. ^{1}H NMR spectrum of C1 recorded in $CDCl_3$.

72
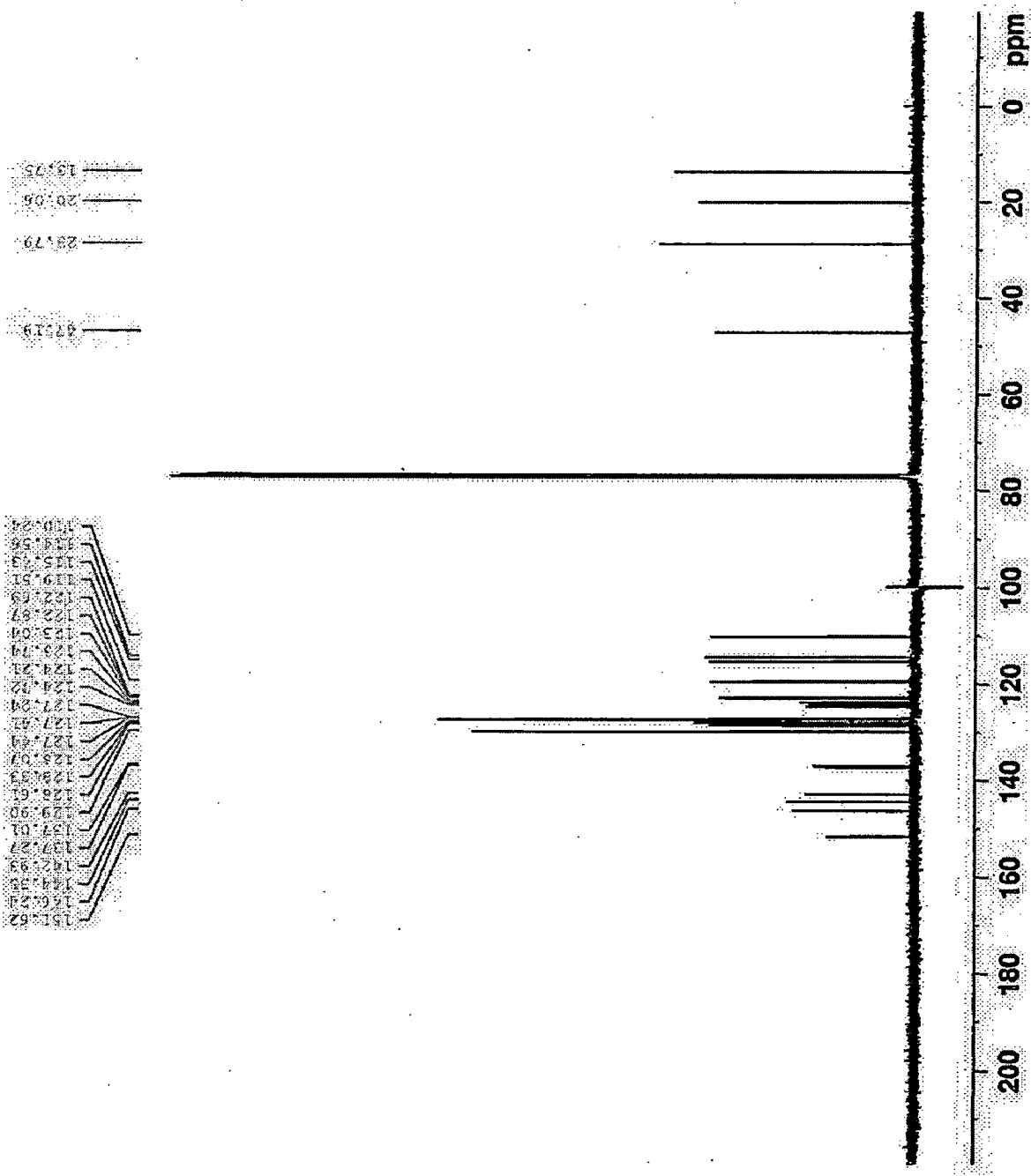
Figure S5. ^{13}C NMR spectrum of C1 recorded in CDCl$_3$.

0.894
0.909
0.924
1.365
1.380
1.395
1.410
1.425
1.440
1.697
1.714
1.729
1.744

3.740
3.755
3.769

6.663
6.680
7.192
7.207
7.225
7.229
7.239
7.241
7.304
7.306
7.311
7.492
7.495
7.506
7.508
7.513
7.517
7.523
7.532
7.537

3.17
2.20
2.06
2.00
1.92
5.08
8.16
6.64
2.01

ppm

0.5 1.0 1.5 2.0 2.5 3.0 3.5 4.0 4.5 5.0 5.5 6.0 6.5 7.0 7.5 8.0 8.5
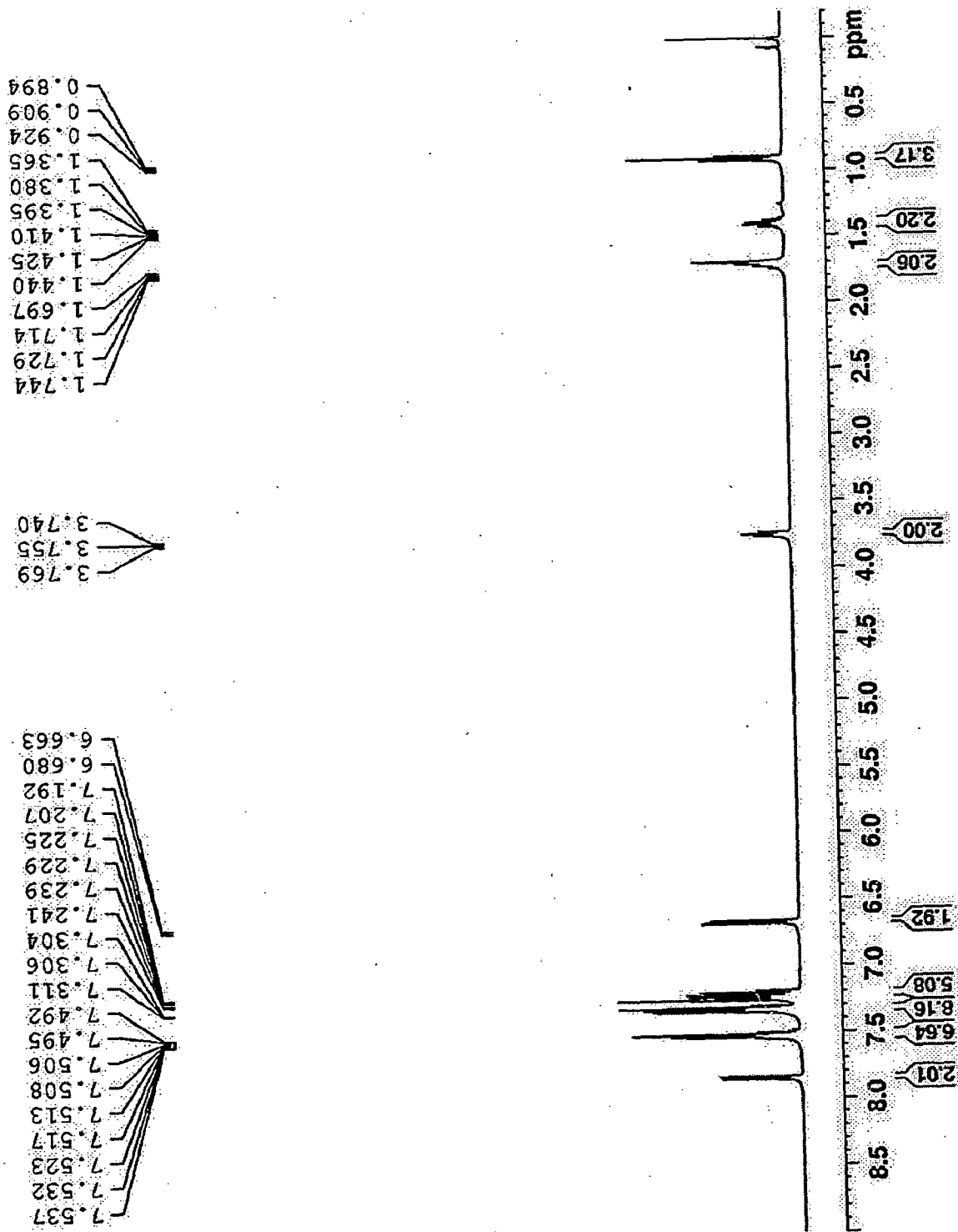
Figure S6. ^{1}H NMR spectrum of C2 recorded in CDCl$_3$.

13.73
20.00
28.65

47.37

110.29
114.73
119.57
122.94
123.14
124.13
124.24
127.44
128.07
128.41
128.72
129.96
136.95
137.29
142.92
145.30
151.39

ppm

20

40

60

80

100

120

140

160

180

200
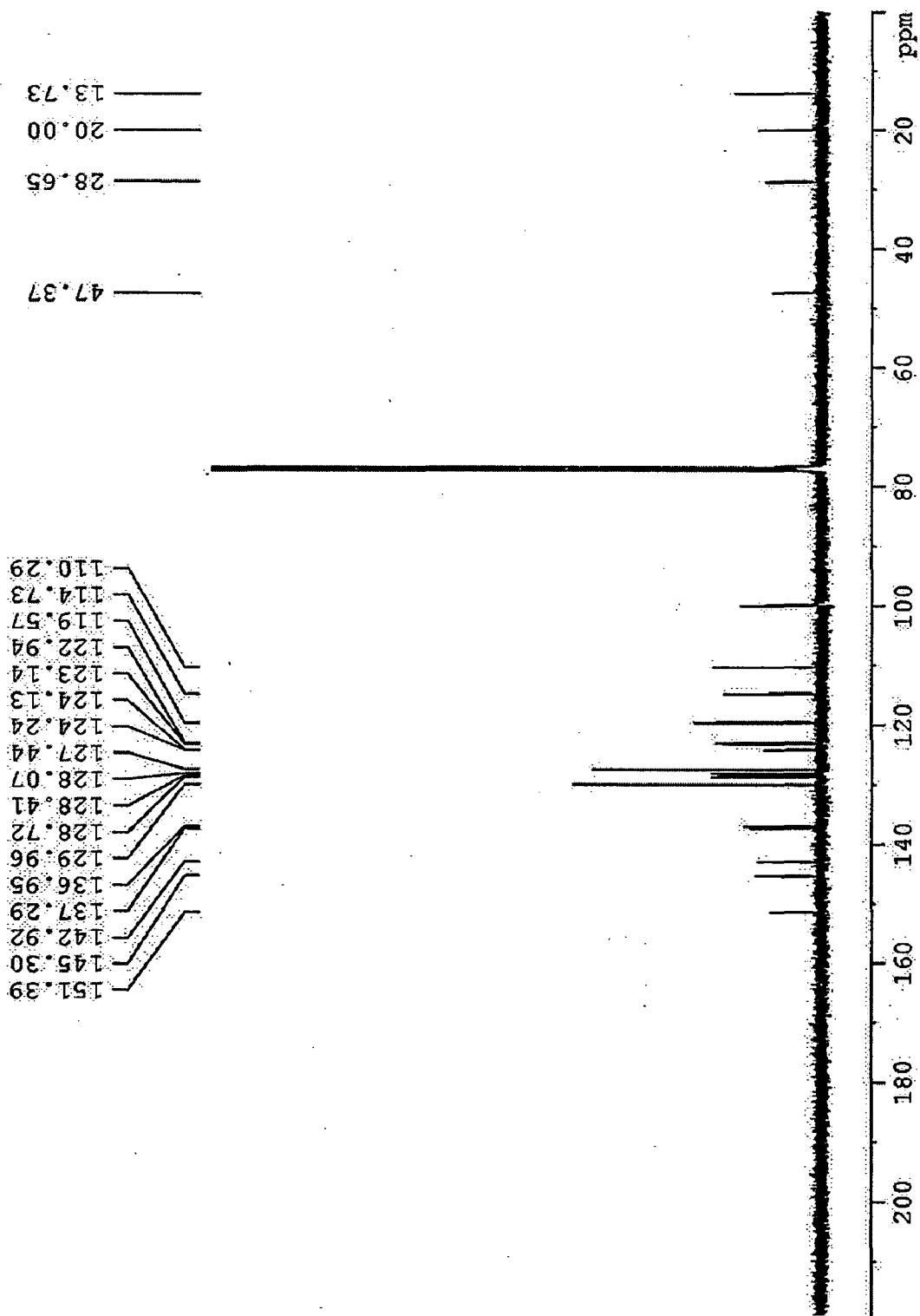
Figure S7. ^{13}C NMR spectrum of **C2** recorded in CDCl$_3$.

75
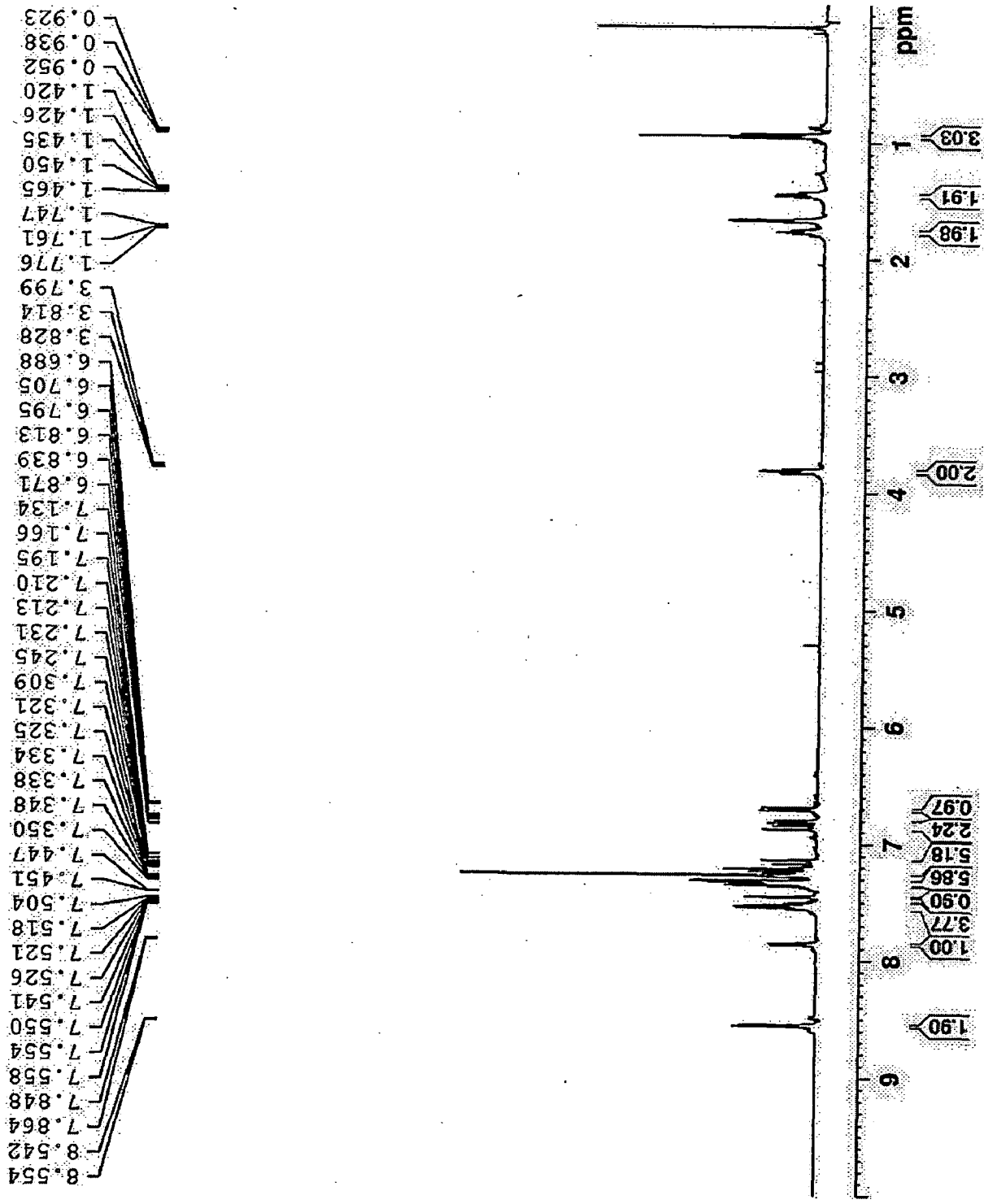
Figure S8. ^{1}H NMR spectrum of **D1** recorded in CDCl$_3$.

76

0.923
0.938
0.952
1.420
1.426
1.435
1.450
1.465
1.747
1.761
1.776
3.799
3.814
3.828
6.688
6.705
6.795
6.813
6.839
6.871
7.134
7.166
7.195
7.210
7.213
7.231
7.245
7.309
7.321
7.325
7.334
7.338
7.348
7.350
7.447
7.451
7.504
7.518
7.521
7.526
7.541
7.550
7.554
7.558
7.848
7.864
8.542
8.554

3.03
1.91
1.98
2.00
0.97
2.24
5.18
5.86
0.90
3.77
1.00
1.90

13.76
20.06
28.77
47.34

110.26
114.52
115.39
119.56
122.91
123.08
123.87
124.18
124.39
124.90
125.86
126.33
127.19
127.32
127.41
127.48
128.09
128.39
128.66
129.94
132.25
137.05
137.34
142.98
143.59
145.81
151.57

Figure S9. ^{13}C NMR spectrum of **D1** recorded in CDCl$_3$.

ppm

0.921
0.936
0.951
1.407
1.428
1.434
1.449
1.464
1.724
1.733
1.748
1.763
1.777
3.797
3.811
3.825
6.685
6.702
6.785
6.803
6.962
7.194
7.211
7.223
7.240
7.250
7.309
7.322
7.328
7.335
7.338
7.344
7.348
7.358
7.403
7.407
7.429
7.433
7.466
7.481
7.503
7.517
7.520
7.525
7.540
7.553
7.847
7.863

3.13
2.27
2.14
1.63
1.01
0.77
1.16
4.96
6.04
1.37
5.26
1.00

ppm
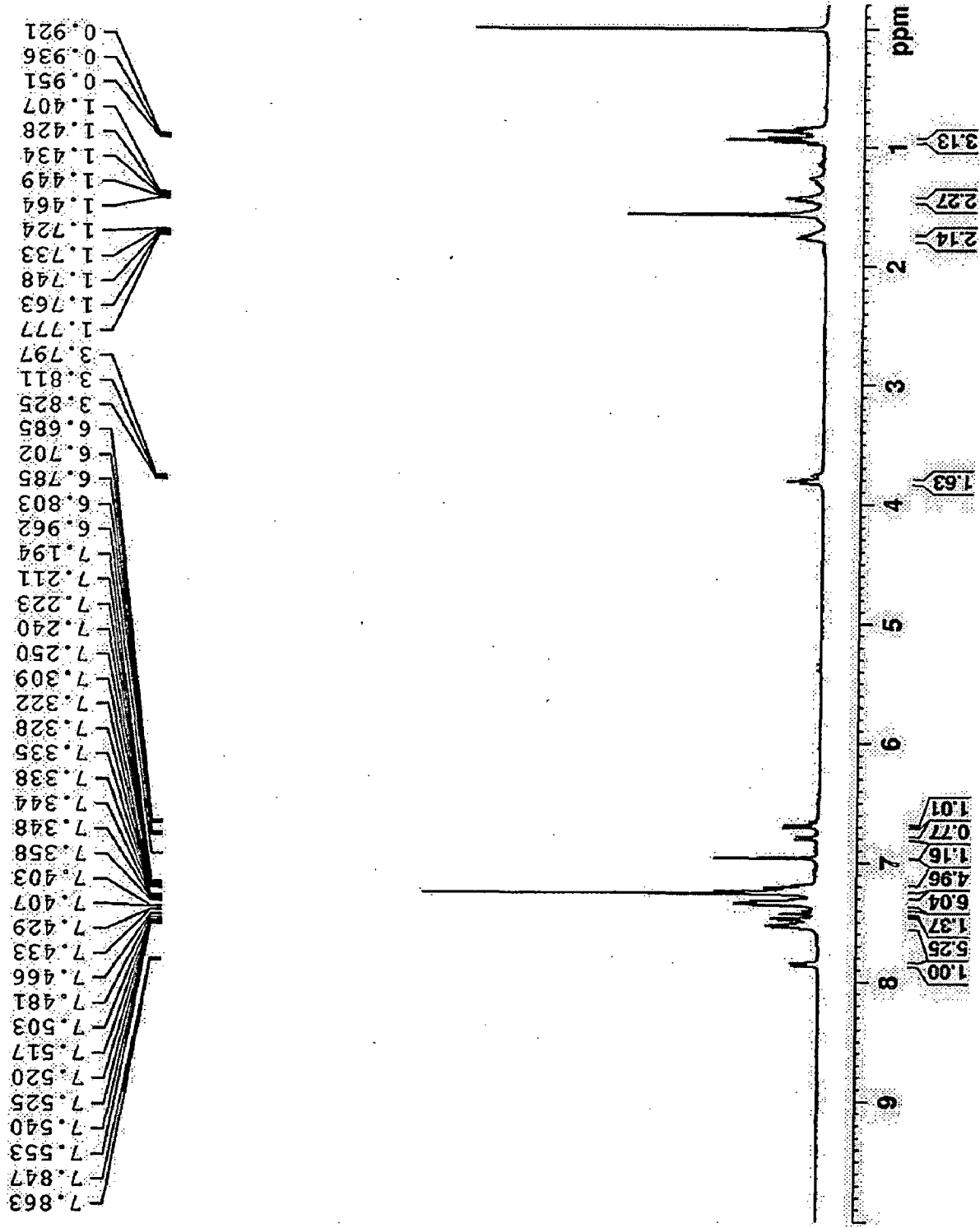
Figure S10. ^{1}H NMR spectrum of **D2** recorded in CDCl$_3$.

13.74
20.03
28.72

47.40
110.28
114.64
115.37
119.55
122.96
123.15
123.97
124.12
124.35
124.56
125.33
126.61
127.47
128.11
128.42
128.69
129.95
130.93
131.68
136.99
137.29
142.91
144.67
145.46
150.10
151.41

200   180   160   140   120   100   80   60   40   20   0   ppm
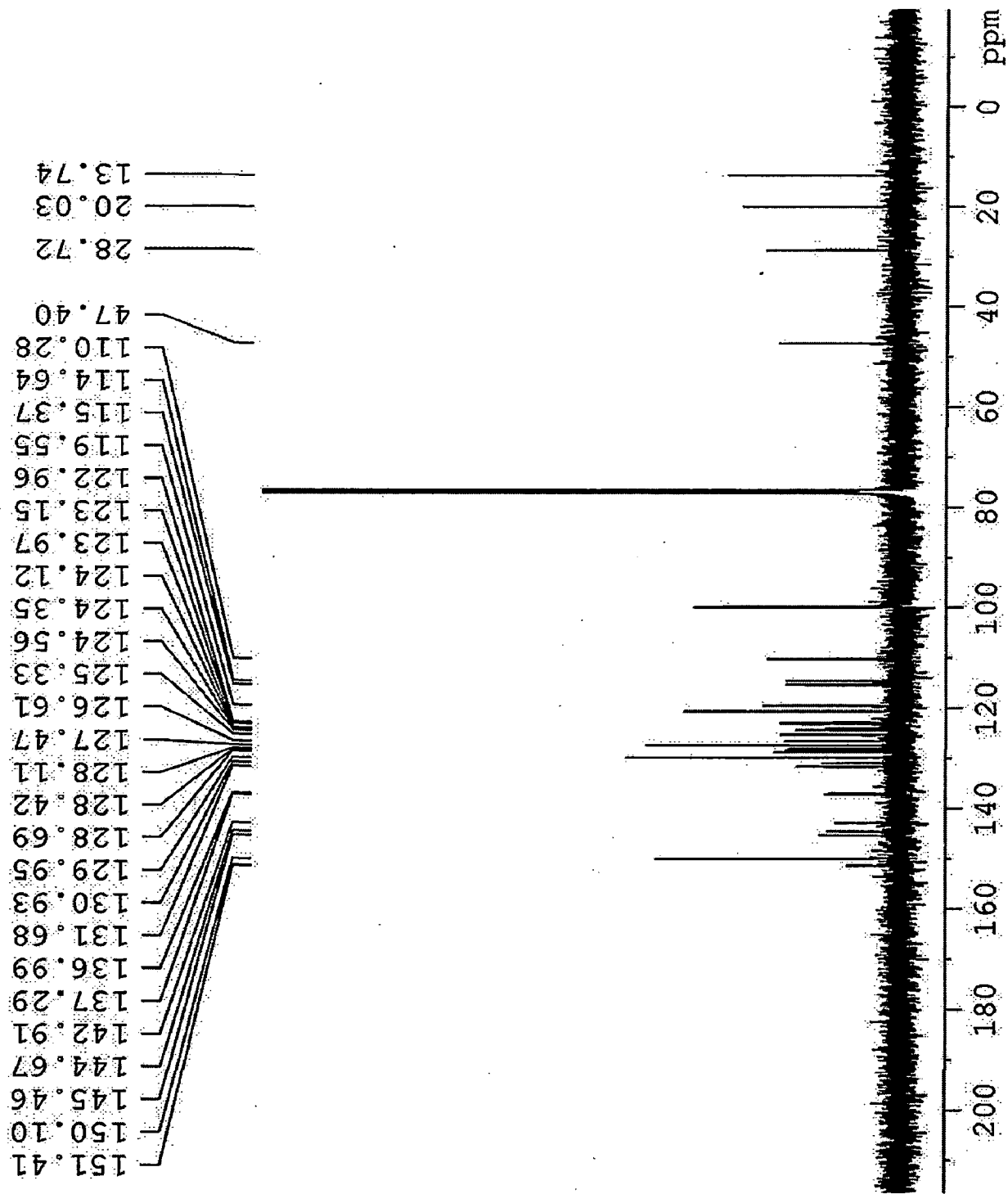
Figure S11. ^{13}C NMR spectrum of **D2** recorded in CDCl$_3$.
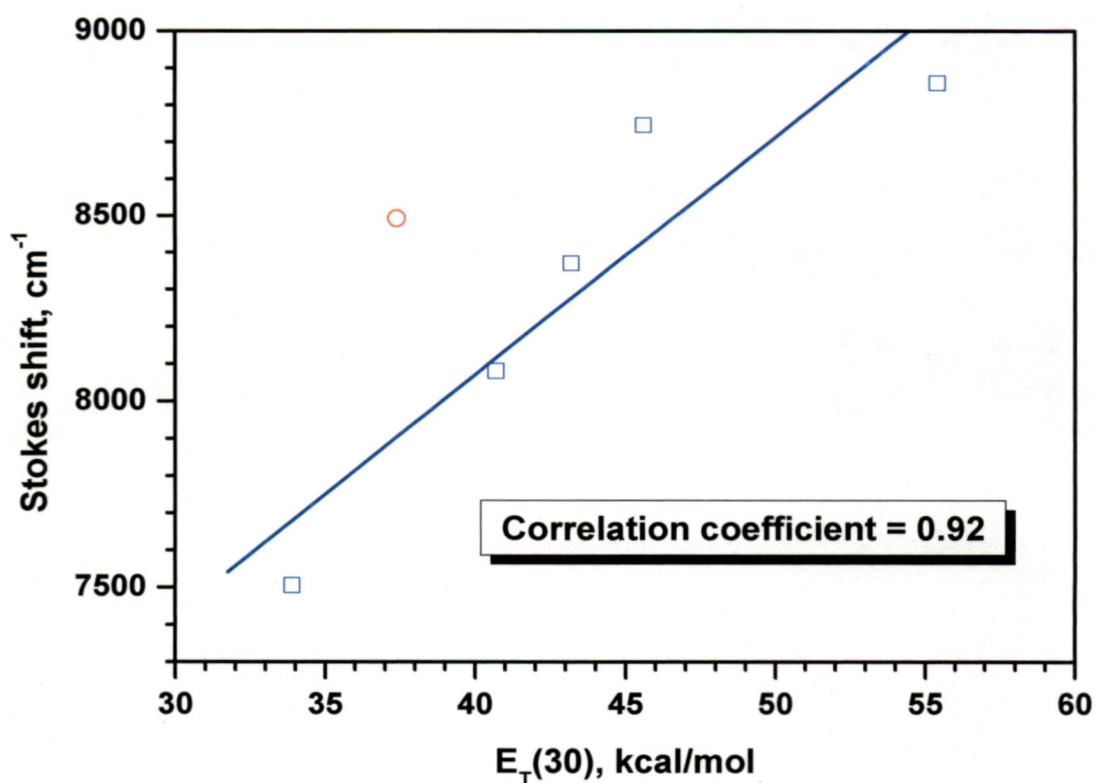
79

Figure 12. Correlation of $E_T(30)$ with Stokes shift observed for C1 in different solvents.
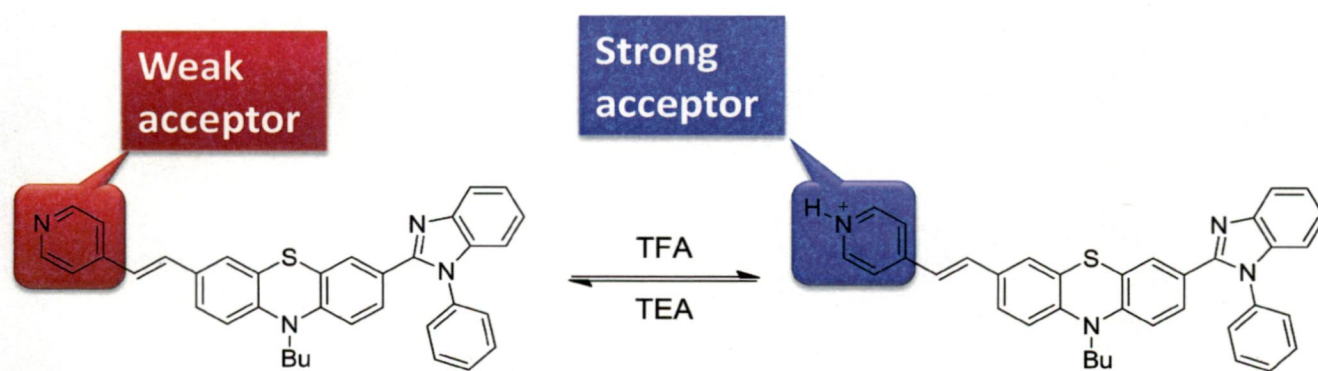

Figure 13. Illustration of protonation-deprotonation equilibrium for **D2**.

Vinylpyridine derivative, **D2** contains a pyridine unit which is capable of interacting with metal salts and hydrogen ions. Such an interaction may alter the electronic properties of the molecule. For instance, protonation of pyridine unit will form a pyridinium ion which is a much stronger acceptor group when compared to pyridine (Figure 13). Incrementation of acceptor

strength by protonation may result in a strong donor-acceptor interaction with phenothiazine which might affect the position of the corresponding charge transfer transition.

Absorption and emission spectra of **D2** in the presence of trifluoroacetic acid was examined in both dichloromethane and toluene. On addition of TFA, **D2** showed a dramatic red-shift in absorption (Figure 14 and 15) and emission profiles (Figure 16 and 17) suggestive of protonation at the pyridine unit as hypothesized above (Figure 13).
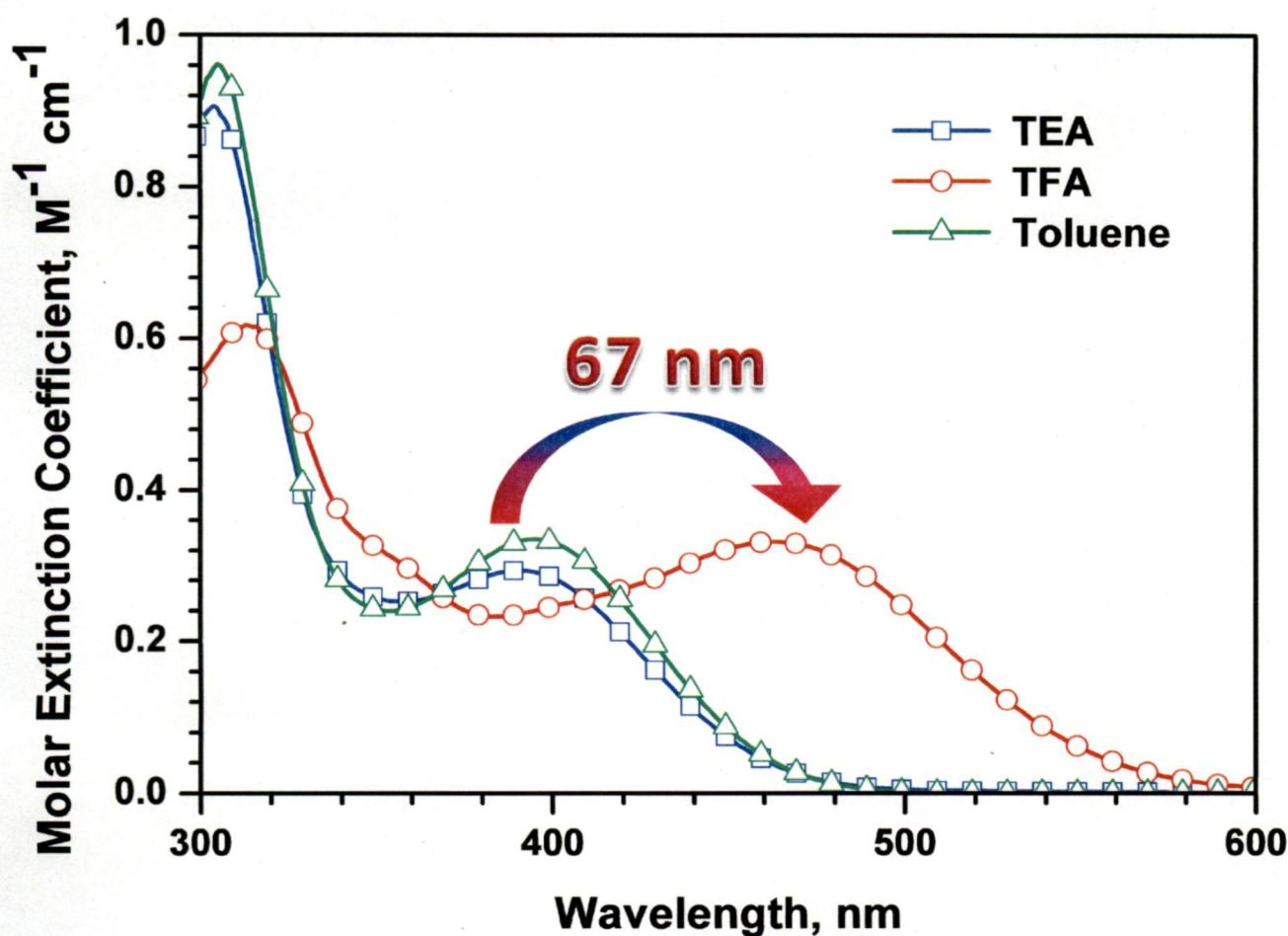

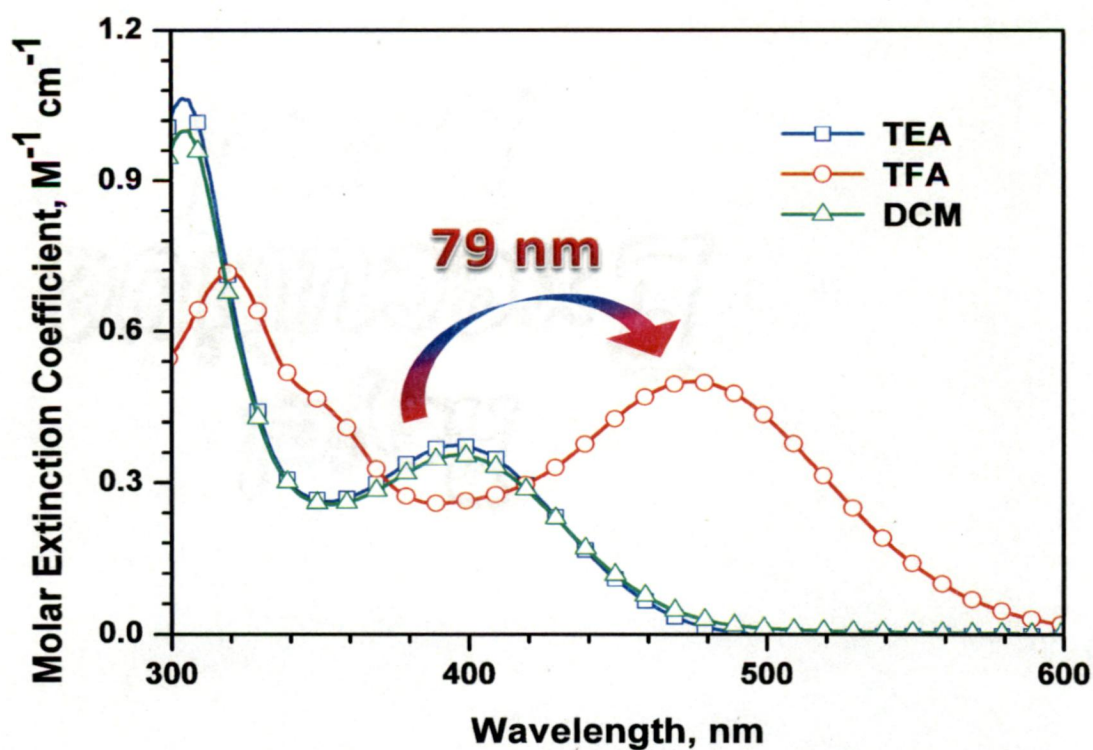**Figure 14**. Absorption changes observed for **D2** on addition of TFA or TEA in toluene.

Figure 15. Absorption changes observed for **D2** on addition of TFA or TEA in dichloromethane.
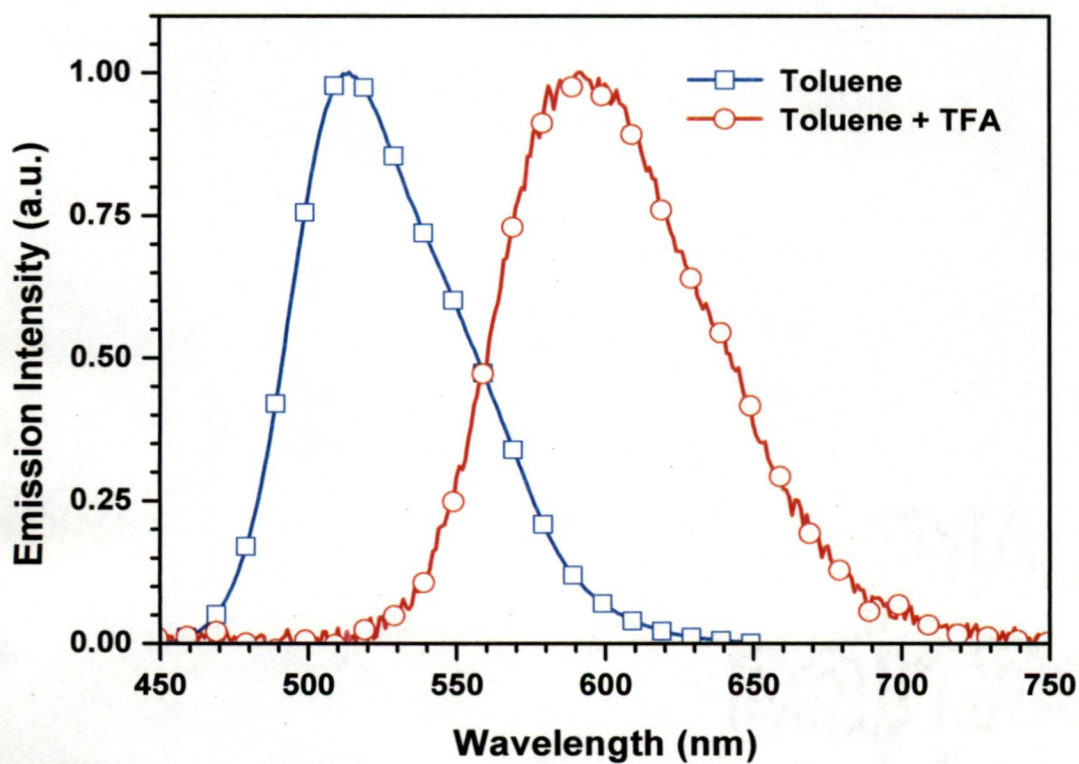

Figure 16. Emission changes observed for **D2** on addition of TFA in toluene.
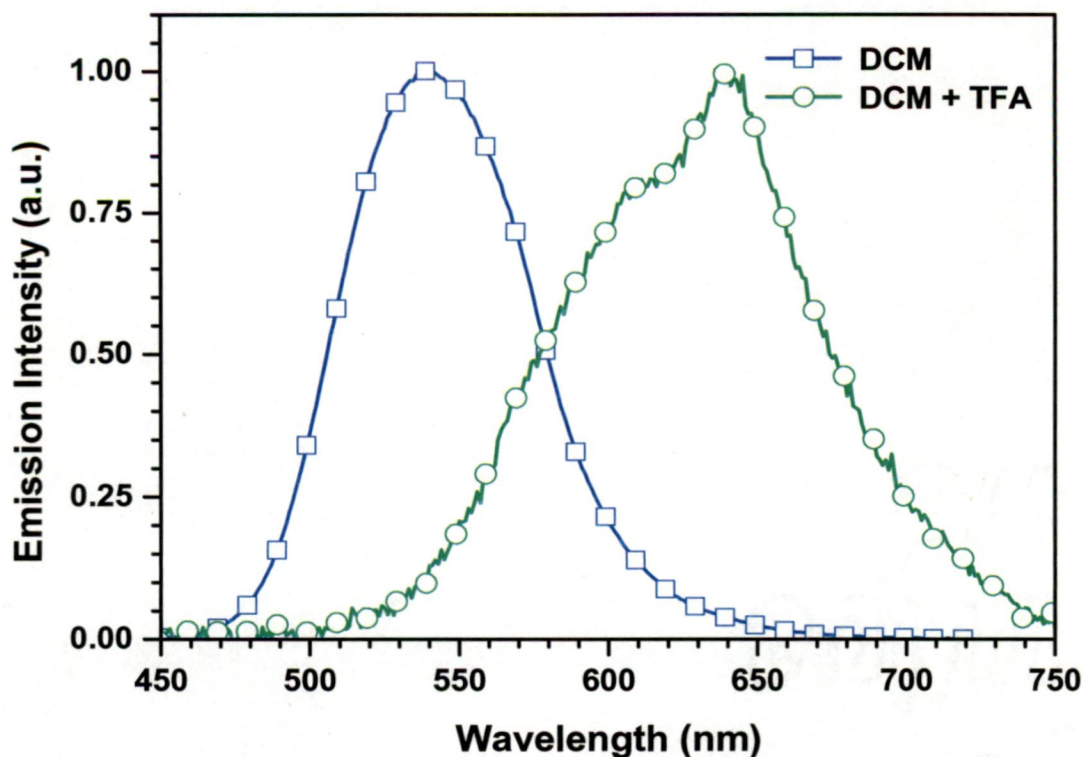
Figure 17. Emission changes observed for **D2** on addition of TFA in dichloromethane.

In toluene, on addition TFA the absorption peak shifted to 462 nm (Figure 14) from 395 nm ($\Delta\lambda$ = 67 nm) and the emission profile changed to 592 nm (Figure 16) from 514 nm ($\Delta\lambda$ = 78 nm) for D2. However the shift was more drastic in dichloromethane solution. The absorption profile exhibited 79 nm change (Figure 15) while the emission profile shifted to longer wavelength by 95 nm (Figure 17). The emission intensity significantly dropped on addition of TFA in dichloromethane. All these observations suggest that **D2** is converted to a more polar molecule on protonation and highly stabilized in polar solvents. The absorption and emission changes observed for **D2** in toluene on incremental addition of TFA is shown in Figures 18 and 19. Nearly 100 equivalents of TFA were required to bring out a complete change in the profiles which points the presence of acid-base equilibrium.
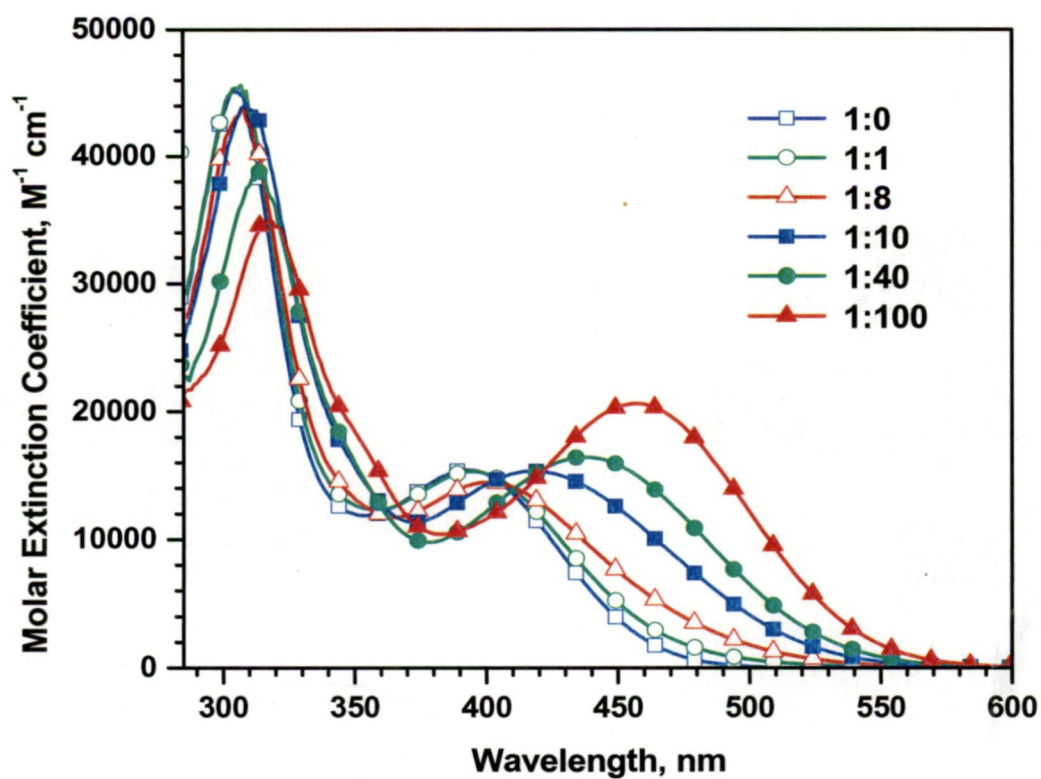
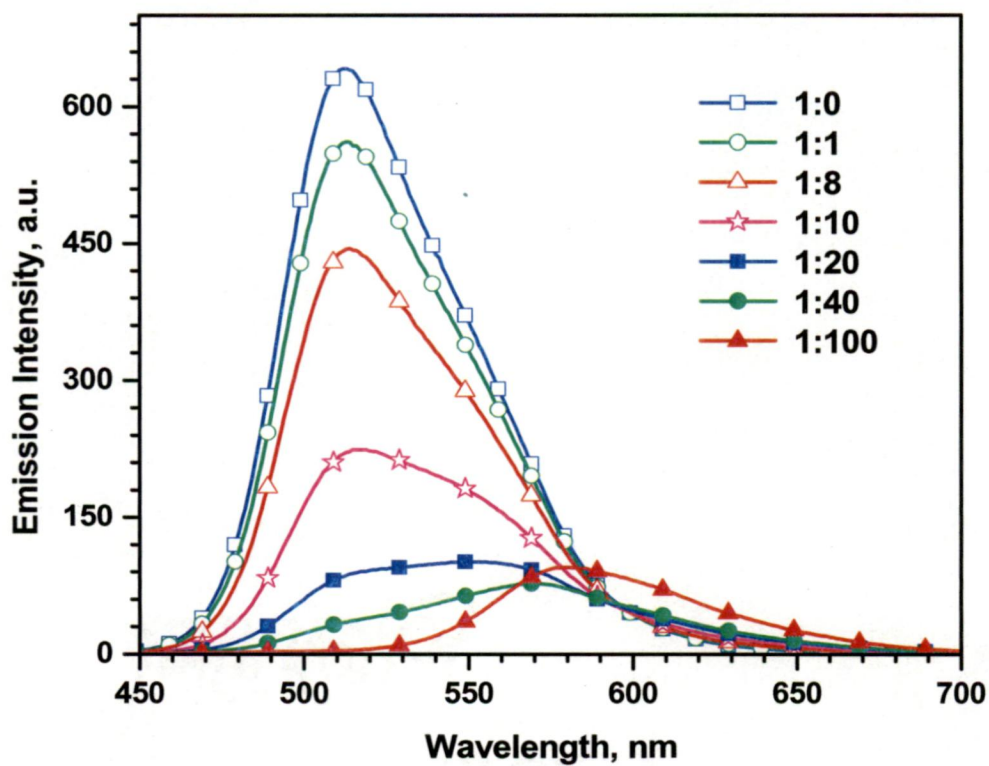**Figure 18.** Absorption changes observed for **D2** in toluene on incremental addition of TFA.

Figure 19. Emission changes observed for **D2** in toluene on incremental addition of TFA.

3.4 Electrochemical characteristics

The electrochemical behaviors of the dyes were investigated by cyclic voltammetric measurements in dichloromethane. Typical cyclic voltammograms recorded for **C1**, **C2** and **D2** are displayed in Figure 20 and the relevant parameters are collected in Table 3.

Table 3. Electrochemical parameters observed for the dyes in dichloromethane

E_{ox} (ΔE_p), V[a]	HOMO, eV[b]	LUMO, eV[c]	E_{0-0}, eV[d]
0.317 (72)	5.12	2.36	2.76
0.365 (74)	5.17	2.46	2.71
-	-		2.58
0.316 (72)	5.12	2.54	2.58

[a] redox potentials with reference to ferrocene which showed oxidation at ~0.23 V when used as internal standard

[b] HOMO = 4.8 + E_{ox}

[c] LUMO = HOMO–E_{0-0}

[d] obtained from optical edge

All the compounds exhibited a quasi-reversible one-electron oxidation redox couple. The half wave potentials for the dyes are more positive (Table 3) than that observed for ferrocene (Figure 20) under similar conditions and is slightly higher than the parent chromophore, 10-*n*-butylphenothiazine. All these data indicate that the phenothiazine chromophore in the present

58

compounds are difficult to oxidize when compared to the parent unit itself which underlines the electron-withdrawing effect exerted by benzimidazole unit on the phenothiazine nucleus. Presence of two benzimidazole units in the molecule **C2** drastically shifts the redox potential anodically (Table 3) which confirms the presence of electron-attracting effect due to benzimidazole.
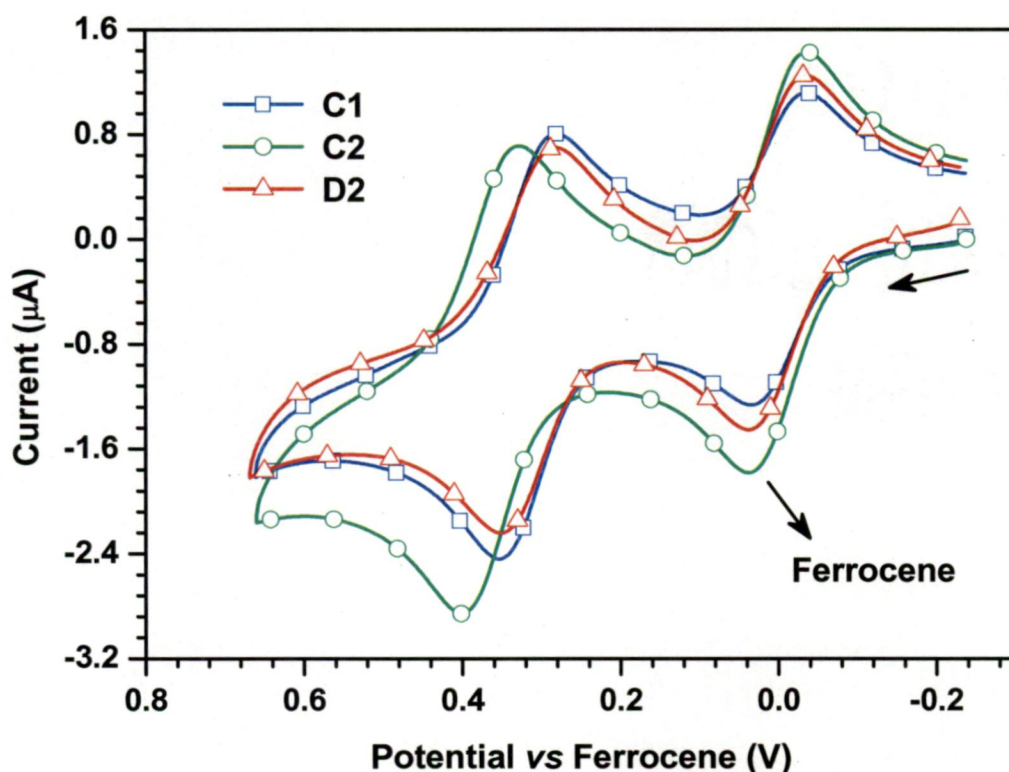
Figure 20. Cyclic voltammograms recorded for the compounds in dichloromethane.

The HOMO and LUMO energy levels of the dyes were deduced from the oxidative potentials and absorption edge (Table 3). The HOMO energy levels of those phenothiazine-based compounds were similar for all the compounds, whereas LUMO energy levels varied dependent upon the additional substituent present on the phenothiazine nucleus. For example, **C1** with only one benzimidazole unit had the same HOMO energy as the pyridyl-substituted derivative **D2**, whereas the LUMO energy of the former was 0.18 eV higher than that of the latter. It is also

interesting to notice that the LUMO energy levels of **D2** was substantially lower than those of **C1** and **C2** which might be due to the delocalization of LUMO into the pyridine segment in **D2**.

3.5 Conclusions

New donor-acceptor compounds based on phenothiazine and benzimidazole units have been synthesized and characterized by spectroscopic methods. Electronic absorption, fluorescence emission and electrochemical studies of the compounds showed the presence of significant donor-acceptor interaction between the phenothiazine donor and benzimidazole acceptor. Direct linking of phenothiazine and benzimidazole, produces charge transfer band in the absorption and emission of the compounds. The different molecular patterns such as a symmetrical bis-acceptor and an asymmetrical mono-acceptor skeletons, and the presence of different additional substituents at phenothiazine nucleus were found to influence the optical and electrochemical properties of the compounds. These inferences suggest that this can be used as an efficient method to a fine tune the electronic parameters such as LUMO levels without significantly affecting the energy levels of HOMO. This may be exploited to design ambipolar molecules with matching energy levels that of the Fermi levels of the electrodes. Such design and outcome will be beneficial to balance the electron or hole injection/transfer in OLED devices.

Chapter 4

Summary

Dipolar compounds are attractive due to their unique properties such as red-shifted absorption and emission, highly polarized excited state which eventually leads to charge separation, ordered solid state arrangements producing high conductivity properties, and balanced charge transport characteristics. Dipolar compounds containing donor fragments such as triphenylamine and carbazole and acceptor moieties such as oxadiazole, quinoxaline, pyridine, benzothiadiazole, benzotriazole, etc. have been designed and their structure property relationship investigated. We hypothesized that the integration of easily oxidizable phenothiazine unit with a moderately electron-accepting benzothiadiazole segment would result in new class of dipolar compounds exhibiting unique optical and electrochemical properties. We have also planned to augment the molecular structure with additional chromophores capable of alternating the electronic structure of phenothiazine.

In this dissertation, we have presented the synthesis and characterization of new donor-acceptor compounds based on phenothiazine and benzimidazole units. The compounds were characterized by routine spectral (^{1}H and ^{13}C NMR and IR) methods and established their molecular composition. Electronic absorption, fluorescence emission and electrochemical studies of the compounds showed the presence of significant donor-acceptor interaction between the phenothiazine donor and benzimidazole acceptor. Direct linking of phenothiazine and benzimidazole, produces charge transfer band in the absorption and emission of the compounds. The different molecular patterns such as a symmetrical bis-acceptor and an asymmetrical mono-

61

acceptor skeletons, and the presence of different additional substituents at phenothiazine nucleus were found to influence the optical and electrochemical properties of the compounds. These inferences suggest that this can be used as an efficient method to a fine tune the electronic parameters such as LUMO levels without significantly affecting the energy levels of HOMO. This may be exploited to design ambipolar molecules with matching energy levels that of the Fermi levels of the electrodes. Such design and outcome will be beneficial to balance the electron or hole injection/transfer in OLED devices.

References

(1)   Tang, C. W.; VanSlyke, S. A. *Appl. Phys. Lett.*, **1987**, *51*, 913-915.

(2)   Baldo, M. A.; Thompson, M. E.; Forrest, S. R. *Nature*, **2000**, *403*, 750-753.

(3)   Chaskar, A.; Chen, H.F.; Wong, K.T. *Adv. Mater.*, **2011**, *23*, 3876-3895.

(4)   Jeon, S. O.; Jang, S. E.; Son, H. S.; Lee, J. Y. *Adv. Mater.*, **2011**, *23*, 1436-1441.

(5)   Tao, Y.; Wang, Q.; Yang, C.; Zhong, C.; Qin, J.; Ma, D. *Adv. Funct. Mater.*, **2010**, *20*, 2923-2929.

(6)   Tao, Y.; Yang, C.; Qin, J. *Chem. Soc. Rev.*, **2011**, *40*, 2943-2970.

(7)   Mishra, A,; Fischer, M. K.; Bäuerle, P.; Angew. Chem. Int. Ed., **2009**, *48*, 2474-2499.

(8)   Lee, K-M.; Wu, S-J.; Chen, C-Y.; Wu, C-G.; Ikegami, M.; Miyoshi, K.; Miyasaka, T.; Ho, K-C. *J. Mater. Chem.*, **2009**, *19*, 5009-5015.

(9)   Lai, R. Y.; Kong, X.; Jenekhe, S. A.; Bard, A. J. *J. Am. Chem. Soc.* **2003**, *125*, 12631-12639.

(10)   Qiu, X. P.; Lu, R.; Zhou, H. P.; Zhang, X. F.; Xu, T. H.; Liu ,X. L.; Zhao, Y. Y. *Tetrahedron Lett.*, **2008**, *49*, 7446-7449.

(11)   Duesing, R.; Tapolsky, G.; Meyer, T. J. *J. Am. Chem. Soc.* **1990**, *112*, 5378-5379.

(12)   Jones Jr, W. E.; Chen, P.; Meyer, T. J. *J. Am. Chem. Soc.* **1992**, *114*, 387-388.

(13)   Spreitzer, H.; Daub, J. *Chem. Eur. J.* **1996**, *2*, 1150-1158.

(14)   Krämer, C. S.; Müller, T. J. J. *Eur. J. Org. Chem.* **2003**, 3534-3548.

(15)   Lai, R. Y.; Fabrizio, E. F.; Lu, L.; Jenekhe, S. A.; Bard, A. J. *J. Am. Chem. Soc.* **2001**, *123*, 9112-9118.

(16)   Kong, X.; Kulkarni, A. P.; Jenekhe, S. A. *Macromolecules* **2003**, *36*, 8992-8999.

(17) Hwang, D-H.; Kim, S-K.; Park, M-J.; Lee, J-H.; Koo, B-W.; Kang, I-N.; Kim, S-H.; Zyung, T. *Chem. Mater.* **2004**, *16*, 1298-1303.

(18) Kim, G.W.; Cho, M.J.; Yu, Y-J.; Kim, Z.H.; Jin, J-I.; Kim, D.Y.; Choi, D.H. *Chem. Mater.* **2007**, *19*, 42-50.

(19) Barberis, V. P.; Mikroyannidis, J. A. *Synthetic Metals.* **2006**, *156*, 1408-1414.

(20) Zhang, X.-H.; Choi, S.-H.; Choi, D. H.; Ahn, K.-H. *Tetrahedron Lett.* **2005**, *46*, 5273-5276.

(21) Kazlauskas, K.; Mikulėnaitė, J.; Karpicz, R.; Gulbinas, V.; Simokaitiene, J.; Michaleviciute, A.; Keruckas, J.; Grazulevicius , J. V. *Dyes Pigm.* **2009**, *83*, 168-173.

(22) Memminger, K.; Oeser, T.; Müller, T. J. J. *Org. Lett.* **2008**, *10*, 2797-2800.

(23) Qiu, X.; Lu, R.; Zhou, H.; Zhang, X.; Xu, T.; Liu, X.; Zhao, Y. *Tetrahedron Lett.* **2007**, *48*, 7582-7585.

(24) Krämer, C. S.; Zeitler, K.; Müller, T. J. J. *Tetrahedron Lett.* **2001**, *42*, 8619-8624.

(25) Krämer, C. S.; Müller, T. J. J. *Eur. J. Org. Chem.* **2003**, *18*, 3534-3548.

(26) Hauck, M.; Schönhaber, J.; Zucchero, A. J.; Hardcastle, K. I.; Müller, T. J. J.; Bunz, U. H. F. *J. Org. Chem.* **2007**, *72*, 6714-6725.

(27) Meyer, T.; Ogermann, D.; Pankrath, A.; Kleinermanns, K.; Müller, T. J. J., *J. Org. Chem.* **2012**, *77*, 3704-3715.

(28) Tian, H.; Yang, X.; Chen, R.; Pan, Y.; Li, L.; Hagfeldt, A.; Sun, L. *Chem. Commun.* **2007**, 3741-3743.

(29) Park, S. S.; Won, Y. S.; Choi, Y. C.; Kim, J. H. *Energy Fuels* **2009**, *23*, 3732-3736.

(30) Cao, D.; Peng, J.; Hong, Y.; Fang, X.; Wang, L.; Meier, H. *Org. Lett.* **2011**, *13*, 1610-1613.

(31) Kim, S. H.; Kim, H. W.; Sakong, C.; Namgoong, J.; Park, S.W.; Ko, M. J.; Lee, C. H.; Lee, W. I.; Kim, J. P. *Org. Lett.* **2011,** *13,* 5784-5787.

(32) Xie, Z.; Midya, A.; Loh, K. P.; Adams, S.; Blackwood, D. J.; Wang, J.; Zhang, X.; Chen, Z. *Prog. Photovolt: Res. Appl.* **2010,** *18,* 573-581.

(33) Wan, Z.; Jia, C.; Duan, Y.; Zhang, J.; Lin, Y.; Shi, Y. *Dyes Pigm.* **2012,** *94,* 150-155.

(34) Wu, W.; Yang, J.; Hua, J.; Tang, J.; Zhang, J.; Long, Y.; Tian, H. *J. Mater. Chem.,* **2010,** *20,* 1772-1779.

(35) Yang, C-J.; Chang, Y. J.; Watanabe, M.; Hon, Y-S.; Chow, T. J. *J. Mater. Chem.,* **2012,** *22,* 4040-4049.

(36) Dong, H.; Chen, B-Z. ; Huang, M.-B. ; Lindh, R. *J. Mater. Chem.,* **2012,** *22,* 889-894.

(37) Sailer, M.; Rominger, F.; Müller, T. J. J. *J. Organomet. Chem.* **2006,** *691,* 299-308.

(38) Takizawa, S.; Montes, V. A.; Anzenbacher Jr., P. *Chem. Mater.* **2009,** *21,* 2452-2458.

(39) Chen, C.-H.; Huang, W.-S.; Lai, M.-Y.; Tsao, W.-C.; Lin, J. T.; Wu, Y.-H.; Ke, T.-H.; Chen, L.-Y.; Wu, C.-C. *Adv. Funct. Mater.* **2009,** *19,* 2661-2670.

(40) Ko, C. W.; Tao, Y. T.; Lin, J. T.; Thomas, K. R. J. *Chem. Mater.* **2002,** *14,* 357-361.

(41) Li, Y.; Fung, M. K. ; Xie, Z.; Lee, S. T.; Huang, L. S. ; Shi, J. *Adv. Mater.* **2002,** *14,* 1317-1321.

(42) Lai, M-Y. ; Chen, C-H. ; Huang, W-S. ; Lin, J. T. ; Ke, T-H. ; Chen, L-Y.; Tsai, M-H. ; Wu, C-C. *Angew. Chem. Int. Ed.* **2008,** *47,* 581-585.

(43) Kumar, S.; Khan, S.A.; Alam, O.; Azim, R.; Khurana, A.; Shaquiquzzaman, M.; Siddiqui, N.; Ahsa W. *Bull. Korean Chem. Soc.* **2011,** *32,* 2260-2266.

(44) Ge, Z.; Hayakawa, T.; Ando, S.; Ueda, M.; Akiike, T.; Miyamoto, H.; Kajita, T.; Kakimoto, M-A. *Chem. Mater.* **2008,** *20,* 2532-2537.

(45) Hung , W-Y.; Chi, L-C.; Chen, W-J; Chen , Y-M.; Chou, S-H. ; Wong, K-T. *J. Mater. Chem.*, **2012**, *20*, 10113-10119.

(46) Huang, J.; Su, J-H.; Li, X.; Lam, M-K.; Fung, K-M.; Fan, H-H.; Cheah, K-W.; Chen, C. H.; Tian, H. *J. Mater. Chem.*, **2011**, *21*, 2957-2964.

(47) Chen , Y-M.; Hung, W-Y.; You, H-W.; Chaskar, A.; Ting, H-C; Chen, H.-F.; Wong, K-T.; Liu, Y-H. *J. Mater. Chem.*, **2011**, *21*, 14971-14978.

(48) Ting, H-C.; Chen, Y-M.; You, H-W.; Hung, W-Y.; Lin, S-H; Chaskar, A.; Chou, S-H.; Chi, Y.; Liu, R-H.; Wong, K-T. *J. Mater. Chem.*, **2012**, *22*, 8399-8407.

(49) Gong, S.; Zhao, Y.; Yang, C.; Zhong, C.; Qin, J.; Ma, D. *J. Phys. Chem. C* **2010**, *114*, 5193-5199.

(50) Yang, X.; Zheng, S.; Bottger, R.; Chae, H. S. ; Tanaka, T. ; Li, S.; Mochizuki, A.; Jabbour, G. E. *J. Phys. Chem. C* **2011**, *115*, 14347-14352.

(51) Selvam, K.; Swaminathan, M. *Tetrahedron Lett.* **2011**, *52*, 3386-3392.

(52) Shao, J.; Ji, S.; Li, X.; Zhao, J.; Zhou, F.; Guo, H. *Eur. J. Org. Chem.* **2011**, 6100-6109.

(53) Kim, S. H.; Kim, H. W.; Sakong, C.; Namgoong, J.; Park, Se W.; Ko, M. J.; Lee, C. H.; Lee, W. I.; Kim, J. P. *Org. Lett.* **2011**, *13*, 5784-5787.

(54) Hauck, M.; Stolte, M.; Schoenhaber, J.; Kuball, H.-G.; Mueller, T. J. J. *Chemistry- Eur. J.* **2011**, *17*, 9984-9998.

(55) Li, Z.; Dong, Q.; Li, Y.; Xu, B.; Deng, M.; Pei, J.; Zhang, J.; Chen, F.; Wen, S.; Gao, Y.; Tian, W. *J. Mater. Chem.* **2011**, *21*, 2159-2168.

(56) Thomas, K. R. J.; Lin, J. T; Tao, Y.-T.; Chuen, C.-H. *Chem. Mater.* **2002**, *14*, 2796-2802.

(57) Thomas, K. R. J.; Lin, J. T; Tao Y.-T. ; Chuen, C.-H. *Adv. Mater.* **2002**, *14*, 822-826.

(58) Chen, S. Y. ; Xu, X. J.; Liu, Y. Q.; Yu, G. ; Sun, X. B. ; Qiu, W. F. ; Ma, Y. Q. ; Zhu, D. B. *Adv. Funct. Mater.* **2005**, *15*, 1541-1546.

(59) Reinhardt, B. A.; Lawrence, L. B.; Clarson, S. J.; Dillard, A. G.; Bhatt, J. C.; Kannan, R.; Yuan, L.; He, G. S.; Prasad, P. N. *Chem. Mater.* **1998**, *10*, 1863-1874.

(60) Abbotto, A.; Beverina, L.; Bozio, R.; Facchetti, A.; Ferrante, C.; Pagani, G. A.; Pedron, D.; Signorini, R. *Chem. Commun.* **2003**, *17*, 2144-2145.

(61) Cho, M. J.; Kim, J. Y.; Kim, J. H.; Lee, S. H.; Dalton, L. R.; Choi, D. H. *Bull Korean Chem Soc.* **2005**, *26*, 77-84.

(62) Wong, M. S.; Li, Z. H.; Tao, Y.; D'Iorio, M. *Chem. Mater.* **2003**, *15*, 1198-1203.

(63) Jiao, G.-S.; Thoresen, L. H.; Burgess, K. *J. Am. Chem. Soc.* **2003**, *125*, 14668-14669.